People's Democratic Republic of Algeria
Ministry of Higher Education and Scientific Research
Mohamed El Bachir El Ibrahimi University of Borj Bou Arréridj
Faculty of Mathematics and Computer Science
Department of Mathematics

THESIS

In order to obtain the Doctorate degree in LMD (3rd cycle)
Branch : Mathematics
Option : Applied Mathematics

THEME

Accélération de la convergence de méthodes numériques pour résoudre des équations intégrales

By: ABDENNEBI Issam

Publicly defended on: 25/06/2025

In front of the jury composed of:

Pr. MEROUANI Abdelbaki	University of Setif 1	**President**
Pr. RAHMOUNE Azedine	University of B.B.A	**Supervisor**
Pr. BENSERIDI Hamid	University of Setif 1	**Examiner**
Dr. ZEGHDANE Rebiha	University of B.B.A	**Examiner**
Dr. BOUKAROURA Ilyas	University of Setif 1	**Examiner**

2024/2025

Acknowledgements

First and foremost, I thank ALLAH for giving me the courage, patience, ability and opportunity to complete this thesis.
I would like to express my sincere gratitude to my supervisor *Pr. Azedine RAHMOUNE* for his help, continuous support, wise advice, encouragement, and invaluable guidance throughout the years of my thesis preparation.
I extend my sincere thanks also to the members of my thesis committee: *Pr. Abdelbaki MEROUANI*, and *Pr. Hamid BENSERIDI* from Mathematics Department, University Ferhat Abbas of Setif 1, *Dr. Rebiha ZEGHDANE* from Mathematics Department, University Mohamed El Bachir El Ibrahimi of Bordj Bou Arreridj and *Dr. Ilyas BOUKAROURA* from Mathematics Department, University Ferhat Abbas of Setif 1, for accepting to evaluate and examine this thesis.
Finally, I would like to express my deepest gratitude to my family for their encouragement and sacrifices, which have been a constant source of inspiration in following my dreams. I also thank my friends and every one who helped me and contributed in any way to the completion of this work.

Abstract

The research work presented in this thesis focuses on improving the convergence speed of numerical methods for solving integral equations. These equations often introduce a very complex behavior, posing significant challenges to traditional numerical techniques, particularly in terms of convergence and accuracy. To address these challenges, we have developed and analyzed an adaptive spectral collocation method for Fredholm and Volterra integral equations of the second kind, which can achieve fast convergence and high accuracy despite the fact that its solution exhibits localized rapid variations, steep gradients, or a steep front. Adaptivity is implemented using a suitable family of one-to-one mappings to generate a new equation with smoother behavior that can be approximated more accurately. The proposed method can achieve exponential accuracy by adjusting a parameter-dependent mapping in the modal approximation according to the given data. Finally, several numerical examples are given to show that the proposed method is preferable to its classical method and some other existing approaches with a relatively smaller number of degrees of freedom.

Keywords: Linear integral equations, mappings for improved accuracy, adaptive spectral collocation method, spectral accuracy, convergence analysis.

Contents

List of Figures

List of Tables

List of Abbreviations

IE	Intergal Eequation;
FIE	Fredholm Integral Equation;
VIE	Volterra Iintegral Equation;
DE	Differential Equation;
IVP	Initial Value Problem;
BVP	Boundary Value Problem;
OP	Orthogonal Polynomial;
JP	Jacobi Polynomial;
LP	Legendre Polynomial;
MJP	Mapped Jacobi Polynomial;
MLP	Mapped Legendre Polynomial;
LBP	Lagrange Basis Polynomial;
MLBP	Mapped Lagrange Basis Polynomial;

List of Symbols

$\mathbb{N}$	set of nonnegative integers;
$L^2(D)$	space of square integrable functions on D;
$\mathcal{C}(D)$	space of continuous functions on D;
$\mathcal{B}(\mathcal{X},\mathcal{Y}), \mathcal{B}(\mathcal{X})$	set of all bounded linear operators;
$\mathcal{B}_c(\mathcal{X},\mathcal{Y}), \mathcal{B}_c(\mathcal{X})$	set of all compact linear operators;
$H^m(D)$, $H^m_{w_{J,\nu}}(D)$	Sobolev spaces with index m on D;
T^*	adjoint of the operator T;
$\mathcal{O}(\cdot)$	order of convergence;
$\|\cdot\|$	norm of an operator;
$(\cdot,\cdot)_w$	inner product of the weighted space $L^2_w(D)$;
$\|\cdot\|_{L^2_w}$	norm of the weighted space $L^2_w(D)$;
$\|\cdot\|_\infty$	uniform norm on D;
cond$(\cdot)$	condition of a matrix;
$\mathcal{P}, \mathcal{P}_N$	projections;
$\mathcal{I}_N, \mathcal{I}^\nu_N$	interpolations;
$\delta_{n,m}$	dalat function equal 1 if $n = m$ and 0 if not;
I, J	intervals are equal to $[-1,1]$, $[a,b]$, respectively;
$J^{\alpha,\beta}_n$	Jacobi polynomial of order n;
$j^{\alpha,\beta}_{n,\nu}$	mapped Jacobi polynomial of order n;
P_n	Legendre polynomial of order n;
$L^{(\nu)}_{J,n}$	mapped Legendre polynomial of order n;
h_j	Lagrange basis polynomial of order j;
$h^{(\nu)}_j$	mapped Lagrange basis function of order j;

Introduction

There is a long history in the development of integral equations (IEs, in short). In the modern scientific community, it is considered traditional that the first origins of the theory of IEs go back to the work of Fourier (1768–1830) on the inversion formula of what is known as the "Fourier transform" which represents, in fact, the inverse operator of an integral operator. In 1823, Abel proposed a generalization of the Tautochrone problem, the solution of which involved solving an IE, which has more recently been designated "an IE of the first kind", and in 1837 Liouville demonstrated that finding a particular solution to a second-order linear differential equation could be achieved by solving an IE of a different type, known as an IE of the second kind, however, the term IE was first suggested by Du Bois-Reymond in 1888. He defined it as an equation in which the unknown function appears under an integral sign (or more integral signs). Starting in 1896, the works of Vito Volterra (1860–1940), Ivar Fredholm (1866–1927), David Hilbert (1862–1943), and Erhard Schmidt (1876–1959) led to the development of IEs as a distinct discipline. (see [13, 2, 94, 71, 17, 21, 83, 64, 37], for more information).

Integral equations (IEs) play an important role in both theoretical and applied mathematics, as they appear in many fields such as engineering science, mathematical physics, biology, and so on [56, 42, 31, 45, 5, 84, 62, 29, 52, 81], and have a close connection to differential equations (DEs, in short). It is well known that numerous initial and boundary value problems associated with both ordinary and partial differential equations can be reformulated as IEs [44, 71]. Since, in many cases, IEs cannot be solved analytically, either the exact solution does not exist or is hard to find. Thus, their solutions must be approximated using so-called numerical methods. Accordingly, several conventional numerical methods have been developed and analyzed for solving IEs, including the degenerate kernel, Nyström and projection methods. For more details on these methods, we refer to [7, 8, 50, 34]. Among these methods, projection methods are the most commonly used approaches for finding numerical solutions of IEs. These methods include the Galerkin method based on the orthogonal projection and the collocation method based on an interpolatory projection (see, e.g. [11, 9, 10, 82]). To improve the accuracy of numerical solutions for IEs, iterated collocation and iterated Galerkin methods have been proposed as effective solution techniques (see, e.g. [36, 11, 58]).

In recent decades, researchers have increasingly focused on high-order numerical techniques, such as spectral methods for solving IEs. These methods possess high-order accuracy and low computational cost. However, they are often not efficient for solving problems that exhibit localized rapid variations, steep gradients, or a steep front. To overcome these challenges, we develop and analyze in this thesis an adaptive spectral collocation method for linear Fredholm and Volterra IEs (FIEs and VIEs) of the second kind, where the underlying solution exhibits localized rapid variations, steep gradients, or a steep front. The proposed strategy involves transforming the given equation into an equivalent one with smoother behavior by using suitable variable transformations, which can then be approximated more accurately. One of the significant advantages of this approach is its flexibility, which stems from the use of a parameter-dependent mapping that enables the recovery of fast convergence and high accuracy, which standard spectral methods may not achieve due to the aforementioned phenomena.

We close this introduction by a summary of the thesis.
This Chapter 1 introduces a detailed classification of IEs (Fredholm, Volterra, singular, linear, and nonlinear) and explores their close connections with DEs. It also introduces some basic concepts of operator theory, such as bounded and compact operators, and compact integral operators which will be required later in the Fredholm Alternative theorem.

Chapter 2 provides a concise overview of numerical methods and their convergence analysis for solving IEs, such as the projection methods, including the Galerkin method and the collocation method, and the quadrature or Nyström method.

Chapter 3 is divided into two sections. In Section 3.1, we review some notions and properties of Jacobi and Legendre polynomials, and their associated Gauss quadrature formulas, which will be used in Section 3.2. This section first introduces a new set of orthogonal functions named MJPs and MLPs, and their associated mapped Gauss quadrature formulas. It also introduces the MLBFs based on the zeros of the MLPs, along with some results on adaptive interpolation and integration errors. In addition, three functions are approximated using the adaptive interpolation at the end of this section to verify its spectral accuracy in comparison with the standard interpolation.

Chapter 4 is divided into three sections. In Section 4.1, we apply the Legendre spectral Galerkin method and its iterated version to solve linear FIEs of the second kind and discuss the convergence results. Finally, three numerical examples are presented to illustrate the convergence rates. In Sections 4.2 and 4.3, we develop and analyze an adaptive spectral collocation method for linear Fredholm and Volterra IEs (FIEs and VIEs) of the second kind, which can achieve fast convergence and high accuracy despite the fact that its solution is exhibits localized rapid variations, steep gradients, or a steep front. Also, we provide error estimates and convergence rates for the proposed numerical scheme in both

the L^2 norm and infinity norm. Finally, several numerical examples are given to demonstrate that the proposed method is more effective than its classical method and some other existing approaches.

Before closing this thesis with conclusion and perspectives, we study in detail how a DE can be transformed into an equivalent IE, incorporating boundary and initial conditions within the studied models, in Appendix A.

Chapter 1

Classifications and some basic from functional analysis for integral equations

In this chapter, we present some concepts and basic results from functional analysis for IEs, which will be used throughout this thesis. The main references of this chapter are [94, 44, 71, 49, 40, 7, 51, 25, 85, 16].

1.1 Classification of integral equations and their relationship to differential equations

1.1.1 Definition

An equation in which the unknown function appears inside an integral is referred to as an integral equation (IE). The standard form of a linear IE is

$$u(x) = f(x) + \lambda \int_{a(x)}^{b(x)} k(x,t)u(t)dt, \tag{1.1}$$

where $a(x)$ and $b(x)$ are the limits of integrations, λ is a non-zero constant parameter, the functions $f(x)$ and $k(x,t)$ are known functions, whereas the function $u(x)$ is the only unknown in the IE that will be determined to appear under the integral sign, and sometimes outside the integral sign . The function $k(x,t)$ is called the *kernel* of the IE and the function $f(x)$ is called the *free term* or the *source function*.

1.1.2 Classifications

Classification of linear integral equations

Linear IEs appear in many forms and can be classified according to the following basic characteristics.

◊ The first characteristic is based on the appearance of the unknown function. If the unknown appears only within the integral, the equation is referred to as an IE of the

first kind. In contrast, if the unknown function appears both inside and outside the integral, the equation is of the second.

◊ The second characteristic is based on the free term. If the free term $f(x)$ is identically zero over the considered domain, i.e., $f(x) = 0$, the IE is homogeneous. Otherwise, it is called *nonhomogeneous* or *inhomogeneous*.

◊ The last characteristic depends on the limits of integration;

(i) If the limits of integration are fixed (e.g., from a to b), the IE is called a Fredholm integral equation (FIE) given in the form:

$$u(x) = f(x) + \lambda \int_a^b k(x,t)u(t)dt.$$

(ii) If one limit of integration is a variable (e.g., from a to x), the IE is called a Volterra integral equation (VIE) given in the form:

$$u(x) = f(x) + \lambda \int_a^x k(x,t)u(t)dt.$$

(iii) If one or both limits of integration become infinite (e.g., from 0 to $+\infty$, or from $-\infty$ to $+\infty$), the IE is called a singular integral equation (SIE) given in the form:

$$u(x) = f(x) + \lambda \int_0^{+\infty} k(x,t)u(t)dt,$$

or

$$u(x) = f(x) + \lambda \int_{-\infty}^{+\infty} k(x,t)u(t)dt.$$

Moreover, an IE is called a SIE if the kernel $k(x,t)$ approaches infinity at one or more points within the range of integration, such as the generalized Abel's IE,

$$f(x) = \int_0^x \frac{1}{(x-t)^\alpha} u(t)dt, \quad 0 < \alpha < 1,$$

and the Wiener-Hopf IE,

$$u(x) = f(x) + \lambda \int_0^{\infty} k(x-t)u(t)dt.$$

Remark 1.1. If the unknown function $u(x)$ appears under the integral sign, and it is given in the functional form $G(u(x))$ such as the power $u(x)$ is no longer unity, e.g., $G(u(x)) = u^m(x)$, $m \neq 1$, or $sin(u(x))$, $cos(u(x))$, $\ln(u(x))$ and $e^{u(x)}$ etc., the above IEs are classified as nonlinear, for examples,

$$u(x) = f(x) + \int_a^b k(x,t)u^2(t)dt,$$

and

$$u(x) = f(x) + \int_a^x k(x,t)\sin(u(t))dt,$$

are called nonlinear FIE and VIE of the second kind, respectively.

Classification of kernel functions

The kernel function is the main part of the IE. Therefore, we shall describe some kernel functions as follows:

- A kernel $k(x,t)$ is called the complex *symmetric* or *Hermitian* if $k(x,t) = \overline{k(t,x)}$, and also it is called symmetric if $k(x,t) = k(t,x)$.
- A kernel $k(x,t)$ is called *degenerate* or *separable* if it can be expressed as the sum of a finite number of terms, each of which is the product of a function of x only and a function of t only, i.e.,
$$k(x,t) = \sum_{j=1}^{n} p_j(x) q_j(x),$$
where $p_j(x)$ and $q_j(x)$, $j = 1, \ldots, n$ are linearly independent sets.
- A kernel $k(x,t)$ is called *non-degenerate* or *non-separable* if it can not be separated as the function of x and function of t.
- A kernel $k(x,t)$ is called *weakly singular* type, in particular, *algebraic* and *logarithmic* type if
$$k(x,t) = \begin{cases} m(x,t)\,|x-t|^{-\alpha}, \\ \\ m(x,t)\,\log|x-t|, \end{cases}$$
where $m(x,t)$ is a sufficiently regular function with $m(x,t) \neq 0$, and α is a positive number *less than one*.

1.1.3 Connection between differential equations and integral equations

There is a close connection between DEs and IEs. In fact, many initial and boundary value problems (IVPs and BVPs, in short) associated with the ordinary and partial-differential equations can be reformulated as IEs. The advantage of the IE reformulation is that associated boundary and initial conditions are incorporated within the IE, in contrast to ordinary differential equations and partial differential equations on which boundary conditions and initial conditions are imposed. For example, the second-order IVP

$$y''(x) + p(x)y'(x) + q(x)y(x) = g(x), \quad y(0) = \alpha,\ y'(0) = \beta,\ x \geq 0, \tag{1.2}$$

can be rewritten as the VIE of the second kind

$$u(x) = f(x) + \int_0^x k(x,t)u(t)dt, \quad x \geq 0, \tag{1.3}$$

in which the kernel $k(x,t)$ is given by

$$k(x,t) = -p(x) + q(x)(t-x)$$

and the free term $f(x)$ is given by

$$f(x) = g(x) - [\beta p(x) + \alpha q(x) + \beta x q(x)].$$

Also, the second-order BVP

$$y''(x) + p(x)y'(x) + q(x)y(x) = g(x), \quad y(0) = \alpha,\ y(1) = \beta, \tag{1.4}$$

can be rewritten as the FIE of the second kind

$$u(x) = f(x) + \int_0^1 k(x,t)u(t)dt, \quad 0 \le x \le 1, \tag{1.5}$$

in which the kernel $k(x,t)$ is given by

$$k(x,t) = \begin{cases} -(p(x) + (x-1)q(x))t, & 0 \le t \le x, \\ \\ (p(x) + xq(x))(1-t), & x \le t \le 1. \end{cases}$$

and the free term is given by

$$f(x) = g(x) - \alpha q(x) - (\beta - \alpha)[p(x) + xq(x).$$

The details of the conversion from the IVP (1.2) to the VIE (1.3) (see Appendix A.1) and the BVP (1.4) to the FIE (1.5) (see Appendix A.2).

1.2 Basic concepts of operator theory and the Fredholm Alternative theorem

1.2.1 Bounded and compact operators

Definition 1.1 (Linear operator). Let T be an operator from a normed space $\mathcal{X}$ to a normed space $\mathcal{Y}$. T is called a *linear operator* if

$$T(\alpha x + \beta y) = \alpha T(x) + \beta T(y), \quad \text{for all } x, y \in \mathcal{X} \text{ and } \alpha, \beta \in \mathbb{C}(or\ \mathbb{R}).$$

For a linear operator T, we usually write $T(x)$ as Tx.

Definition 1.2 (Bounded operator). A linear operator $T : \mathcal{X} \to \mathcal{Y}$, where $\mathcal{X}$ and $\mathcal{Y}$ are normed spaces, is called *bounded* if there is a real number $M > 0$ such that

$$\|Tx\|_{\mathcal{Y}} \le M\|x\|_{\mathcal{X}}, \quad \text{for all } x \in \mathcal{X}. \tag{1.6}$$

The smallest possible value of M that satisfy the inequality (1.6) is called the *norm* of the linear operator T and it is denoted by $\|T\|$, i.e.,

$$\|T\| := \sup\{\|Tx\|_{\mathcal{Y}} : \ x \in \mathcal{X}, \ \|x\|_{\mathcal{X}} \leq 1\}.$$

We denote the set of all bounded linear operators from a normed space $\mathcal{X}$ to a normed space $\mathcal{Y}$ by $\mathcal{B}(\mathcal{X}, \mathcal{Y})$. That is,

$$\mathcal{B}(\mathcal{X}, \mathcal{Y}) = \{T : \mathcal{X} \to \mathcal{Y} : T \text{ is linear and bounded}\},$$

and in the case that $\mathcal{X} = \mathcal{Y}$ we denote it simply by $\mathcal{B}(\mathcal{X})$.

Compact operators are very important in applications. For example, they play a central role in the theory of IEs and in various problems of mathematical physics. Before presenting the concept of compact operators, we first recall that a set $\mathcal{U}$ in a normed space $\mathcal{X}$ is called compact if each sequence in $\mathcal{U}$ has a convergent subsequence. A set is called relatively compact if its closure is compact.

Definition 1.3 (Compact operator). [7] Let $\mathcal{X}$ and $\mathcal{Y}$ be normed vector spaces, and let $T : \mathcal{X} \to \mathcal{Y}$ be linear. Then T is *compact* if the set $\{Tx : x \in \mathcal{X}, \|x\|_{\mathcal{X}} \leq 1\}$ has compact closure in $\mathcal{Y}$. This is equivalent to saying that for every bounded sequence $\{x_n\} \subset \mathcal{X}$, the sequence $\{Tx_n\}$ has a subsequence that is convergent to some point in $\mathcal{Y}$.

Definition 1.4. We use the notation $\mathcal{B}_c(\mathcal{X}, \mathcal{Y})$ for the set of all compact linear operators from a normed space $\mathcal{X}$ to a normed space $\mathcal{Y}$. If $T \in \mathcal{B}_c(\mathcal{X}, \mathcal{Y})$ then T is bounded.

The following theorem states conditions under which the limit of a sequence of compact linear operators is compact.

Theorem 1.1 (Sequence of compact operators). *Let $\{T_n\}$ be a sequence of compact linear operators from a normed space $\mathcal{X}$ into a* Banach *space $\mathcal{Y}$. If $\{T_n\}$ is uniformly convergent to an operator T, say,*

$$\lim_{n\to\infty} \|T_n - T\| \to 0.$$

Then the operator T is compact.

Proof. See [51, p. 408]. □

Definition 1.5 (Adjoint and self-adjoint operators). Let $\mathcal{X}$ and $\mathcal{Y}$ be (real or complex) Hilbert spaces with inner products denoted by $(\cdot, \cdot)$.

(i) If $T \in \mathcal{B}(\mathcal{X}, \mathcal{Y})$, the operator $T^* \in \mathcal{B}(\mathcal{Y}, \mathcal{X})$ is said to be the *adjoint* of T if it satisfies

$$(Tx, y) = (x, T^*y), \ \text{ for all } x \in \mathcal{X} \text{ and } y \in \mathcal{Y};$$

(ii) $T \in \mathcal{B}(\mathcal{X})$ is called *self-adjoint* (or Hermitian) if $T^* = T$, i.e., if

$$(Tx, y) = (x, Ty), \ \text{ for all } x, y \in \mathcal{X}.$$

If $\mathcal{X}$ is a real Hilbert space, such an operator is often called *symmetric*.

Theorem 1.2. *If $\mathcal{X}$ and $\mathcal{Y}$ are Hilbert spaces and $T \in \mathcal{B}_c(\mathcal{X}, \mathcal{Y})$ is compact, then the adjoint operator $T^* \in \mathcal{B}_c(\mathcal{Y}, \mathcal{X})$ is also compact.*

Proof. See [49, Theorem 4.10]. □

1.2.2 Compact integral operators

We consider here two classes of compact integral operators on continuous and square-integrable function spaces, that play an important role in studying numerical methods for IEs in Chapters 2 and 4.

Let $\mathcal{X}$ be a Banach space, usually $\mathcal{X} = \mathcal{C}(D)$ or $\mathcal{X} = L^2(D)$ with norm $\|\cdot\|_\infty$ or $\|\cdot\|_{L^2}$, respectively. Consider the linear integral operator $\mathcal{K}$ defined on $\mathcal{X}$ by the formula

$$(\mathcal{K}u)(x) = \int_D k(x,t)u(t)dt, \quad x \in D, \tag{1.7}$$

where the integration domain D is an often compact subset of $\mathbb{R}^n$ for some $n \geq 1$, and the function $k(x,t)$ is called the kernel of the integral operator $\mathcal{K}$. To prove that $\mathcal{K}$ is compact, one needs conditions on the kernel $k(x,t)$ that make $\mathcal{K}$ compact. To this end, we have the following lemma and theorem.

Lemma 1. *(i) If $k \in L^2(D \times D)$, then the corresponding integral operator $\mathcal{K}$ given in (1.7) is a compact operator in $\mathcal{B}_c(L^2(D))$.*

(ii) If D is compact and $k \in \mathcal{C}(D \times D)$, then the corresponding integral operator $\mathcal{K}$ given in (1.7) is a compact operator in $\mathcal{B}_c(\mathcal{C}(D))$.

Proof. See [40, p. 168]. □

A more general criterion in the case of $\mathcal{X} = \mathcal{C}(D)$ is the following.

Theorem 1.3. *Let $k(x,t)$ is Riemann integrable as a function of t, for all $t \in D$. If the following assumptions hold:*

$$A_1.\ \lim_{h\to 0} w(h) = 0, \qquad w(h) \equiv \max_{\substack{x,y\in D \\ |x-y|\leq h}} \int_D |k(x,t) - k(y,t)|dt,$$

$$A_2.\ \max_{x\in D} \int_D |k(x,t)|dt < \infty.$$

Then the integral operator defined by (1.7) is a compact operator in $\mathcal{B}_c(\mathcal{C}(D))$.

Proof. To prove this theorem, we first recall the Arzelà–Ascoli theorem which states that a set $\mathcal{S}$ is relatively compact in $\mathcal{C}(D)$ if and only if $\mathcal{S}$ is uniformly bounded and equicontinuous ([22, Theorem A.43]).

Using A_1, if the function u is bounded and integrable, then $\mathcal{K}u$ is continuous with

$$|\mathcal{K}u(x) - \mathcal{K}u(y)| \leq w(|x-y|)\|u\|_\infty, \tag{1.8}$$

and using A_2, then $\mathcal{K}$ is bounded with

$$\|\mathcal{K}\| = \max_{x\in D} \int_D |k(x,t)|dt.$$

To show that $\mathcal{K}$ is compact, it suffices to show that the set

$$\mathcal{S} = \{\mathcal{K}u : u \in \mathcal{C}(D) \text{ and } \|u\|_\infty \leq 1\}$$

is a relatively compact in $\mathcal{C}(D)$", i.e., the closure of this set is compact in $\mathcal{C}(D)$, which is equivalent to show that $\mathcal{S}$ is uniformly bounded and equicontinuous. For any $u \in \mathcal{C}(D)$, we have

$$\|\mathcal{K}u\|_\infty = \max_{x\in D} |\int_D k(x,t)u(t)dt| \leq \max_{x\in D} \int_D |k(x,t)u(t)|dt,$$

and using A_2, we obtain that

$$\|\mathcal{K}u\|_\infty \leq \|\mathcal{K}\|\|u\|_\infty,$$

hence for all function u such that $\|u\|_\infty \leq 1$ it holds

$$\|\mathcal{K}u\|_\infty \leq \|\mathcal{K}\|.$$

Then, $\mathcal{S}$ is uniformly bounded. In addition, $\mathcal{S}$ is equicontinuous form (1.8). Thus, by Arzela-Ascoli theorem, $\mathcal{S}$ is a relatively compact set in $\mathcal{C}(D)$, i.e., the closure of this set is compact in $\mathcal{C}(D)$, then $\mathcal{K} \in \mathcal{B}_c(\mathcal{C}(D))$ is compact.

□

1.2.3 The Fredholm Alternative theorem

The following theorems quoted from [7, p. 13] and [22, p. 500], respectively.

Theorem 1.4 (Fredholm Alternative). *Let $\mathcal{X}$ be a Banach space, and let $\mathcal{K} \in \mathcal{B}_c(\mathcal{X})$ be compact. Then the equation $(\lambda - \mathcal{K})x = y$, $\lambda \neq 0$, has a unique solution $x \in \mathcal{X}$ if and only if the homogeneous equation $(\lambda - \mathcal{K})z = 0$ has only the trivial solution $z = 0$. In such a case, the operator $(\lambda - \mathcal{K}) : \mathcal{X} \xrightarrow[onto]{1-1} \mathcal{X}$ has a bounded inverse $(\lambda - \mathcal{K})^{-1}$.*

Let $\mathcal{X}$ be a Hilbert space, with inner product and norm $(\cdot,\cdot)$ and $\|\cdot\|$, respectively. Consider the linear operator equation and its adjoint operator equation

$$(\mathcal{I} - \mathcal{K})u = f \quad (a); \qquad (\mathcal{I} - \mathcal{K}^*)v = g \quad (b)$$

and the corresponding homogeneous equations

$$(\mathcal{I} - \mathcal{K})u = 0 \quad (c); \qquad (\mathcal{I} - \mathcal{K}^*)v = 0 \quad (d)$$

respectively, where $\mathcal{I}$ is the identity operator and $\mathcal{K}^*$ is the adjoint operator of $\mathcal{K} \in \mathcal{B}_c(\mathcal{X})$.

Also, the following theorem called the *Fredholm Alternative*.

Theorem 1.5. *If $\mathcal{K} \in \mathcal{B}_c(\mathcal{X})$ is compact, then the following statements hold:*

(i) *Equation* (a) *is uniquely solvable for an arbitrarily given* $f \in \mathcal{X}$ *if and only if equation* (b) *is so for an arbitrarily given* $g \in \mathcal{X}$.

(ii) *Equation* (a) *(or equation* (b)*) is uniquely solvable for an arbitrarily given* $f \in \mathcal{X}$ *(or* $g \in \mathcal{X}$*) if and only if the corresponding homogeneous equation* (c) *(or equation* (d)*) has only a zero solution.*

(iii) *In the case that equation* (c) *only has a zero solution, the inverse operator* $(\mathcal{I} - \mathcal{K})^{-1}$ *exists on the entire space* $\mathcal{X}$ *and is bounded, i.e.,* $(\mathcal{I} - \mathcal{K})^{-1} \in \mathcal{B}(\mathcal{X})$*, so that the solution* $u \in \mathcal{X}$ *of equation* (a) *satisfies*

$$\|u\| \leq C\|f\|,$$

for a constant $C > 0$*, independent of* $f \in \mathcal{X}$.

For more information on the Fredholm Alternative see e.g., Kress [49, Chapter 3].

Chapter 2

Numerical methods for integral equations

This chapter provides a concise overview of numerical methods and their convergence analysis for solving IEs, for example, the projection methods, including Galerkin method based on the orthogonal projection and the collocation method based on an interpolatory projection, and the quadrature or Nyström method. For more details on these methods, we refer to [7, 8, 6, 50, 49, 35, 70].

2.1 Projection methods

In this section, we describe the projection methods to solve approximately the following operator equation of the second kind

$$u - \mathcal{K}u = f, \tag{2.1}$$

where $\mathcal{K}$ is an integral operator defined on a Banach space $\mathcal{X}$. Before describing these methods, we first introduce the concept of projection operator in the following subsection.

2.1.1 Projection operator

Definition 2.1. Let $\mathcal{X}$ be a normed space and $\mathcal{V} \subset \mathcal{X}$ a nontrivial subspace. A bounded linear operator $\mathcal{P} : \mathcal{X} \to \mathcal{V}$ is called a *projection operator* or a simply *projection* from $\mathcal{X}$ onto $\mathcal{V}$ if for all $x \in \mathcal{V}$ we have

$$\mathcal{P}x = x.$$

The element $\mathcal{P}x$ is called the projection of x onto $\mathcal{V}$.

Theorem 2.1. *Let $\mathcal{P} \in \mathcal{B}(\mathcal{X})$ be a bounded operator, where $\mathcal{X}$ be a normed space. Then $\mathcal{P}$ is a projection operator on $\mathcal{X}$ if and only if $\mathcal{P} = \mathcal{P}^2$. Moreover, in this case, if $\mathcal{P} \neq 0$ then $\|\mathcal{P}\| \geq 1$.*

Proof. Let $\mathcal{P} : \mathcal{X} \to \mathcal{V}$ be a projection. Then for all $x \in \mathcal{X}$ we have

$$\mathcal{P}^2 x = \mathcal{P}(\mathcal{P}x) = \mathcal{P}x,$$

Conversely, let $\mathcal{P}^2 = \mathcal{P}$ and set $\mathcal{V} := \mathcal{P}(\mathcal{X})$. Then for all $v \in \mathcal{V}$ we may write $v = \mathcal{P}x$ for some $x \in \mathcal{X}$ and obtain

$$\mathcal{P}v = \mathcal{P}^2 x = \mathcal{P}x = v.$$

Finally, it follows from the equation $\mathcal{P} = \mathcal{P}^2$ that

$$\|\mathcal{P}\|^2 \geq \|\mathcal{P}^2\| = \|\mathcal{P}\|,$$

which imply that $\|\mathcal{P}\| \geq 1$ when $\mathcal{P} \neq 0$. □

2.1.2 Collocation and Galerkin methods

For introducing these methods, let $\mathcal{X}$ be a Banach space and consider the linear integral operator $\mathcal{K}$ defined on $\mathcal{X}$ by the formula

$$(\mathcal{K}u)(x) = \int_D k(x,t)u(t)dt. \tag{2.2}$$

From (2.2) and (2.1), it follows that

$$u(x) - \int_D k(x,t)u(t)dt = f(x), \tag{2.3}$$

To solve the equation (2.3) numerically, we choose a sequence of finite dimensional subspaces $\mathcal{X}_n \subset \mathcal{X}, n \geq 1$, with $\mathcal{X}_n$ having dimension N_n. If $\{\phi_j : j = 1, \ldots, N_n\}$ is a basis of $\mathcal{X}_n$, then we seek a function $u_n \in \mathcal{X}_n$ so that it can be written as

$$u_n(x) = \sum_{j=1}^{N_n} c_j \phi_j(x). \tag{2.4}$$

Since $u_n(x)$ in general will not solve (2.3) exactly, we consider the function $r_n(x)$ given by

$$\begin{aligned} r_n(x) &= u_n(x) - \int_D k(x,t)u_n(t)dt - f(x) \\ &= \sum_{j=1}^{N_n} c_j[\phi_j(x) - \int_D k(x,t)\phi_j(x)] - f(x). \end{aligned} \tag{2.5}$$

where $r_n(x)$ is called the *residual* in the approximation of the equation when using $u \approx u_n$. Symbolically, we write (2.3) as

$$(\mathcal{I} - \mathcal{K})u = f, \tag{2.6}$$

and also the quantity (2.5) as

$$r_n = (\mathcal{I} - \mathcal{K})u_n - f. \tag{2.7}$$

The unknown coefficients $c_j, j = 1, \ldots, N_n$ are chosen by forcing $r_n(x)$ to be approximately zero in some sense. The hope is that the resulting function $u_n(x)$ will be a good approximation of the exact solution $u(x)$. How this is done depends on the method used. We will

review some of the principal strategies for making r_n small, as presented in the following methods

• Collocation method

For the collocation scheme, the most common choice for $\mathcal{X}$ is $\mathcal{C}(D)$. The idea behind this method is to make the residual $r_n(x)$ small by forcing $r_n(x)$ to be zero at the collocation points $x_j, j = 1, \ldots, N_n$, that is,

$$r_n(x_i) = 0, \quad i = 1, \ldots, N_n, \tag{2.8}$$

or equivalently,

$$u_n(x_i) - (\mathcal{K}u_n)(x_i) = f(x_i).$$

This yields the linear equations

$$\sum_{j=1}^{N_n} c_j \left[\phi_j(x_i) - (\mathcal{K}\phi_j)(x_i)\right] = f(x_i), \quad i = 1, \ldots, N_n. \tag{2.9}$$

Let us denote

$$\mathbf{E}_n = \left[\phi_j(x_i) : i, j = 1, \ldots, N_n\right], \quad \mathbf{K}_n = \left[(\mathcal{K}\phi_j)(x_i) : i, j = 1, \ldots, N_n\right],$$

and

$$\mathbf{c}_n = \left[c_j : j = 1, \ldots, N_n\right], \quad \mathbf{f}_n = \left[f(x_j) : j = 1, \ldots, N_n\right].$$

Then, (2.9) can be written in the matrix-vector form

$$(\mathbf{E}_n - \mathbf{K}_n)\mathbf{c}_n = \mathbf{f}_n. \tag{2.10}$$

If this linear system have a unique solution, then the unknown vector $\mathbf{c}_n$ can be determined and the approximation $u_n(x)$ is well defined.

• Galerkin's method

For the Galerkin scheme, the standard choice for $\mathcal{X}$ is $L^2(D)$ or another Hilbert space, with inner product denoted by $(\cdot, \cdot)$. The Galerkin method is based on the principle of making the residual r_n "small" by requiring that

$$(r_n, \phi_i) = 0, \quad i = 0, \ldots, N_n, \tag{2.11}$$

this is equivalent to

$$(u_n, \phi_i) - (\mathcal{K}u_n, \phi_i) = (f, \phi_i).$$

This yields the linear equations

$$\sum_{j=1}^{N_n} c_j \left[(\phi_j, \phi_i) - (\mathcal{K}\phi_j, \phi_i)\right] = (f, \phi_i), \quad i = 1, \ldots, N_n. \tag{2.12}$$

Let us denote

$$\mathbf{E}_n = \left[(\phi_j, \phi_i) : i, j = 1, \ldots, N_n\right], \quad \mathbf{K}_n = \left[(\mathcal{K}\phi_j, \phi_i) : i, j = 1, \ldots, N_n\right],$$

and

$$\mathbf{c}_n = \left[c_j : j = 1, \ldots, N_n\right], \quad \mathbf{f}_n = \left[(f, \phi_j) : j = 1, \ldots, N_n\right].$$

Then, (2.12) can be written in the matrix-vector form

$$(\mathbf{E}_n - \mathbf{K}_n)\mathbf{c}_n = \mathbf{f}_n. \tag{2.13}$$

If this linear system have a unique solution, then the unknown vector $\mathbf{c}_n$ can be determined and the approximation $u_n(x)$ is well defined.

According to [7, pp. 52–54], (2.8) and (2.11) may be written as

$$\mathcal{P}_n r_n = 0,$$

is equivalent to

$$\mathcal{P}_n(\mathcal{I} - \mathcal{K})u_n = \mathcal{P}_n f, \quad u_n \in \mathcal{X}_n. \tag{2.14}$$

where $\mathcal{P}_n$ is a projection onto $\mathcal{X}_n$. Since $\mathcal{P}_n u_n = u_n$, the above equation can be written as follows:

$$(\mathcal{I} - \mathcal{P}_n\mathcal{K})u_n = \mathcal{P}_n f. \tag{2.15}$$

We may consider this as the defining equation for the Galerkin and collocation methods, with the appropriate choice of $\mathcal{P}_n$. In the Galerkin method, $\mathcal{P}_n$ is the orthogonal projection from $\mathcal{X} := L^2(D)$ to $\mathcal{X}_n$, defined by

$$(\mathcal{P}_n u, \phi) = (u, \phi), \quad \text{for all } u \in \mathcal{X} \text{ and } \phi \in \mathcal{X}_n$$

while for the collocation method, $\mathcal{P}_n$ is the interpolatory projection from $\mathcal{X} := \mathcal{C}(D)$ to $\mathcal{X}_n$, defined for $u \in \mathcal{X}$ by

$$\mathcal{P}_n u(x_i) = u(x_i), \quad \text{for all } i \in \{1, \ldots, N_n\},$$

where $\{x_i\}_{i=0}^{N_n}$ is a set of distinct nodes in D.

2.1.3 Theoretical aspects of projection methods

The following results for projection methods quoted from [7, pp. 55-58].

Lemma 2 ([7]). *Let $\mathcal{X}$ be a Banach space, and let $\{\mathcal{P}_n\}$ be a family of bounded projections on $\mathcal{X}$ with*

$$\mathcal{P}_n u \to u \quad \text{as } n \to \infty, \text{ for all } u \in \mathcal{X}.$$

Let $\mathcal{K} \in \mathcal{B}_c(\mathcal{X})$ be compact. Then,

$$\|\mathcal{K} - \mathcal{P}_n\mathcal{K}\| \to 0 \quad \text{as } n \to \infty.$$

Theorem 2.2. *Assume $\mathcal{K} : \mathcal{X} \to \mathcal{X}$ is bounded, with $\mathcal{X}$ be a Banach space, and $(\mathcal{I} - \mathcal{K}) : \mathcal{X} \to \mathcal{X}$ is one-to-one and onto. Further if*

$$\|\mathcal{K} - \mathcal{P}_n\mathcal{K}\| \to 0 \quad \text{as } n \to \infty,$$

then for all sufficiently large n, say $n \geq n_0$, the operator $(\mathcal{I} - \mathcal{P}_n\mathcal{K})^{-1}$ exists as a bounded operator from $\mathcal{X}$ to $\mathcal{X}$. Also, it is uniformly bounded:

$$\sup_{n \geq n_0} \|(\mathcal{I} - \mathcal{P}_n\mathcal{K})^{-1}\| < \infty.$$

Proof. See [7]. □

Theorem 2.3. *For all solutions u_n and u to (2.15) and (2.6), respectively, one can obtain that*

$$\frac{1}{\|\mathcal{I} - \mathcal{P}_n\mathcal{K}\|}\|u - \mathcal{P}_n u\| \leq \|u - u_n\| \leq \|(\mathcal{I} - \mathcal{P}_n\mathcal{K})^{-1}\|\|u - \mathcal{P}_n u\|.$$

Proof. See [7]. □

Theorem 2.3 shows that u_n converges to u if and only if $\mathcal{P}u_n$ converges to u. Further, if convergence does occur, then $\|u - u_n\|$ and $\|u - \mathcal{P}_n u\|$ tend to zero with exactly the same speed.

According to the above lemma and theorems, we can conclude if equation (2.1) is uniquely solvable for all $f \in \mathcal{X}$, then the equation (2.15) is uniquely solvable for all sufficiently large n, say $n \geq n_0$, and the inverse operators $(\mathcal{I} - \mathcal{P}_n\mathcal{K})^{-1}$ exists and are uniformly bounded for $n \geq n_0$.

2.1.4 Condition numbers

In the context of approximate methods, we need to introduce the concept of the *condition number* of a linear operator, which is used to indicate how sensitive the solution of an equation may be to small relative changes in the input data. A problem is called *well-conditioned* if the perturbation of the input error is not much larger than "1". While if the error is strongly increased, the problem is called *ill-conditioned*.

Definition 2.2. Let $T \in \mathcal{B}(\mathcal{X}, \mathcal{Y})$ be a bounded operator from a Banach space $\mathcal{Y}$ into a Banach space $\mathcal{Y}$ with bounded inverse $T^{-1} \in \mathcal{B}(\mathcal{Y}, \mathcal{X})$. The quantity

$$cond(T) = \|T\|\|T^{-1}\|$$

is called the *condition number* of T, denoted by $\kappa := cond(T)$.

Clearly, the inequality $\kappa := cond(T) \geq 1$ is always satisfied, as demonstrated below

$$\|T\|\|T^{-1}\| \geq \|TT^{-1}\| = \|\mathcal{I}\| = 1.$$

Theorem 2.4. *If* $\det(\boldsymbol{E}_n) \neq 0$ *and denoting by* $\boldsymbol{A}_n = \boldsymbol{E}_n - \boldsymbol{K}_n$ *the matrix of the system of equations* (2.10) *then the condition number of the linear system* (2.10) *of the collocation method satisfies*

$$\kappa := cond(\boldsymbol{A}_n) \leq \|\mathcal{P}_n\|_\infty^2 \, cond(\boldsymbol{E}_n) \, cond(\mathcal{I} - \mathcal{P}_n\mathcal{K}).$$

Proof. See [7, pp. 90–92] or [22]. □

Corollary 2.1. *If* $\phi_j = h_j$ *is the j-th Lagrange interpolation polynomial associated with distinct nodes* $\{x_j, j = 1, \ldots, N\}$ *in* D*, then the condition number of the linear system* (2.10) *of the collocation method satisfies*

$$\kappa := cond(\boldsymbol{A}_n) \leq \|\mathcal{P}_n\|_\infty^2 \, cond(\mathcal{I} - \mathcal{P}_n\mathcal{K}),$$

where

$$\|\mathcal{P}_n\|_\infty := \max_{x \in D} \sum_{j=1}^{N_n} |h_j(x)|.$$

Theorem 2.5. *Denoting by* $\boldsymbol{A}_n = \boldsymbol{E}_n - \boldsymbol{K}_n$ *the matrix of the system of equations* (2.13) *then the condition number of the linear system* (2.13) *for the Galerkin method has the bound*

$$\kappa := cond(\boldsymbol{A}_n) \leq cond(\boldsymbol{E}_n) \, cond(\mathcal{I} - \mathcal{P}_n\mathcal{K}).$$

Proof. See [7, pp. 96–97] or [22]. □

Corollary 2.2. *If* $(\phi_i, \phi_j) = \delta_{i,j}, i, j = 1, \ldots, N_n$*, then the condition number of the linear system* (2.13) *for the Galerkin method has the bound*

$$\kappa := cond(\boldsymbol{A}_n) \leq cond(\mathcal{I} - \mathcal{P}_n\mathcal{K}).$$

2.2 Quadrature methods

In this section we introduce the quadrature (Nyström) method for solving IEs of the second kind with continuous kernel. This method discretizes the IE by directly replacing the integral appearing in the IE by numerical quadratures.

2.2.1 Numerical quadratures

Let $\Omega := [a, b] \subset \mathbb{R}$ be a bounded interval and $g \in \mathcal{C}(\Omega)$. To approximate the integral

$$Q(g) := \int_a^b g(t)dt, \tag{2.16}$$

we consider numerical quadrature rules of the form

$$Q_n(g) := \sum_{j=1}^{n} \omega_j^{(n)} g(t_j^{(n)}), \tag{2.17}$$

where $t_j^{(n)}, j = 1, \ldots, n$ are quadrature nodes (distinct) and $\omega_j^{(n)} j = 1, \ldots, n$ are real quadrature weights.

Remark 2.1. It is easily seen that Q and Q_n defined in (2.16) and (2.17) respectively, are linear functionals from $\mathcal{C}(\Omega)$ to $\mathbb{R}$. The norm of Q_n is defined with

$$\|Q_n\| = \sup_{\|g\|=1} |Q_n(g)| = \sum_{j=1}^{n} |\omega_j^{(n)}|,$$

plays an important role in the convergence of $Q_n(g)$ to $Q(g)$ for all continuous functions.

There are many well-known numerical methods for computing a definite integral, such as the trapezoidal rule, Simpson's rule, and Gaussian quadrature, the latter of which is generally the most accurate. In the following, we quote some examples of quadrature rules from [47, pp. 481–497].

Example 2.1. Consider the trapezoidal quadrature rule

$$\begin{aligned} T_h(g) := Q_n(g) &= h\left[\frac{1}{2}g(t_0^{(n)}) + g(t_1^{(n)}) + \cdots + g(t_{n-1}^{(n)}) + \frac{1}{2}g(t_n^{(n)})\right], \\ &= \sum_{j=0}^{n} \omega_{j,T}^{(n)} g(t_j^{(n)}), \end{aligned} \tag{2.18}$$

for the integral $Q(g)$, where $h := (b-a)/n$, $t_j^{(n)} = a + jh$, $j = 0, \ldots, n$ and

$$\omega_{j,T}^{(n)} = \begin{cases} \frac{h}{2}, & j = 0, n, \\ \\ h, & \text{otherwis.} \end{cases} \tag{2.19}$$

When $g \in \mathcal{C}^2(\Omega)$, the error of the trapezoidal rule has the estimate [47, p. 481]

$$|Q(g) - T_h(g)| \leq \frac{b-a}{12} h^2 \|g^{(2)}\|_\infty.$$

Example 2.2. Consider the Simpson quadrature rule

$$\begin{aligned} S_h(g) := Q_n(g) &= \frac{h}{3}\left[g(t_0^{(n)}) + 4g(t_1^{(n)}) + 2g(t_2^{(n)}) + \cdots + 2g(t_{n-2}^{(n)}) + 4g(t_{n-1}^{(n)}) + g(t_n^{(n)})\right], \\ &= \sum_{j=0}^{n} \omega_{j,S}^{(n)} g(t_j^{(n)}), \end{aligned} \tag{2.20}$$

for the integral $Q(g)$, where $h := (b-a)/n$ (n is even), $t_j^{(n)} = a + jh$, $j = 0, \ldots, n$ and

$$\omega_{j,S}^{(n)} = \begin{cases} \frac{h}{3}, & j = 0, n, \\ \frac{2h}{3}, & j = 2, 4, \ldots, n-2, \\ \frac{4h}{3}, & \text{otherwis.} \end{cases} \tag{2.21}$$

When $g \in \mathcal{C}^4(\Omega)$, the error of the Simpson's rule has the estimate [47, p. 483]

$$|Q(g) - S_h(g)| \leq \frac{b-a}{180} h^4 \|g^{(4)}\|_\infty.$$

This example illustrates that, as the step size h tends to zero, the error associated with Simpson's rule diminishes more rapidly than that of the trapezoidal rule. This implies that the Nyström method using the Simpson's rule has a faster convergence than the trapezoidal rule.

Example 2.3. Let $\{\phi_j : 1 \leq j \leq n\}$ be a set of orthogonal polynomials of degree $\leq n$ on Ω with respect to a non-negative weight function w. Consider the Gaussian quadrature rule

$$G_n(g) := Q_n(g) = \sum_{j=1}^{n} \omega_j^{(n)} g(t_j^{(n)}),$$

for the integral $Q(g)$, where the points $t_j^{(n)}$ are the zeros of the function ϕ_n and

$$w_j^{(n)} := \int_a^b w(t) \prod_{\substack{i=1 \\ i \neq j}}^{n} \frac{t - t_i^{(n)}}{t_j^{(n)} - t_i^{(n)}} dt, \quad j = 1, \ldots, n.$$

When $g \in \mathcal{C}^{2n}(\Omega)$, the error of the Gaussian quadrature rule has the estimate [47, p. 497]

$$Q(g) - G_n(g) = \frac{g^{(2n)}(\xi)}{(2n)!} \int_a^b q_n^2(t) w(t) dt, \tag{2.22}$$

where $\xi \in (a, b)$ and q_n is the polynomial

$$q_n(t) = \prod_{i=1}^{n} (t - t_i^{(n)}).$$

Remark 2.2. If $\Omega := [-1, 1]$, $w(x) = 1$ and $\{\phi_j(x) := P_j(x) : 1 \leq j \leq n\}$ is chosen to be the set of LPs see Chapter 3, then the error term (2.22) is given by [76, p. 105] or [32]

$$Q(g) - G_n(g) = \frac{2^{2n+1}(n!)^4}{(2n+1)!((2n)!)^3} g^{(2n)}(\xi), \quad -1 < \xi < 1.$$

This example demonstrates that the Nyström method, when combined with the Gaussian quadrature formula, achieves rapid convergence.

Definition 2.3. A sequence (Q_n) of quadrature rules is called convergent if

$$Q_n(g) \to Q(g) \text{ as } n \to \infty, \text{ for all } g \in \mathcal{C}(\Omega),$$

i.e., if the sequence (Q_n) converges pointwise[1] to the functional Q on $\mathcal{C}(\Omega)$.

The following theorem guarantees the convergence of many common quadrature formula, and in particular of the trapezoidal rule, Simpson's rule and Gaussian quadrature rules.

Theorem 2.6 ([50], Theorem 12.4)**.** *The quadrature rules (Q_n) converges if and only if*

$$Q_n(g) \to Q(g) \text{ as } n \to \infty, \text{ for all } g \text{ in some dense subset}^2\ \mathcal{U} \subset \mathcal{C}(\Omega) \text{ and}$$

$$\sup_{n\in\mathbb{N}} \sum_{j=1}^{n} |\omega_j^{(n)}| < \infty.$$

2.2.2 Nyström's method

The quadrature (Nyström) method is among the simplest numerical methods for solving IEs. It was originally introduced to handle approximations based on the numerical integration of the integral operator in IEs. To describe this method, we consider the linear functional equation of the form

$$u(x) - \mathcal{K}u(x) = f(x), \tag{2.23}$$

where the operator $\mathcal{K}$ is given by

$$(\mathcal{K}u)(x) := \int_a^b k(x,t)u(t)dt, \quad x \in \Omega, \tag{2.24}$$

with a continuous kernel $k \in \mathcal{C}(\Omega \times \Omega)$. To solve the equation (2.23) numerically, we consider a sequence (Q_n) of numerical quadrature rules for the integral operator (2.24). This integral operator is approximated by a sequence of numerical integration operators defined by

$$(\mathcal{K}_n u)(x) = \sum_{j=1}^{n} \omega_j^{(n)} k(x, t_j^{(n)}) u(t_j^{(n)}), \quad x \in \Omega, \tag{2.25}$$

where $t_j^{(n)}$ in Ω are quadrature nodes and $\omega_j^{(n)}$ are real quadrature weights of a quadrature rule $Q_n(g)$ with $g = k_x u$, where $k_x(\cdot) = k(x, \cdot)$. The most natural way of approximating the solution of (2.23) is to replace the integral (2.24) by a numerical quadrature given in (2.25), it follows that

$$u(x) - \sum_{j=1}^{n} \omega_j^{(n)} k(x, t_j^{(n)}) u(t_j^{(n)}) \simeq f(x),$$

[1] A sequence (Q_n) of functions defined on $\mathcal{C}(\Omega)$ is said to be converge pointwise to a functional Q on $\mathcal{C}(\Omega)$ if, for every $g \in \mathcal{C}(\Omega)$ and very $\varepsilon > 0$, there exists $N \in \mathbb{N}$ such that for all $n \geq N$ we have $|Q_n(g) - Q(g)| < \varepsilon$.

[2] A subset W of a normed vector space V is said to be dense in V if for each $v \in V$ and each $\epsilon > 0$ there exists an element $w \in W$ such that $\|v - w\| \leq \epsilon$.

If $u_n(x)$ is defined as the solution to

$$u_n(x) - \sum_{j=1}^{n} \omega_j^{(n)} k(x, t_j^{(n)}) u_n(t_j^{(n)}) = f(x) \tag{2.26}$$

then evaluating $u_n(x)$ at $x = x_i^{(n)}, i = 1, \ldots, n$, gives the following set of algebraic equations for $u_i^{(n)} := \{u_n(t_i^{(n)})\}_{i=1}^n$:

$$u_i^{(n)} - \sum_{j=1}^{n} \omega_j^{(n)} k(x_i^{(n)}, t_j^{(n)}) u_j^{(n)} = f(x_i^{(n)}), \quad i = 1, \ldots, n. \tag{2.27}$$

If the above linear system has a unique solution, then the solution reads as

$$u_n(x) := \sum_{j=1}^{n} \omega_j^{(n)} k(x, t_j^{(n)}) u_j^{(n)} + f(x), \quad x \in \Omega.$$

Equation (2.23) can be rewritten as

$$u - \mathcal{K}u = f, \tag{2.28}$$

and also the numerical IE (2.26) as

$$u_n - \mathcal{K}_n u_n = f. \tag{2.29}$$

We summarize the above discussion in the following theorem.

Theorem 2.7 (Nyström's method). *For the solution u_n of (2.26), let $u_j^{(n)} := u(t_j^{(n)})$ and $k_{ij}^{(n)} := k(x_i^{(n)}, t_j^{(n)})$, $j = 1, \ldots, n$ for $n \in \mathbb{N}$. Then $[u_1^{(n)}, \ldots, u_n^{(n)}]^T$ satisfies the following linear system*

$$\begin{bmatrix} 1 - \omega_1^{(n)} k_{11}^{(n)} & -\omega_2^{(n)} k_{12}^{(n)} & \cdots & -\omega_n^{(n)} k_{1n}^{(n)} \\ -\omega_1^{(n)} k_{21}^{(n)} & 1 - \omega_2^{(n)} k_{22}^{(n)} & \cdots & -\omega_n^{(n)} k_{2n}^{(n)} \\ \vdots & \vdots & \ddots & \vdots \\ -\omega_1^{(n)} k_{n1}^{(n)} & -\omega_2^{(n)} k_{n2}^{(n)} & \ldots & 1 - \omega_n^{(n)} k_{nn}^{(n)} \end{bmatrix} \begin{bmatrix} u_1^{(n)} \\ u_2^{(n)} \\ \vdots \\ u_n^{(n)} \end{bmatrix} = \begin{bmatrix} f(x_1^{(n)}) \\ f(x_2^{(n)}) \\ \vdots \\ f(x_n^{(n)}) \end{bmatrix}. \tag{2.30}$$

Conversely, if $[u_1^{(n)}, \ldots, u_n^{(n)}]^T$ is a solution of (2.30), then the function u_n defined by

$$u_n(x) := f(x) + \sum_{j=1}^{n} \omega_j^{(n)} k(x, t_j^{(n)}) u_j^{(n)}, \quad x \in \Omega \tag{2.31}$$

solves equation (2.26).

Proof. The first statement is trivial. Next, if $[u_1^{(n)}, \ldots, u_n^{(n)}]^T$ is a solution of (2.30), then we have from (2.31) and (2.30) that

$$u(x_i^{(n)}) = f(x_i^{(n)}) + \sum_{j=1}^{n} \omega_j^{(n)} k(x_i^{(n)}, t_j^{(n)}) u_j^{(n)} = u_i^{(n)}, \quad i = 1, \ldots, n. \tag{2.32}$$

From (2.31) and the above equation, we find that u_n satisfies (2.26). □

The error estimate for the Nyström method is quite straightforward using the results given in [50, 22]. Recall that the error analyses of projection methods depended on showing $\|\mathcal{K} - \mathcal{K}_n\|$ converges to zero as n increases, with $\mathcal{K}_n = \mathcal{P}_n\mathcal{K}$ the approximation to the integral operator $\mathcal{K}$. This cannot be done here; in fact,

$$\|\mathcal{K} - \mathcal{K}_n\| \geq \|\mathcal{K}\|.$$

To see this, for any small positive constant ϵ we can choose a function $\varphi_\epsilon \in \mathcal{X} = \mathcal{C}(\Omega)$ such that $\|\varphi_\epsilon\|_\infty = 1$, $\varphi_\epsilon(x) = 1$ for all $x \in \Omega$ with $\min_{j\in\{1,\dots,n\}} |x - x_j| \geq \epsilon$ and $\varphi_\epsilon(x_j) = 0$ for all $j \in \{1, \dots, n\}$. For this choice of φ_ϵ, we have that

$$\begin{aligned}
\|\mathcal{K} - \mathcal{K}_n\| = \sup_{u\in\mathcal{X},\|u\|_\infty\leq 1} \|(\mathcal{K} - \mathcal{K}_n)u\|_\infty &\geq \sup_{u\in\mathcal{X},\|u\|_\infty\leq 1} \sup_{\epsilon>0} \|(\mathcal{K} - \mathcal{K}_n)(u\varphi_\epsilon)\|_\infty \\
&= \sup_{u\in\mathcal{X},\|u\|_\infty\leq 1} \sup_{\epsilon>0} \|\mathcal{K}(u\varphi_\epsilon)\|_\infty \\
&= \sup_{u\in\mathcal{X},\|u\|_\infty\leq 1} \|\mathcal{K}u\|_\infty = \|\mathcal{K}\|.
\end{aligned}$$

Theorem 2.8 ([22]). *If the sequence of quadrature rules is convergent, then the sequence $\{\mathcal{K}_n\}$ of quadrature operators is collectively compact and pointwise convergent on $\mathcal{C}(\Omega)$. Moreover, if u and u_n are the solution of equations (2.23) and the Nyström method, respectively, then there exist a positive constant c and a positive integer N such that for all $n \geq N$,*

$$\|u - u_n\|_\infty \leq c\|(\mathcal{K}_n - \mathcal{K})u\|_\infty.$$

Theorem 2.8 indicates that the error $\|u - u_n\|_\infty$ converges to zero in the same order as the numerical integration error

$$\|(\mathcal{K}_n - \mathcal{K})u\|_\infty = \max_{x\in\Omega} \left| \sum_{j=1}^{n} \omega_j^{(n)} k(x, t_j^{(n)}) u(t_j^{(n)}) - \int_\Omega k(x,t)u(t)dt \right|. \tag{2.33}$$

Implementation

In order to obtain the approximate solution of (2.23), one needs to employ a quadrature rule to approximate the integral in (2.24). The straightforward application of the repeated trapezoidal rule (2.18) or the repeated Simpson's rule (2.20) to the integral in (2.24) takes the form

$$(\mathcal{K}_n u(x) = \sum_{j=0}^{n} w_j^{(n)} K(x, t_j^{(n)}) u(t_j^{(n)}), \quad x \in \Omega, \tag{2.34}$$

where $w_j^{(n)} = w_{j,T}^{(n)}$ or $w_{j,S}^{(n)}$ are given by (2.19) and (2.21), respectively. This gives the following approximating equation

$$u_n(x) - \sum_{j=0}^{n} w_j^{(n)} k(x, t_j^{(n)}) u_n(t_j^{(n)}) = f(x). \tag{2.35}$$

Substituting $x_i = t_i^{(n)}, i = 0, 1, \ldots, n$ in (2.35), we get

$$u_i^{(n)} - \sum_{j=0}^{n} w_j^{(n)} k(t_i^{(n)}, t_j^{(n)}) u_j^{(n)} = f(t_i^{(n)}), \quad i = 0, 1, \ldots, n,$$

where $u_i^{(n)}$ is the approximate value of the exact solution at the points $t_i^{(n)}$. The Nyström interpolation formula is given by

$$u_n(x) = \sum_{j=0}^{n} \omega_j^{(n)} k(x, t_j^{(n)}) u_j^{(n)} + f(x), \quad x \in \Omega.$$

From (2.33), the numerical integration error for the trapezoidal rule is

$$\|(\mathcal{K}_n - \mathcal{K})u\|_\infty \leq \frac{b-a}{12} h^2 \max_{x,t\in\Omega} \left| \frac{\partial^2}{\partial t^2} k(x,t)u(t) \right|, \tag{2.36}$$

under the assumption $u \in \mathcal{C}^2(\Omega)$ and $k(x,t) \in \mathcal{C}^2(\Omega \times \Omega)$. Similarly, for the Simpson's rule is

$$\|(\mathcal{K}_n - \mathcal{K})u\|_\infty \leq \frac{b-a}{180} h^4 \max_{x,t\in\Omega} \left| \frac{\partial^4}{\partial t^4} k(x,t)u(t) \right|, \tag{2.37}$$

under the assumption $u \in \mathcal{C}^4(\Omega)$ and $k(x,t) \in \mathcal{C}^4(\Omega \times \Omega)$. From (2.36) (or (2.37)), we see the Nyström method using the trapezoidal rule (or the Simpson's rule) converges with an order of $\mathcal{O}(h^2)$ (or $\mathcal{O}(h^4)$). This shows that, as the step size h tends to zero, the error for Simpson's rule converges to zero faster than the error for the trapezoidal rule.

Numerical test

Consider the following IE

$$u(x) - \frac{1}{5} \int_0^1 e^{xt} u(t) dt = f(x), \quad x \in \Omega := [0, 1], \tag{2.38}$$

where $f(x)$ is chosen so that the exact solution is $u(x) = e^{-x}\cos(x)$. Table 2.1 shows the absolute error between the approximate and exact solutions at the some selected points on Ω. In this table, $|u(x) - u^{\mathrm{T}}(x)|$ and $|u(x) - u^{\mathrm{S}}(x)|$ denote the absolute errors of the Nyström method using Trapezoidal and Simpson's rules for $n = 4$, respectively.

TABLE 2.1: Numerical results for Eq. (2.38)

x	$\lvert u(x) - u^{\mathrm{T}}(x)\rvert$	$\lvert u(x) - u^{\mathrm{S}}(x)\rvert$
0	4.59e−04	1.04e−05
0.25	9.95e−05	8.02e−06
0.5	2.69e−04	4.45e−06
0.75	6.44e−04	5.56e−07
1	1.01e−03	2.61e−06

Chapter 3

Generalities about spectral approximation

Spectral approximations including Legendre, Chebyshev and Gegenbaure approximations, which are special cases of Jacobi approximations, have gained tremendous success in a variety of applications, such as root-finding algorithms, Gaussian quadrature rules and spectral methods for differential, integral and integro-differential equations (see, e.g., [57, 91, 20, 89, 18, 32, 14, 90, 78, 23, 93, 48, 46, 77, 80, 38, 92, 69] and the references therein). One of the most significant advantages of these approximations is that their convergence behavior depends solely on the smoothness properties of the functions involved and fast convergence can be achieved if the functions to be approximated are sufficiently smooth. These approximations have certain limitations; for example, they are not efficient in approximating problems that exhibit localized rapid variations, steep gradients, or a steep front. To address this, we develop in this chapter an adaptive approach which has the advantage of accelerating convergence even when the functions to be approximated exhibit such complex behaviors.

3.1 Standard spectral approximation

In spectral methods for non-periodic problems, the approximation is based on the expansion of a function in terms of an infinite sequence of orthogonal trial functions, which is given by

$$u(x) = \sum_{n=0}^{\infty} \widehat{u}_n \phi_n(x), \tag{3.1}$$

where $u(x)$ is the function to approximate and $\{\widehat{u}_n\}$ represents the spectral coefficients associated with a set of polynomials $\phi_n(x)$. The set $\{\phi_n(x)\}$ is orthogonal with respect to a positive weight function $w(x)$ on the interval J, if the following equality holds

$$(\phi_n, \phi_m)_w = \int_a^b \phi_n(x)\phi_m(x)w(x)dx = \gamma_n \delta_{n,m}, \tag{3.2}$$

where $\gamma_n = (\phi_n, \phi_m)_w$ and $\delta_{n,m}$ is the Kronecker delta function. The integral of (3.2) represents the weighted inner product of the functions ϕ_n and ϕ_m. In case the weighted inner

product of a function with itself is taken the square of the norm is given by

$$\|u\|^2_{L^2_w} = (\phi_n, \phi_m)_w = \int_a^b u^2(x)w(x)dx, \tag{3.3}$$

where the weighted space $L^2_w(J)$ defined by

$$L^2_w(J) := \{u : u \text{ is measurabe and } \|u\|_{L^2_w} < \infty\}. \tag{3.4}$$

3.1.1 Orthogonal projection and discussion of convergence

Definition 3.1. Let $\mathcal{V} \subset \mathcal{X}$ be a subset of a normed space $\mathcal{X}$. An element $\phi^* \in \mathcal{V}$ is called a *best approximation* to an arbitrary element $u \in \mathcal{X}$ if it minimizes the distance to u among all elements of $\mathcal{V}$; that is

$$\|u - \phi^*\|_{\mathcal{X}} = \inf_{\phi \in \mathcal{V}} \|u - \phi\|_{\mathcal{X}}.$$

i.e., $\phi^* \in \mathcal{V}$ has smallest distance from u.

Lemma 3 ([78]). *For any $u \in L^2_w(J)$ and $N \in \mathbb{N}$, there exists a unique $q^*_N \in \mathbb{P}_N$, such that*

$$\|u - q^*_N\|_{L^2_w} = \inf_{q_N \in \mathbb{P}_N} \|u - q_N\|_{L^2_w},$$

where $\mathbb{P}_N$ denotes the space of polynomials of degree at most N,

$$q^*_N(x) = \sum_{n=0}^{N} \widehat{u}_n \phi_n(x), \quad \widehat{u}_n = \frac{(u, \phi_n)_w}{\|\phi_n\|^2_w},$$

and $\{\phi_n\}_{n=0}^N$ forms an L^2_w-orthogonal basis of $\mathbb{P}_N$.

In particular, we denote the *best approximation polynomial* q^*_N by $\mathcal{P}_N u$, which represents the L^2_w-orthogonal projection of u and is characterized by the following orthogonality conditions

$$(u - \mathcal{P}_N u, p)_w = 0, \quad \forall p \in \mathbb{P}_N, \tag{3.5}$$

where

$$\mathcal{P}_N u(x) = \sum_{n=0}^{N} \widehat{u}_n \phi_n(x), \qquad \widehat{u}_n = \frac{(u, \phi_n)_w}{\|\phi_n\|^2_w}. \tag{3.6}$$

with the truncated error

$$u - \mathcal{P}_N u = \sum_{n=N+1}^{\infty} \widehat{u}_n \phi_n.$$

It is not difficult to show that $\mathcal{P}_N u$ is the orthogonal projection of u onto $\mathbb{P}_N$ under the inner product defined in $L^2_w(J)$. To do this, we first have form (3.5) that

$$(u - \mathcal{P}_N u, p_m)_w = \sum_{n=N+1}^{\infty} \widehat{u}_n (\phi_n, p_m)_w.$$

Since the polynomials ϕ_n, $(0 \leq n \leq N)$ form a basis for $\mathbb{P}_N$, any polynomial $p \in \mathbb{P}_N$ can be expanded with respect to this basis. Eq. (3.5) follows noticing that for $m \leq N$,

$$(\phi_n, p_m)_w = 0, \text{ for all } n \geq N+1$$

because of orthogonality property.

The convergence of the orthogonal projection is established in the following theorem.

Theorem 3.1. *For any $u \in L^2_w(J)$, we have*

$$\lim_{N\to\infty} \|u - \mathcal{P}_N u\|_{L^2_w} = 0.$$

Proof. See [32]. □

3.1.2 Jacobi polynomials and Gauss quadrature

An important class of classical orthogonal polynomials (OPs) called the Jacobi polynomials, named after mathematician Carl Gustav Jacob Jacobi, are a two parameter family of ordered complete sets of classical OPs on the standard interval I, orthogonal with respect to the Jacobi weight

$$w^{\alpha,\beta}(y) = (1-y)^\alpha (1+y)^\beta, \ \ \alpha, \beta > -1.$$

It is well known that the Jacobi polynomials (JPs) with basis parameters α and β are typically denoted by $J_n^{\alpha,\beta}(y), n \in \mathbb{N}$, and satisfy the orthogonality condition [39]:

$$\int_{-1}^{1} J_n^{\alpha,\beta}(y) J_m^{\alpha,\beta}(y) w^{\alpha,\beta}(y) dy = \gamma_n^{\alpha,\beta} \delta_{n,m}, \tag{3.7}$$

where $\delta_{n,m}$ is the Kronecker function, and the normalizing constant $\gamma_n^{\alpha,\beta}$ is given by [39]:

$$\gamma_n^{\alpha,\beta} = \frac{2^{\alpha+\beta+1}}{2n+\alpha+\beta+1} \frac{\Gamma(n+\alpha+1)\Gamma(n+\beta+1)}{\Gamma(n+1)\Gamma(n+\alpha+\beta+1)}.$$

Also, they satisfy the following three-term recurrence relation [87, (1.4.3)]:

$$\begin{aligned} &J_0^{\alpha,\beta}(y) = 1, \quad J_1^{\alpha,\beta}(y) = \tfrac{1}{2}(\alpha+\beta+2)y + \tfrac{1}{2}(\alpha-\beta), \\ &J_{n+1}^{\alpha,\beta}(y) = (a_n^{\alpha,\beta} y - b_n^{\alpha,\beta}) J_n^{\alpha,\beta}(y) - c_n^{\alpha,\beta} J_{n-1}^{\alpha,\beta}(y), \quad n \geq 1, \end{aligned} \tag{3.8}$$

where

$$\begin{cases} a_n^{\alpha,\beta} &= \dfrac{(2n+\alpha+\beta+1)(2n+\alpha+\beta+2)}{2(n+1)(n+\alpha+\beta+1)}, \\ b_n^{\alpha,\beta} &= -\dfrac{(\alpha^2-\beta^2)(2n+\alpha+\beta+1)}{2(n+1)(n+\alpha+\beta+1)(2n+\alpha+\beta)}, \\ c_n^{\alpha,\beta} &= \dfrac{(n+\alpha)(n+\beta)(2n+\alpha+\beta+1)}{2(n+1)(n+\alpha+\beta+1)(2n+\alpha+\beta)}. \end{cases}$$

The following important Gauss-Quadrature theorem, which established in [78].

Theorem 3.2 (Gauss Quadrature). *Let $\{x_j\}_{j=0}^N$ be the set of zeros of the orthogonal polynomial p_{N+1}. Then there exists a unique set of quadrature weights $\{\omega_j\}_{j=0}^N$, defined by*

$$\omega_j = \int_a^b h_j(x)w(x)dx$$

where

$$h_j(x) = \prod_{\substack{i=0 \\ i\neq j}}^{N} \frac{x - x_i}{x_j - x_i}, \quad 0 \leq j \leq N, \tag{3.9}$$

is the Lagrange basis polynomials (LBPs) associated with $\{x_j\}_{j=0}^N$, such that

$$\int_a^b p(x)w(x)dx = \sum_{j=0}^{N} p(x_j)\omega_j, \quad \forall p \in \mathbb{P}_{2N+1}.$$

Moreover, the quadrature weights are all positive and are given by

$$\omega_j = \frac{k_{N+1}}{k_N} \frac{\|p_N\|_w^2}{p_N(x_j)p'_{N+1}(x_j)}, \quad 0 \leq j \leq N,$$

where k_j is the leading coefficient of the polynomial p_j.

Lemma 4. *If $x_0, x_1, \ldots, x_N$ are the zeros of the polynomial $p_{N+1}(x)$, then the LBPs (3.9) can be expressed as*

$$h_j(x) = \frac{p_{N+1}(x)}{(x - x_j)p'_{N+1}(x_j)}. \tag{3.10}$$

Proof. Let $p_{N+1}(x)$ be the polynomial of degree $N+1$ having $N+1$ distinct real roots are the interpolation nodes x_j, defined by

$$p_{N+1}(x) \equiv \prod_{j=0}^{N}(x - x_j)$$

which is equivalently

$$p_{N+1}(x) = (x - x_j)q_{N+1}(x), \tag{3.11}$$

where

$$q_{N+1}(x) \equiv \prod_{\substack{i=0 \\ i\neq j}}^{N}(x - x_i).$$

Differentiation of (3.11) gives

$$p'_{N+1}(x) = q_{N+1}(x) + (x - x_j)q'_{N+1}(x),$$

in which setting $x = x_j$ yields

$$p'_{N+1}(x_j) = q_{N+1}(x_j).$$

Assuming

$$h_j(x) = a_j \frac{p_{N+1}(x)}{(x - x_j)},$$

the requirement $h_j(x_j) = 1$ leads, via l'Hôpital's rule to

$$1 = a_j \lim_{x \to x_j} \frac{p_{N+1}(x)}{(x - x_j)} = a_j p'_{N+1}(x_j) = a_j q_{N+1}(x_j).$$

Therefore, for any $j = 0, \ldots, N$ the LBPs defined in (3.9), can also be expressed more succinctly in the following form

$$h_j(x) = \frac{p_{N+1}(x)}{(x - x_j) p'_{N+1}(x_j)}.$$

□

Figure 3.1 illustrates the LBPs $h_j(x)$ for $0 \leq j \leq 3$, defined on the interval $[-1, 1]$,

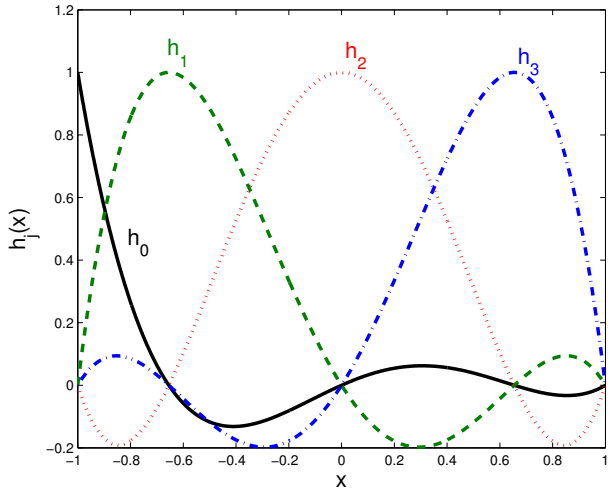

FIGURE 3.1: LBPs $h_j(x)$ with $j = 0, 1, 2, 3$, defined on the interval $[-1, 1]$.

One of the most widely used methods in numerical integration is Jacobi-Gauss quadrature rule. This quadrature rule is of importance in the numerical analysis for the approximate evaluation of integrals, which is demonstrated in [78]:

Lemma 5 (Jacobi-Gauss quadrature). *Let* $\{\sigma_j := \sigma_{N,j}^{\alpha,\beta}\}_{j=0}^{N}$ *be the zeros of* $J_{N+1}^{\alpha,\beta}(y)$*, while the quadrature weights* $\{\omega_{N,j}^{\alpha,\beta}\}_{j=0}^{N}$ *are given by*

$$\omega_{N,j}^{\alpha,\beta} = \frac{\Gamma(N+\alpha+2)\Gamma(N+\beta+2)}{(N+1)!\Gamma(N+\alpha+\beta+2)} \frac{2^{\alpha+\beta+1}}{(1-\sigma_j^2)[\partial_y J_{N+1}^{\alpha,\beta}(\sigma_j)]^2}. \tag{3.12}$$

Then

$$\int_{-1}^{1} p(y) w^{\alpha,\beta}(y) dy = \sum_{j=0}^{N} p(\sigma_j)\, \omega_{N,j}^{\alpha,\beta}, \quad \forall p \in \mathbb{P}_{2N+1}. \tag{3.13}$$

3.1.3 Legendre polynomials

The *Legendre polynomials* (LPs) are important special cases of the JPs obtained by seeting $\alpha = \beta = 0$. They are denoted by $P_n(y) := J_n^{0,0}(y), n \in \mathbb{N}$, from the recurrence relation of the JPs (3.8), we can find that $P_n(y)$ satisfy the three-term recursion [79]:

$$(n+1)P_{n+1}(y) = (2n+1)yP_n(y) - nP_{n-1}(y), \quad n \geq 1,$$

with $P_0(y) = 1$ and $P_1(y) = y$ (In Figure 3.2, the graphs of the LPs $P_n(y)$ for $1 \leq n \leq 4$, are drawn.). They form an $L^2(I)$-orthogonal system on the interval I with respect to the uniform weight function, that is

$$\int_{-1}^{1} P_n(y)P_m(y)dy = \gamma_n \delta_{n,m}, \quad \gamma_n = \frac{2}{2n+1}, \quad n = 0, 1, \cdots. \tag{3.14}$$

For $N \in \mathbb{N}$, let $\{\sigma_{N,j} := \sigma_{N,j}^{0,0}\}_{j=0}^{N}$ be the Legendre-Gauss nodes, and there holds

$$\int_{-1}^{1} \phi(y)dy = \sum_{j=0}^{N} \phi(\sigma_{N,j})\omega_{N,j}, \ \ \forall \phi \in \mathbb{P}_{2N+1}, \tag{3.15}$$

where $\{\omega_{N,j} := \omega_{N,j}^{0,0}\}_{j=0}^{N}$ are the corresponding quadrature weights given by

$$\omega_{N,j} = \frac{2}{(1-\sigma_{N,j}^2)[P'_{N+1}(\sigma_{N,j})]^2}, \quad 0 \leq j \leq N.$$

The discrete inner product for $U, V \in \mathcal{C}(I)$ is define as

$$(U, V)_N = \sum_{j=0}^{N} U(\sigma_{N,j})V(\sigma_{N,j})\omega_{N,j}. \tag{3.16}$$

The Legendre-Gauss interpolation operator $\mathcal{I}_N : \mathcal{C}(I) \to \mathbb{P}_N$, is defined by

$$\mathcal{I}_N U(y) \in \mathbb{P}_N, \text{ such that } \mathcal{I}_N U(\sigma_{N,i}) = U(\sigma_{N,i}), \ i = 0, 1, \ldots, N. \tag{3.17}$$

Moreover, such polynomial is unique and can be written in Lagrange form as

$$\mathcal{I}_N U(y) = \sum_{j=0}^{N} U(\sigma_{N,j})h_j(y),$$

where

$$h_j(y) = \prod_{\substack{i=0 \\ i \neq j}}^{N} \frac{y - \sigma_{N,i}}{\sigma_{N,j} - \sigma_{N,i}}. \tag{3.18}$$

For additional properties of JPs/LPs, see e.g. [19, 86, 4, 27]).

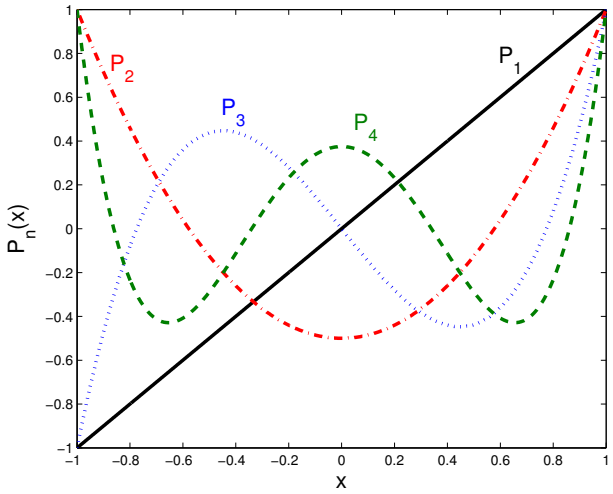

FIGURE 3.2: LPs $P_n(x)$ with $n = 1, 2, 3, 4$ defined on the interval $[-1, 1]$.

3.2 Improved spectral approximation via use of mappings

3.2.1 Mappings for improvement accuracy

Mappings are used most frequently for the treatment of geometries that differ from standard intervals. They can also be used to improve accuracy and reduce computational costs in spectral methods. Before presenting these mappings defined on the standard interval I, we first define the general form of a mapping between the intervals I and J by

$$x = \varphi_{a,b}(\nu; y) := \frac{b+a}{2} + \frac{b-a}{2}\rho(\nu; y), \quad y \in I,\ x \in J,\ \nu \in \mathscr{D}_\nu, \tag{3.19}$$

where ν is a parameter vector, $\mathscr{D}_\nu$ is the feasible domain of ν and $\rho(\nu; y)$ is an appropriate mapping of the standard interval I onto itself with $\rho(\nu; \pm 1) = \pm 1$. Moreover, we assume the following properties hold

$$\frac{dx}{dy} = \varphi'_{a,b}(\nu; y) = \frac{b-a}{2}\rho'(\nu; y) > 0, \quad \nu \in \mathscr{D}_\nu, \tag{3.20}$$

and

$$\varphi_{a,b}(\nu; -1) = a, \quad \varphi_{a,b}(\nu; +1) = b, \quad \nu \in \mathscr{D}_\nu.$$

The mapping (3.19) is explicitly invertible, and denote its inverse mapping by

$$y = \varphi^{-1}_{a,b}(\nu; x) = \rho^{-1}\left(\nu; \frac{2}{b-a}x - \frac{b+a}{b-a}\right) = \psi_{a,b}(\nu; x), \quad x \in J,\ \nu \in \mathscr{D}_\nu. \tag{3.21}$$

In the literature, there are many one-to-one mappings defined on the standard interval I that can be used to describe the above strategy. In this context, we present two valuable

sets of one-to-one mappings, the first one is given by:

$$z = \rho_1(\nu; y) := \frac{\arcsin(\nu y)}{\arcsin(\nu)}, \quad y \in I,\ \nu \in \mathscr{D}_\nu, \tag{3.22}$$

its inverse, consisting of

$$y = \rho_1^{-1}(\nu; z) = \sin(\theta z)/\nu, \quad y, z \in I,\ \nu \in \mathscr{D}_\nu,$$

where $\theta = \arcsin(\nu)$, $\mathscr{D}_\nu$ is the feasible domain of ν defined by $\mathscr{D}_\nu := \{\nu : 0 < \nu < 1\}$, and the second one is given by:

$$z = \rho_2(\nu; y) = \nu_2 + \tan(a_1(y - a_0))/\nu_1, \quad y \in I,\ \nu \in \mathscr{D}_\nu, \tag{3.23}$$

its inverse, consisting of

$$y = \rho_2^{-1}(\nu; z) = a_0 + \arctan(\nu_1(z - \nu_2))/a_1, \quad y, z \in I,\ \nu \in \mathscr{D}_\nu,$$

where the feasible domain of $\nu = (\nu_1, \nu_2)$ is defined by:

$$\mathscr{D}_\nu := \{(\nu_1, \nu_2) :\ \nu_1 > 0,\ -1 \le \nu_2 < 1\},$$

and the values of a_0 and a_1 are chosen to satisfy the condition $\rho_2'(\nu; y) > 0$ for all $y \in I$. In Figures 3.3 and 3.4, we plot the mapping derivatives of $\rho_1(\nu; y)$ and $\rho_2(\nu; y)$ for various values of the mapping parameter ν. Note that, when $\nu \to 0$ the mapping (3.22) reduces to a unity mapping, and also with the mapping (3.23) when $\nu_1 \to 0$.

The major effect of the combination of $\rho_1(\nu; y)$ with the mapping (3.19) is to obtain a more uniform distribution of the grid points in the interval J when $\nu \to 1$ (see Figure 3.5), while the combination of $\rho_2(\nu; y)$ clusters the points near (see Figure 3.7)

$$x = \frac{b + a}{2} + \frac{b - a}{2}\nu_2 \ \text{ for } \nu_1 > 1.$$

3.2.2 Mapped Jacobi polynomials

For $\alpha, \beta > -1$, let $J_n^{\alpha,\beta}(y)$ be the classical JP of degree n defined on the standard interval I, whose properties are summarized in Subsection 3.1.2. According to (3.21), we define the so-called *mapped Jacobi polynomial* (MJP) of degree n on the finite interval J by

$$j_{\nu,n}^{\alpha,\beta}(x) = J_n^{\alpha,\beta}(\psi_{a,b}(\nu; x)), \quad n = 0, 1, \ldots,\ \nu \in \mathscr{D}_\nu, \tag{3.24}$$

and denote its the weight function by

$$w_{J,\nu}^{\alpha,\beta}(x) = w^{\alpha,\beta}(y)\frac{dy}{dx} = w^{\alpha,\beta}(y)(\varphi_{a,b}'(\nu; y))^{-1} > 0, \tag{3.25}$$

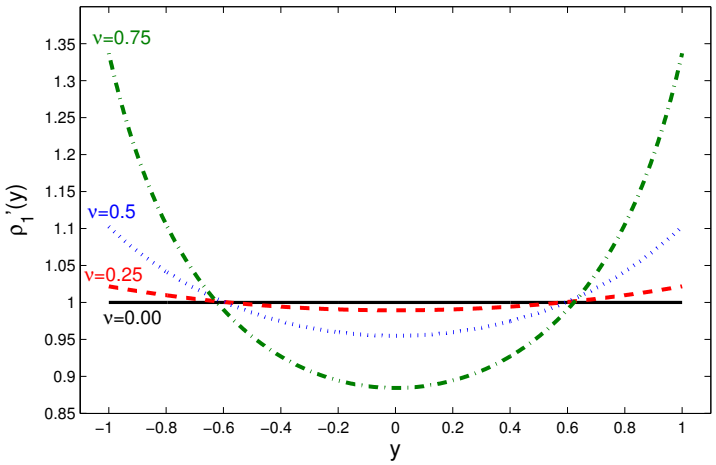

FIGURE 3.3: The mapping derivative of $\rho_1(\nu; y)$ for various values of the mapping parameter ν.

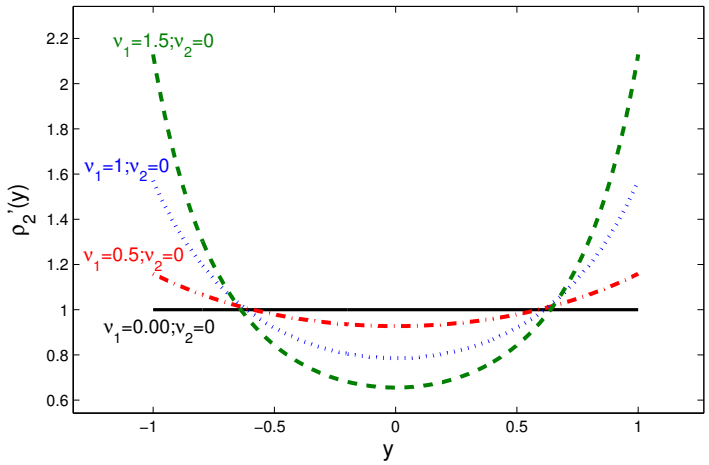

FIGURE 3.4: The mapping derivative of $\rho_2(\nu; y)$ for various values of the mapping parameter ν_1 and fixed $\nu_2 = 0$.

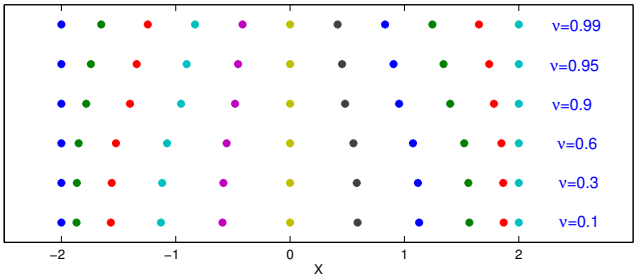

FIGURE 3.5: Illustration of the effect of the combination of $\rho_1(\nu; y)$ with the mapping (3.19) for various values of the mapping parameter ν.

with $w^{\alpha,\beta}(y) = (1-y)^{\alpha}(1+y)^{\beta}$ is the original *Jacobi* weight function. From (3.20) and (3.21), we have

$$\psi'_{a,b}(\nu; x) = \frac{dy}{dx} = \left(\frac{dx}{dy}\right)^{-1} = (\varphi'_{a,b}(\nu; y))^{-1},$$

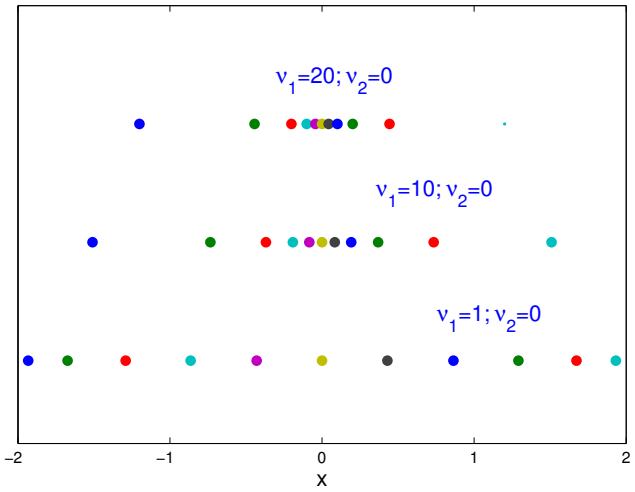

FIGURE 3.6: Illustration of clustering of grid points near $x = 0$ using the combination of $\rho_2(\nu; y)$ with the mapping (3.19) for various values of the mapping parameter ν_1 and fixed $\nu_2 = 0$.

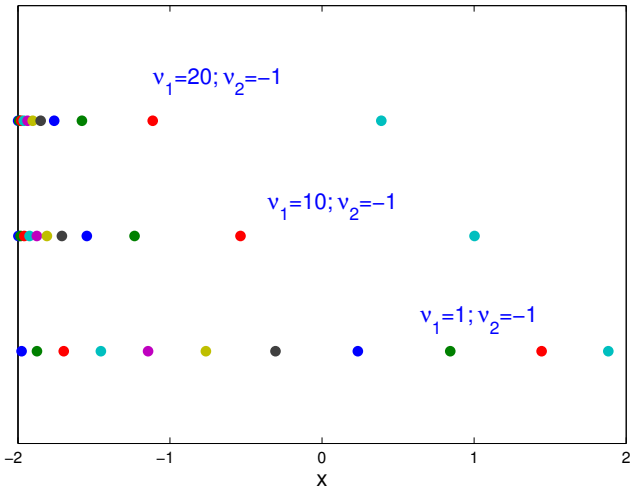

FIGURE 3.7: Illustration of clustering of grid points near $x = -2$ using the combination of $\rho_2(\nu; y)$ with the mapping (3.19) for various values of the mapping parameter ν_1 and fixed $\nu_2 = -1$.

and substituting $y = \psi_{a,b}(\nu; x)$ in (3.25), we obtain that

$$w^{\alpha,\beta}_{J,\nu}(x) = w^{\alpha,\beta}(\psi_{a,b}(x))\psi'_{a,b}(\nu; x).$$

Let us now present important properties of the MJPs.

Lemma 6. *For $\alpha, \beta > -1$, the MJPs $j^{\alpha,\beta}_{\nu,n}(x)$ are orthogonal with respect to the weight function $w^{\alpha,\beta}_{J,\nu}(x)$, i.e.,*

$$\int_a^b j^{\alpha,\beta}_{\nu,n}(x) j^{\alpha,\beta}_{\nu,m}(x) w^{\alpha,\beta}_{J,\nu}(x) dx = \gamma^{\alpha,\beta}_n \delta_{n,m}. \tag{3.26}$$

Proof. Using the substitution $y = \psi_{a,b}(\nu; x)$, we have

$$\int_a^b j_{\nu,n}^{\alpha,\beta}(x) j_{\nu,m}^{\alpha,\beta}(x) w_{J,\nu}^{\alpha,\beta}(x) dx = \int_{-1}^{1} J_n^{\alpha,\beta}(y) J_m^{\alpha,\beta}(y) w^{\alpha,\beta}(y) dy.$$

Then we have the orthogonality (3.26) from (3.7). □

Theorem 3.3. *The MJPs are generated using the following three-term recurrence relation:*

$$\begin{aligned} &j_{\nu,0}^{\alpha,\beta}(x) = 1, \quad j_{\nu,1}^{\alpha,\beta}(x) = (a_0^{\alpha,\beta}\psi_{a,b}(x) - b_0^{\alpha,\beta}), \\ &j_{\nu,n+1}^{\alpha,\beta}(x) = (a_n^{\alpha,\beta}\psi_{a,b}(x) - b_n^{\alpha,\beta}) j_{\nu,n}^{\alpha,\beta}(x) - c_n^{\alpha,\beta} j_{\nu,n-1}^{\alpha,\beta}(x), \quad n \geq 1, \end{aligned} \tag{3.27}$$

where $a_n^{\alpha,\beta}$, $b_n^{\alpha,\beta}$ and $c_n^{\alpha,\beta}$ are as in Equation (3.8).

Proof. The three-term recurrence relation (3.27) is a straightforward result from the corresponding three-term recurrence relation of JPs with the mapping (3.21). □

By using Lemma 5, we introduce the following lemma.

Lemma 7 (Mapped Jacobi-Gauss quadrature)**.** *For $\alpha, \beta > -1$, let $\{\sigma_{N,j}^{\alpha,\beta}, w_{N,j}^{\alpha,\beta}\}_{j=0}^{N}$ be the set of Jacobi-Gauss quadrature nodes and weights. Denoting the set of mapped Jacobi-Gauss quadrature nodes and weights by*

$$\left\{\zeta_{\nu,j}^{\alpha,\beta} := \varphi_{a,b}(\nu; \sigma_{N,j}^{\alpha,\beta}), \quad \omega_{\nu,j}^{\alpha,\beta} := \omega_{N,j}^{\alpha,\beta}\right\}_{j=0}^{N}.$$

Then

$$\int_a^b q(x) w_{J,\nu}^{\alpha,\beta}(x) dx = \sum_{j=0}^{N} q(\zeta_{\nu,j}^{\alpha,\beta})\, \omega_{\nu,j}^{\alpha,\beta}, \quad \forall q \in \mathbb{Q}_{2N+1,\nu},$$

where

$$\mathbb{Q}_{N,\nu} := span\{1, \psi_{a,b}(\nu; x), (\psi_{a,b}(\nu; x))^2, \ldots, (\psi_{a,b}(\nu; x))^N\}.$$

Proof. According to Lemma 5, for any polynomial $p \in \mathbb{P}_{2N+1}$ we have

$$\int_{-1}^{1} p(y) w^{\alpha,\beta}(y) dy = \sum_{j=0}^{N} p(\sigma_{N,j}^{\alpha,\beta})\, \omega_{N,j}^{\alpha,\beta}. \tag{3.28}$$

Since $p = q \circ \varphi \in \mathbb{P}_{2N+1}$ if $q = p \circ \psi \in \mathbb{Q}_{2N+1,\nu}$, we can obtain that from the above Gauss-Jacobi quadrature rule,

$$\begin{aligned} \int_a^b q(x) w_{J,\nu}^{\alpha,\beta}(x) dx. &= \int_{-1}^{1} q(\varphi_{a,b}(\nu; y)) w^{\alpha,\beta}(y) dy \\ &= \sum_{j=0}^{N} q(\varphi_{a,b}(\nu; \sigma_{N,j}^{\alpha,\beta}))\, \omega_{N,j}^{\alpha,\beta} = \sum_{j=0}^{N} q(\zeta_{\nu,j}^{\alpha,\beta})\, \omega_{\nu,j}^{\alpha,\beta}. \end{aligned}$$

□

3.2.3 Mapped Lagrange basis functions

According to (3.21), we define the j-th mapped Lagrange basis function (MLBF) related to the mapped points $\{\zeta_{N,i} := \zeta_{N,i}^{0,0}\}_{i=0}^{N}$ in J as

$$h_j^{(\nu)}(x) := \prod_{\substack{i=0 \\ i\neq j}}^{N} \frac{\psi_{a,b}(\nu;x) - \psi_{a,b}(\nu;\zeta_{\nu,i})}{\psi_{a,b}(\nu;\zeta_{\nu,j}) - \psi_{a,b}(\nu;\zeta_{\nu,i})}, \quad 0 \le j \le N. \tag{3.29}$$

It is clear that the new basis functions (3.29) satisfies the property of the Kronecker delta, $h_j^{(\nu)}(\zeta_{\nu,i}) = \delta_{i,j}$ at $\zeta_{\nu,i}$, which reduces the computational cost. The first four LBPs and MLBFs using the two-parameter mapping (3.23) are illustrated in Figure 3.8.

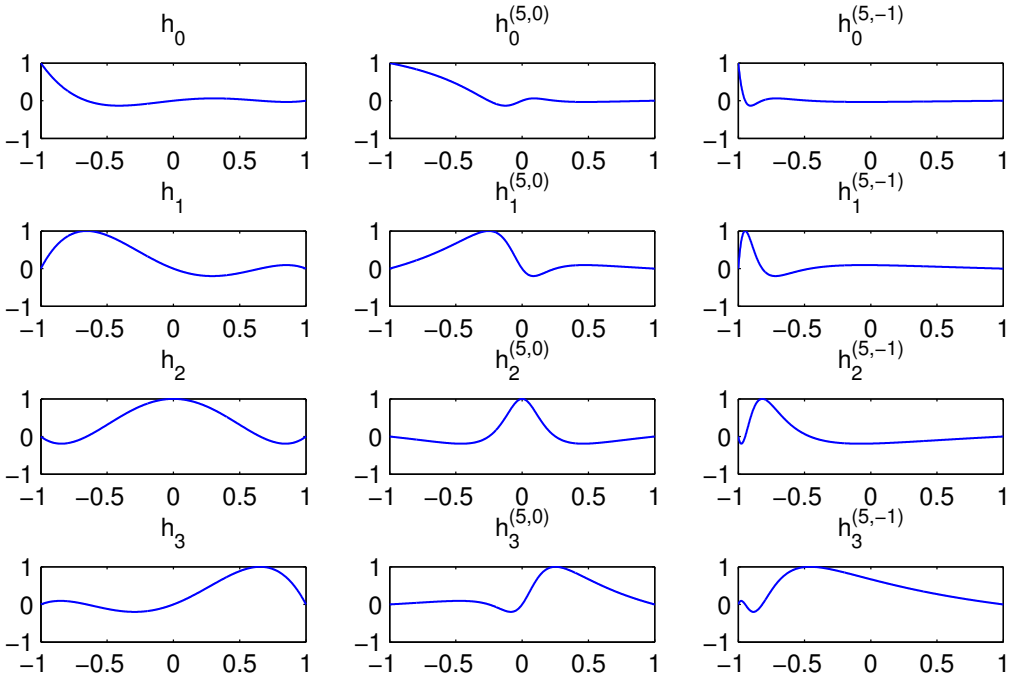

FIGURE 3.8: LBPs h_j and MLBFs $h_j^{(\nu_1,\nu_2)}$ with $j = 0,1,2,3$, defined on the interval $[-1,1]$.

Lemma 8. *If $\zeta_{\nu,0},\zeta_{\nu,1},\ldots,\zeta_{\nu,N}$ are the zeros of the mapped polynomial $\pi_{\nu,N+1}(x)$, then the MLBFs (3.29) can be expressed as*

$$h_j^{(\nu)}(x) = a_j \frac{\pi_{\nu,N+1}(x)}{\psi_{a,b}(\nu;x) - \psi_{a,b}(\nu;\zeta_{\nu,j})}, \qquad \nu \in \mathscr{D}_\nu, \tag{3.30}$$

where

$$a_j = \frac{\psi'_{a,b}(\nu;\zeta_{\nu,j})}{\pi'_{\nu,N+1}(x)|_{x=\zeta_{\nu,j}}}, \quad 0 \le j \le N.$$

Proof. Let the mapped polynomial $\pi_{\nu,N+1}(x)$ whose $N+1$ distinct real roots are the mapped interpolation nodes $\zeta_{\nu,j}$ defined as

$$\pi_{\nu,N+1}(x) = \prod_{j=0}^{N}(\psi_{a,b}(\nu;x) - \psi_{a,b}(\nu;\zeta_{\nu,j})),$$

which is equivalently

$$\pi_{\nu,N+1}(x) = (\psi_{a,b}(\nu;x) - \psi_{a,b}(\nu,\zeta_{\nu,j}))q_{\nu,N+1}(x), \tag{3.31}$$

where

$$q_{\nu,N+1}(x) \equiv \prod_{\substack{i=0\\ i\neq j}}^{N}(\psi_{a,b}(\nu;x) - \psi_{a,b}(\nu;\zeta_{\nu,i})).$$

Differentiation of (3.31) gives

$$\pi'_{\nu,N+1}(x) = \psi'_{a,b}(\nu,x)q_{\nu,N+1}(x) + (\psi_{a,b}(\nu;x) - \psi_{a,b}(\nu;\zeta_{\nu,j}))q'_{N+1}(x),$$

in which setting $x = \zeta_{\nu,j}$ yields

$$\pi'_{\nu,N+1}(x)|_{x=\zeta_{\nu,j}} = \pi'_{\nu,N+1}(\zeta_{\nu,j}) = \psi'_{a,b}(\nu,\zeta_{\nu,j})q_{\nu,N+1}(\zeta_{\nu,j}),$$

where

$$\psi'_{a,b}(\nu;\zeta_{\nu,j}) > 0 \text{ for all } j \in \{0,1,\dots,N\}.$$

Assuming

$$h_j^{(\nu)}(x) = a_j\frac{\pi_{\nu,N+1}(x)}{\psi_{a,b}(\nu;x) - \psi_{a,b}(\nu;\zeta_{\nu,j})},$$

the requirement $h_j^{(\nu)}(\zeta_{\nu,j}) = 1$ leads, via l'Hopital's rule to

$$1 = a_j\lim_{x\to\zeta_{\nu,j}}\frac{\pi_{\nu,N+1}(x)}{\psi_{a,b}(\nu;x) - \psi_{a,b}(\nu;\zeta_{\nu,j})} = a_j\frac{\pi'_{\nu,N+1}(\zeta_{\nu,j})}{\psi'_{a,b}(\nu;\zeta_{\nu,j})} = a_jq_{\nu,N+1}(\zeta_{\nu,j}).$$

Therefore, for any $j = 0,\dots,N$ the MLBFs, defined in (3.29), can also be expressed more succinctly in the following form

$$h_j^{(\nu)}(x) = a_j\frac{\pi_{\nu,N+1}(x)}{\psi_{a,b}(\nu;x) - \psi_{a,b}(\nu;\zeta_{\nu,j})}.$$

□

3.2.4 Mapped Legendre polynomials

The *mapped Legendre polynomials* (MLPs) can be obtained directly by setting $\alpha = \beta = 0$ in the MJPs as follows:

$$L_{J,n}^{(\nu)}(x) = j_{\nu,n}^{0,0}(x), \quad n \in \mathbb{N},\ \nu \in \mathscr{D}_\nu.$$

Also, from the recurrence relation of the MJPs (3.27), we can find that $L_{J,n}^{(\nu)}(x)$ satisfy the three-term recursion

$$L_{J,0}^{(\nu)}(x) = 1, \quad L_{J,1}^{(\nu)}(x) = \psi_{a,b}(x),$$

$$(n+1)L_{J,n+1}^{(\nu)}(x) = (2n+1)\psi_{a,b}(x)L_{J,n}^{(\nu)}(x) - nL_{J,n-1}^{(\nu)}(x), \quad n \geq 1.$$

(In Figure 3.9, the graphs of the LPs P_n and MLPs $L_n^{(\nu)}$, with $n = 1,2,3,4$, defined on the interval $[-1,1]$, are drawn). The set of MLPs is orthogonal on J with respect to the weight function denoted by

$$w_{J,\nu}(x) := \psi'_{a,b}(\nu;x) = \frac{1}{\varphi'_{a,b}(\nu;y)} = \frac{2}{(b-a)\rho'(\nu;y)}, \quad \nu \in \mathscr{D}_\nu. \tag{3.32}$$

According to (3.26), the orthogonality relation for the MLPs therefore changes to

$$\int_a^b L_{J,n}^{(\nu)}(x)L_{J,m}^{(\nu)}(x)w_{J,\nu}(x)dx = \int_{-1}^{1} P_n(y)P_m(y)dy = \gamma_n\delta_{n,m}, \quad \forall n,m \in \mathbb{N},$$

Let us define the weighted space $L^2_{w_{J,\nu}}(J)$ by

$$L^2_{w_{J,\nu}}(J) = \{u : u \text{ is measurable and } \|u\|_{w_{J,\nu}} < \infty\},$$

where

$$\|u\|_{w_{J,\nu}} := \left(\int_a^b |u(x)|^2 w_{J,\nu}(x)dx\right)^{\frac{1}{2}}.$$

Let $u, v : J \to \mathbb{R}$ be two continuous functions. Their inner product is defined by

$$(u,v)_{w_{J,\nu}} := \int_a^b u(x)v(x)w_{J,\nu}(x)dx.$$

For $\nu \in \mathscr{D}_\nu$, let $\mathcal{X}_N^\nu$ denotes the finite-dimensional subspace on J that is spanned by the first $N+1$ MLPs, namely,

$$\mathcal{X}_N^\nu := \text{span}\{L_{J,n}^{(\nu)}(x) \mid x \in J,\ n = 0,1,\ldots,N\}.$$

Applying the mapping (3.19) to the standard Legendre-Gauss quadrature formula (3.15) leads to the mapped Legendre-Gauss quadrature

$$\int_a^b \phi(x)w_{J,\nu}(x)dx = \sum_{j=0}^{N} \phi(\zeta_{N,j}^{(\nu)})\omega_{N,j}^{(\nu)}, \ \forall \phi \in \mathcal{X}_{2N+1}^\nu, \tag{3.33}$$

where

$$\zeta_{N,j}^{(\nu)} = \varphi_{a,b}(\nu;\sigma_{N,j}), \ \ \omega_{N,j}^{(\nu)} = \omega_{N,j}, \ 0 \leq j \leq N.$$

Accordingly, the discrete inner product and the corresponding discrete norm can be defined as follows

$$(u,v)_{w_{J,\nu},N} = \sum_{j=0}^{N} u(\zeta_{N,j}^{(\nu)}) v(\zeta_{N,j}^{(\nu)}) \omega_{N,j}^{(\nu)}, \quad \|u\|_{w_{J,\nu},N} = (u,u)_{w_{J,\nu},N}^{\frac{1}{2}}. \tag{3.34}$$

The mapped Legendre-Gauss interpolation operator $\mathcal{I}_N^\nu : \mathcal{C}(J) \to \mathcal{X}_N^\nu$, is defined by

$$\mathcal{I}_N^\nu u \in \mathcal{X}_N^\nu \text{ such that } (\mathcal{I}_N^\nu u)(\zeta_{N,i}^{(\nu)}) = u(\zeta_{N,i}^{(\nu)}),\ i = 0, 1, \cdots, N.$$

By setting $U_\nu(y) := u(x) = u(\varphi_{a,b}(\nu; y))$, we have

$$\mathcal{I}_N^\nu u(x) = (\mathcal{I}_N U_\nu)(y) = (\mathcal{I}_N U_\nu)(\psi_{a,b}(\nu; x)). \tag{3.35}$$

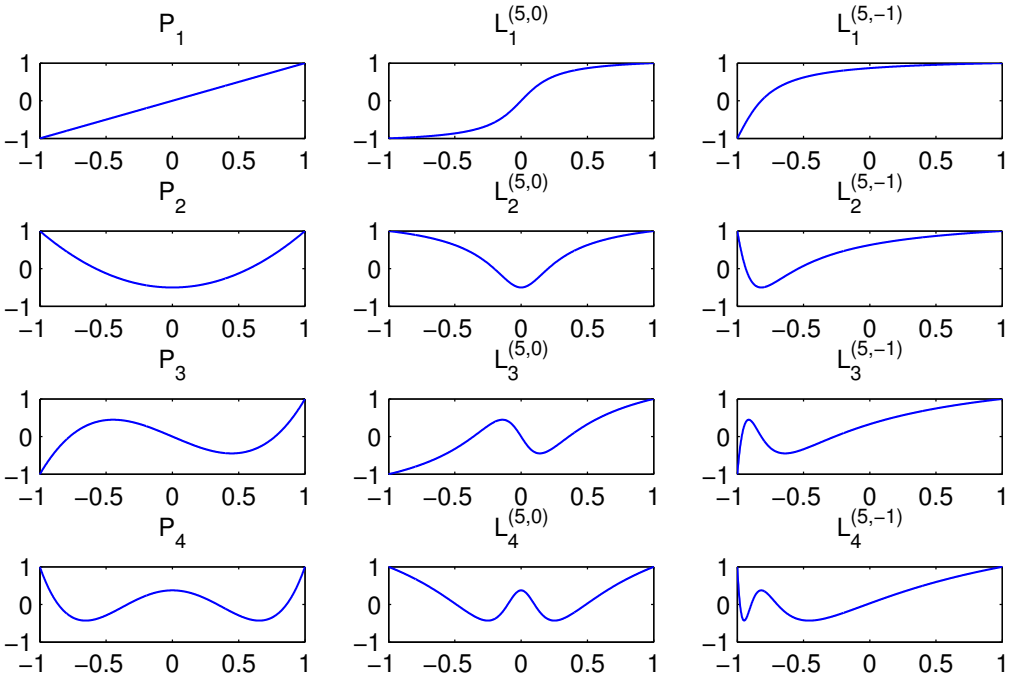

FIGURE 3.9: LPs P_n and MLPs $L_n^{(\nu_1,\nu_2)}$ with $n = 1, 2, 3, 4$, defined on the interval $[-1, 1]$.

3.2.5 Adaptive interpolation and integration errors

In order to estimate the error between u and its interpolant $\mathcal{I}_N^\nu u$, we introduce the following differential operator

$$\partial_y U_\nu = \mu_\nu(x)\frac{du}{dx} =: D_x u, \quad \mu_\nu(x) = \frac{dx}{dy},$$
$$\partial_y^m U_\nu = \mu_\nu(x)\frac{d}{dx}\left(\mu_\nu(x)\frac{du}{dx}\left(\cdots\left(\mu_\nu(x)\frac{du}{dx}\right)\cdots\right)\right) =: D_x^m u, \quad m \geq 1.$$

For $\nu \in \mathscr{D}_\nu$ and a non-negative integer m, define

$$H^m_{w_{J,\nu}}(J) = \{u \mid D_x^r u \in L^2_{w_{J,\nu}}(J),\ 0 \leq r \leq m\},$$

with the following norm

$$\|u\|_{H^m_{w_{J,\nu}}} = \left(\sum_{r=0}^{m} \|D_x^r u\|^2_{L^2_{w_{J,\nu}}}\right)^{\frac{1}{2}},$$

and the seminorm on $H^m_{w_{J,\nu}}(J)$ is defined by

$$|u|_{H^{m;N}_{w_{J,\nu}}} = \left(\sum_{r=\min(m,N+1)}^{m} \|D_x^r u\|^2_{L^2_{w_{J,\nu}}}\right)^{\frac{1}{2}},$$

which implies that if $N \geq m-1$ then $|u|_{H^{m;N}_{w_{J,\nu}}} = \|D_x^m u\|_{L^2_{w_{J,\nu}}}$, In particular, $H^0_{w_{J,\nu}}(J) = L^2_{w_{J,\nu}}(J)$ and

$$\|u\|_{H^0_{w_{J,\nu}}} = \|u\|_{L^2_{w_{J,\nu}}} = \|U_\nu\|_{L^2}. \tag{3.36}$$

The following error estimate is satisfied if $u \in H^m_{w_{J,\nu}}(J)$, for some $m \geq 1$,

$$\|u - \mathcal{I}_N^\nu u\|_{L^2_{w_{J,\nu}}} \leq CN^{-m}|u|_{H^{m;N}_{w_{J,\nu}}}. \tag{3.37}$$

where C is independent of N. To prove this error estimate, we use the estimate (5.4.33) in [19, p. 289], it is mentioned that if $U_\nu \in H^m(I)$ with $m \geq 1$, we have

$$\|U_\nu - \mathcal{I}_N U_\nu\|_{L^2} \leq CN^{-m}|U_\nu|_{H^{m;N}}. \tag{3.38}$$

Also, if $N \geq m-1$, we have $|U_\nu|_{H^{m;N}} = \|\partial_y^m U_\nu\|_{L^2}$, where

$$\|\partial_y^m U_\nu\|_{L^2} = \left(\int_{-1}^{1} |\partial_y^m U_\nu(y)|^2 dy\right)^{1/2} = \left(\int_a^b |D_x^m u(x)|^2 w_{J,\nu}(x)dx\right)^{1/2} = \|D_x^m u\|_{L^2_{w_{J,\nu}}}. \tag{3.39}$$

Then, by (3.38), (3.39) and (3.36), we obtain the desired estimate (3.37). From the inequality (3.37) (or inequality (3.38)), it can be seen that for a sufficiently regular function, the difference between u and its interpolant $\mathcal{I}_N^\nu u$ (or U_ν and its interpolant $\mathcal{I}_N U_\nu$) decays faster than any finite power of $1/N$. It implies that the error decays exponentially.

Moreover, using the interpolation estimate (3.37), it can be proved the following integration error estimate if $u \in H^m_{w_{J,\nu}}(J)$, with $m \geq 1$,

$$\left| \int_a^b u(x) w_{J,\nu}(x) dx - \sum_{j=0}^{N} u(\zeta_{N,j}^{(\nu)}) \omega_{N,j}^{(\nu)} \right| \leq \widetilde{C} N^{-m} |u|_{H^{m;N}_{w_{J,\nu}}}, \tag{3.40}$$

where $\widetilde{C}$ is independent of N. To prove the above estimate for the mapped Legendre Gauss quadrature error, we have

$$\sum_{j=0}^{N} u(\zeta_{N,j}^{(\nu)}) \omega_{N,j}^{(\nu)} = \int_a^b \mathcal{I}_N^\nu u(x) w_{J,\nu}(x) dx, \tag{3.41}$$

and

$$\int_a^b w_{J,\nu}(x) dx = \int_a^b \psi'_{a,b}(x) dx = 2.$$

Applying the Cauchy–Schwarz inequality, we obtain the following result

$$\begin{aligned} \left| \int_a^b u(x) w_{J,\nu}(x) dx - \sum_{j=0}^{N} u(\zeta_{N,j}^{(\nu)}) \omega_{N,j}^{(\nu)} \right| &= \left| \int_a^b u(x) w_{J,\nu}(x) dx - \int_a^b \mathcal{I}_N^\nu u(x) w_{J,\nu}(x) dx \right| \\ &= \left| \int_a^b (u(x) - \mathcal{I}_N^\nu u(x)) w_{J,\nu}(x) dx \right| \\ &\leq \sqrt{2} \| u - \mathcal{I}_N^\nu u \|_{L^2_{w_{J,\nu}}}. \end{aligned}$$

Consequently, combining (3.37) leads to the desired result (3.40).

3.2.6 Numerical experiments

Here, we approximate three functions defined on the interval $[a, b]$,

$$\begin{aligned} f_1(x) &= \cos(kx) e^{-x^2}, \quad x \in J_1 := [-4, 4], \\ f_2(x) &= \exp\left(-\frac{(x-\lambda)^2}{2k^2} \right), \quad x \in J_2 := [0, 10], \\ f_3(x) &= \frac{r}{(x-\lambda)^2 + k^2}, \quad x \in J_3 := [-1, 1], \end{aligned}$$

by $\mathcal{I}_N^\nu f$ for which the computational errors $e_{\nu,N} := \| f - \mathcal{I}_N^\nu f \|_{L^2_{w_{J,\nu}}}$. The first one has the localized rapid region for some k, the second and third functions have the steep gradients near $x = \lambda$ for some k. In Figure 3.10, we show the convergence curves for the adaptive interpolation error of the function $f_1(x)$ obtained by the adaptive interpolation using the combination of $\rho_1(\nu; y)$ with the mapping (3.19) and its standard interpolation. Also, in Figures 3.11 and 3.12 (top), we show the convergence curves for the adaptive interpolation error of the functions $f_2(x)$ and $f_3(x)$ obtained by the adaptive interpolation using the combination of $\rho_2(\nu; y)$ with the mapping (3.19) and its standard interpolation. In addition, Figure 3.12 (bottom) illustrates the adaptive integration error for $f_3(x)$. The advantage of the presented adaptive interpolation is that only a small number at the adaptive

data points gives satisfactory numerical results, rather than using the standard interpolation which required a large number at the data points of the shifted Legendre-Gauss nodes. The adaptive interpolation approaches the standard interpolation, if the parameter mapping $\nu \to 0$.

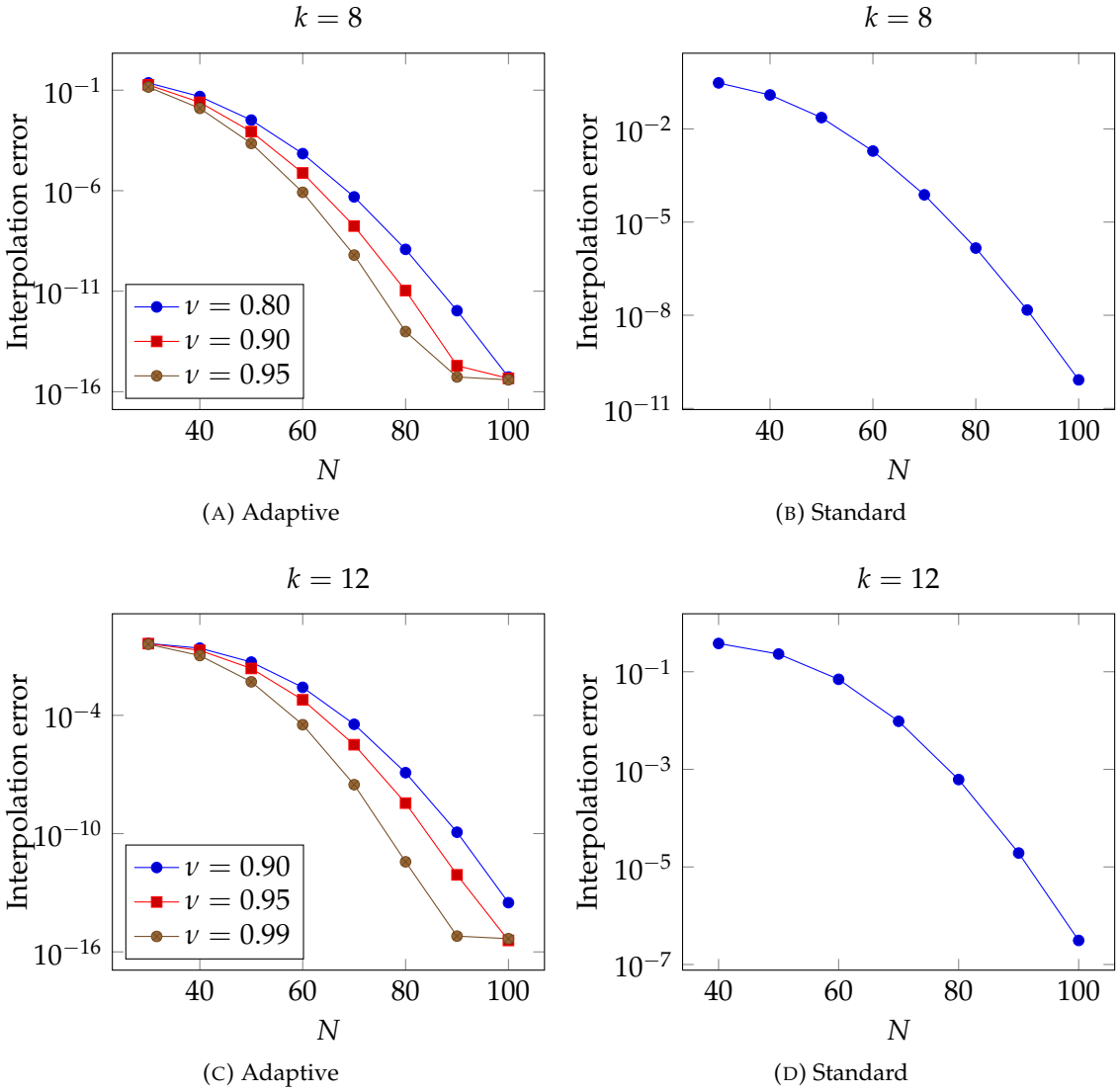

(A) Adaptive

(B) Standard

(C) Adaptive

(D) Standard

FIGURE 3.10: Behavior of the interpolation error for the function $f_1(x) = \cos(kx)e^{-x^2}$ defined on the interval J_1.

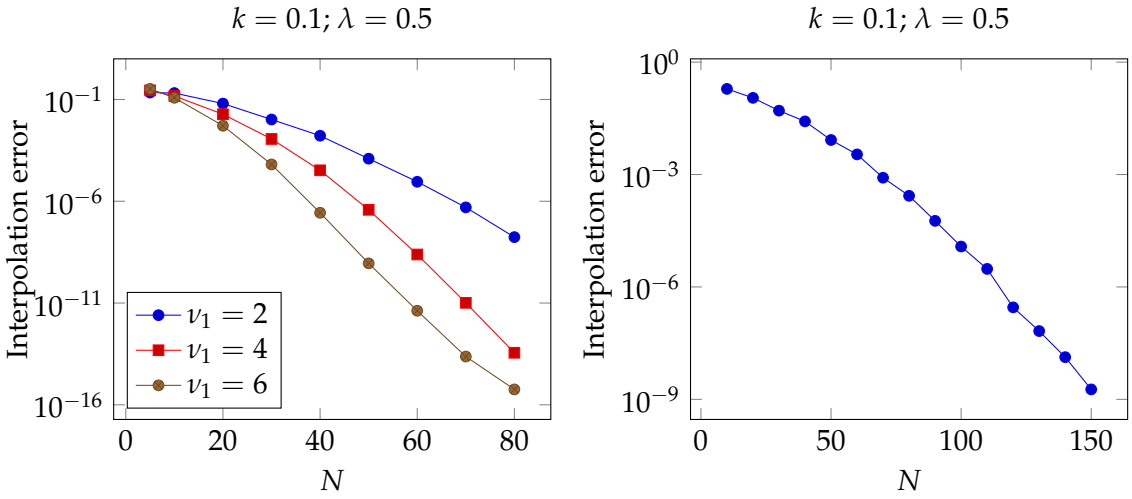

(A) Adaptive, with various ν_1 and fixed $\nu_2 = -0.9$

(B) Standard

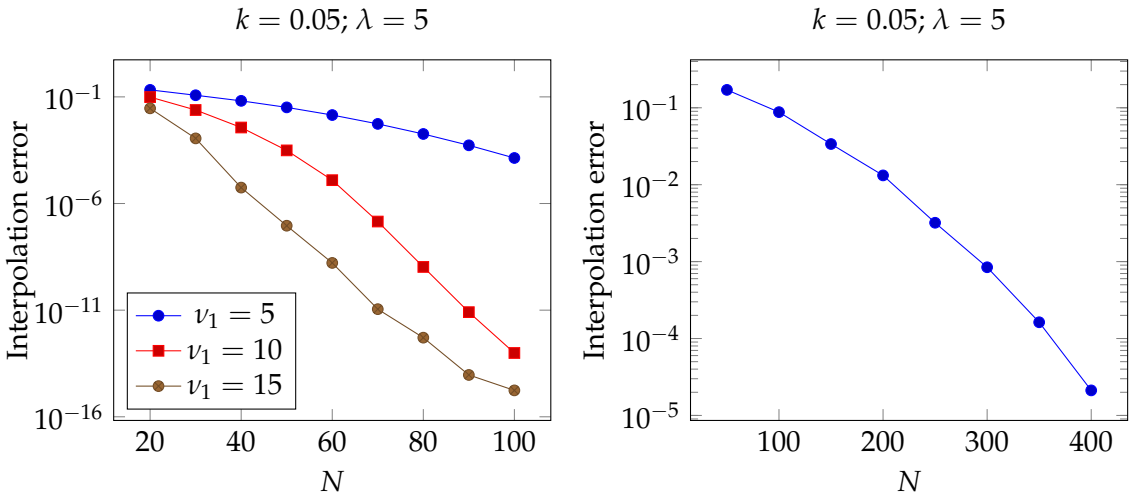

(C) Adaptive, with various ν_1 and fixed $\nu_2 = 0$

(D) Standard

FIGURE 3.11: Behavior of the interpolation error for the function $f_2(x) = e^{-(x-\lambda)^2/2k^2}$ defined on the interval J_2.

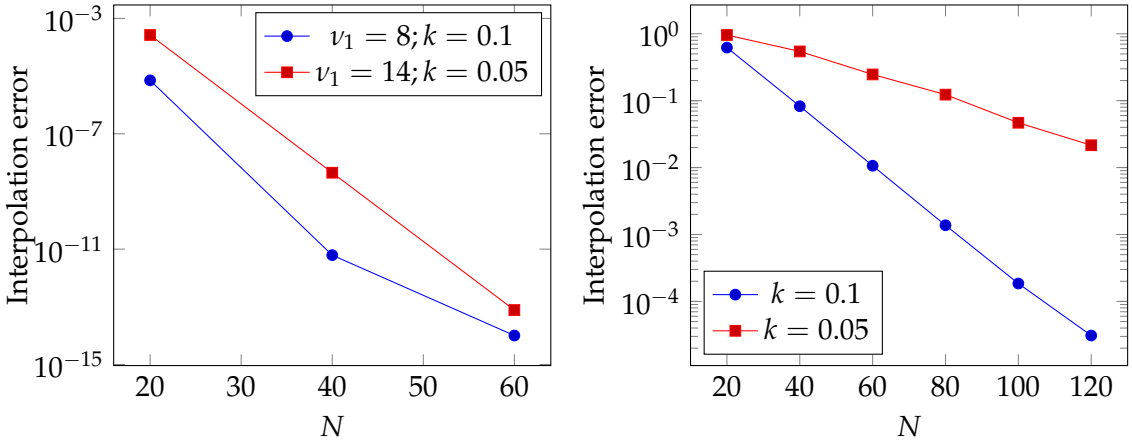

(A) Adaptive, with various ν_1 and fixed $\nu_2 = 0$

(B) Standard

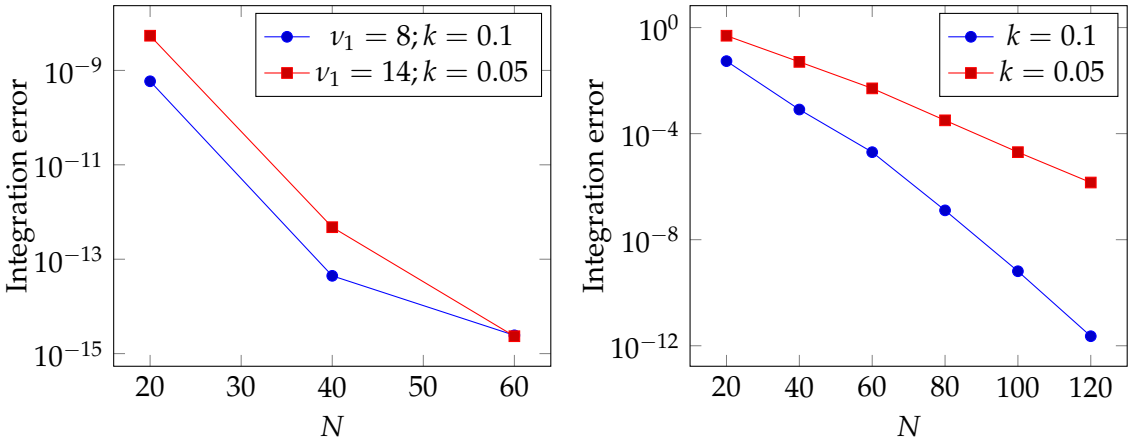

(C) Adaptive, with various ν_1 and fixed $\nu_2 = 0$

(D) Standard

FIGURE 3.12: Behavior of the interpolation error (top) and the integration error (bottom) for the function $f_3(x) = k/((x-\lambda)^2 + k^2)$ defined on the interval J_3, with various k and fixed $\lambda = 0.2$

Chapter 4

Accurate spectral solution methods for Fredholm and Volterra integral equations of the second kind

Over the years, various numerical techniques have been developed and successfully applied to solve a wide variety of differential, integral, and integro-differential equations, where the main goal of these techniques has been to produce computationally efficient and highly accurate numerical methods (see, e.g., [54, 41, 15, 28, 68, 72, 75, 12, 66, 65, 33, 46] and the references therein). Within this context, spectral methods are one of the high accuracy numerical tools that have been used to solve IEs. For instance, truncated Bernstein series have been proposed to approximate some classes of IEs in [60]. The so-called Boubaker Polynomials Expansion Scheme (BPES) has been used for obtaining an analytical solution of Love's IE in [53], and has been also successfully applied for obtaining its approximate solution in [63]. Chebyshev and Legendre polynomials have been employed to obtain the approximate solution of FIEs in [55] respectively in [59, 30]. A Legendre spectral-collocation method was proposed for linear VIEs of the second kind in [88]. Also, a spectral Petrov-Galerkin methods was proposed in [95] for linear Volterra type IEs of the second kind. Spectral collocation methods based on the scaled Laguerre functions and the mapped Gegenbauer rational functions (MGRF) have been proposed in [73] and [74], respectively, to solve linear FIEs on the half-line and the whole line.

Unfortunately, the despite excellent property of very high accuracy, the effectiveness of spectral methods may be hindered in situations, such as localized rapid variations, steep gradients, or a steep front. This chapter deals with this issue by proposing an efficient and accurate spectral approach for solving linear IEs of the second kind of the following form:

$$u(x) - \int_{\Omega} k(x,t)u(t)dt = f(x), \quad a \leq x \leq b, \tag{4.1}$$

where k and f are given functions, and u is the solution to be determined. Depending on the domain $\Omega = [a,b]$ or $\Omega = [a,x]$, Equation (4.1) is named a linear FIE or a linear VIE, respectively.

The content of this chapter is divided into three sections. In the first Section 4.1, we

apply the Legendre spectral Galerkin method and its iterated version to solve linear FIEs of the second kind and discuss the convergence results. In the second and last Sections 4.2 and 4.3, we develop and analyze an adaptive spectral collocation method for FIEs and VIEs of the second kind, even if the equation exhibits localized rapid variations, steep gradients, or a steep front.

4.1 Solving FIEs by using an accurate spectral Galerkin method

Let $\Omega \equiv [-1,1]$ in the equation (4.1), then this equation becomes

$$u(x) - \int_{-1}^{1} k(x,t)u(t)dt = f(x), \quad -1 \leq x \leq 1. \tag{4.2}$$

where k and f are given functions, and u is the solution to be determined. Equation (4.2) can be written in a compact symbolic form as follows

$$(\mathcal{I} - \mathcal{K})u = f, \tag{4.3}$$

where the operator $\mathcal{K}$ is given by

$$(\mathcal{K}u)(x) := \int_{-1}^{1} k(x,t)u(t)dt.$$

If the kernel function $k(x,t) \in L^2(I \times I)$, then $\mathcal{K} \in \mathcal{B}_c(L^2(I))$ is compact (see Lemma 1 in Chapter 1). The importance of $\mathcal{K}$ being compact is that the Fredholm theory then applies to the solvability theory for (4.3) (see, Subsection 1.2.3 in Chapter 1).

In this section, we apply the Legendre spectral Galerkin method and its iterated version to solve the equation (4.2) and discuss the convergence results. Finally, some numerical examples are presented to show effectiveness of the presented method.

4.1.1 Numerical scheme

Before describing the Legendre spectral Galerkin method and its iterated version for solving FIE (4.2), we first recall some notations. Let $\mathcal{X}_N$ be the set of all LPs of degree $\leq N$ defined on I, and let the orthogonal projection operator $\mathcal{P}_N : \mathcal{X} := L^2(I) \to \mathcal{X}_N$ be defined by

$$(\mathcal{P}_N u, \phi) = (u, \phi), \text{ for all } u \in \mathcal{X}, \phi \in \mathcal{X}_N.$$

where (f,g) is the L^2 inner product given by

$$(f,g) = \int_{-1}^{1} f(x)g(x)dx,$$

and the associated norm is

$$\|f\|_{L^2} = \left(\int_{-1}^{1} f^2(t)dt \right)^{\frac{1}{2}}.$$

The Galerkin method for solving (4.2) is to find $u_N \in \mathcal{X}_N$ such that (see Section 2.1.2 in Chapter 2)

$$u_N - \mathcal{P}_N \mathcal{K} u_N = \mathcal{P}_N f, \tag{4.4}$$

or equivalently,

$$(u_N, \phi) - (\mathcal{K} u_N, \phi) = (f, \phi), \text{ for all } \phi \in \mathcal{X}_N. \tag{4.5}$$

To find u_N, write

$$u_N = \sum_{n=0}^{N} \widetilde{u}_n \phi_n,$$

with $\{\phi_n : n = 0, \ldots, N\}$ a basis for $\mathcal{X}_N$, then the coefficients $\widetilde{u}_n$ are obtained by solving the linear system

$$\sum_{n=0}^{N} \widetilde{u}_n \left[(\phi_n, \phi_m) - (\mathcal{K}\phi_n, \phi_m) \right] = (f, \phi_m), \quad m = 0, \ldots, N. \tag{4.6}$$

If the basis is orthonormal, then $(\phi_m, \phi_n) = \delta_{m,n}$; The integrals $(\mathcal{K}\phi_n, \phi_m)$ must be calculated numerically. For the inner product, the discrete inner product (3.16) is used. For the integral operator $\mathcal{K}\phi_n$, the Gauss-Legendre quadrature formula (3.15) is used.

4.1.2 Convergence analysis

The convergence analysis for the Galerkin method (4.4) is quite straightforward using the results given in [7]. According to Lemma 2 in Chapter 2, the compactness of the operator $\mathcal{K}$, it follows that

$$\|\mathcal{K} - \mathcal{P}_N \mathcal{K}\|_{L^2} \to 0, \quad \text{as } N \to \infty.$$

In the classical Galerkin method, (4.2) is approximated by

$$(\mathcal{I} - \mathcal{P}_N \mathcal{K}) u_N = \mathcal{P}_N f. \tag{4.7}$$

and its corresponding iterated Galerkin solution is defined by

$$\widetilde{u}_N = \mathcal{K} u_N + f, \tag{4.8}$$

Using $\mathcal{P}_N \widetilde{u}_N = u_N$ and from the equation (4.8), it follows that

$$(\mathcal{I} - \mathcal{K}\mathcal{P}_N) \widetilde{u}_N = f, \tag{4.9}$$

this iterated solution may converge to u at a faster rate than the approximation u_N does.

From the theory of FIEs (see Theorem 1.5 in Chapter 1), the inverse operator $(\mathcal{I} - \mathcal{K})^{-1}$ exists as a bounded operator on $L^2(I)$. By Theorem 2.2 in Chapter 2, we can conclude if (4.3) is uniquely solvable for all $f \in \mathcal{X}$, then the Galerkin equation (4.7) is uniquely solvable for sufficiently large N, say $N \geq n_0$, and the operator $(\mathcal{I} - \mathcal{P}_N \mathcal{K})^{-1}$ exists as a

bounded operator from $L^2(I)$ into itself and is uniformly bounded,

$$M \equiv \sup_{N \geq n_0} \|(\mathcal{I} - \mathcal{P}_N \mathcal{K})^{-1}\| < \infty.$$

Also, we have (see [7, Lemma 3.4.1])

$$(\mathcal{I} - \mathcal{K}\mathcal{P}_N)^{-1} = \left[\mathcal{I} + \mathcal{K}(\mathcal{I} - \mathcal{P}_N \mathcal{K})^{-1}\mathcal{P}_N\right].$$

The existence and boundedness of $(\mathcal{I} - \mathcal{P}_N\mathcal{K})^{-1}$ follows from that of $(\mathcal{I} - \mathcal{K}\mathcal{P}_N)^{-1}$,

$$c \equiv \sup_{N \geq n_0} \|(\mathcal{I} - \mathcal{K}\mathcal{P}_N)^{-1}\| < \infty.$$

From the equation (4.7), it follows that

$$u - u_N = u - \mathcal{P}_N f + \mathcal{P}_N \mathcal{K} u_N. \tag{4.10}$$

Moreover, applying the projection $\mathcal{P}_N$ to both sides of operator equation (4.3) yields

$$\mathcal{P}_N u - \mathcal{P}_N \mathcal{K} u = \mathcal{P}_N f.$$

and substituting this equation into (4.10) leads to the equation

$$u - u_N = \mathcal{P}_N \mathcal{K}(u - u_N) + u - \mathcal{P}_N u.$$

Solving for $u - u_N$ from the above equation gives

$$u - u_N = (\mathcal{I} - \mathcal{P}_N \mathcal{K})^{-1}(u - \mathcal{P}_N u), \tag{4.11}$$

and by applying $\|\cdot\|_{L^2}$ on both sides of (4.11) yields

$$\|u - u_N\|_{L^2} \leq \|(\mathcal{I} - \mathcal{P}_N \mathcal{K})^{-1}\| \|u - \mathcal{P}_N u\|_{L^2}.$$

For the error in $\widetilde{u}_n$, first rewrite (4.3) as

$$(\mathcal{I} - \mathcal{K}\mathcal{P}_N)u = f + \mathcal{K}u - \mathcal{K}\mathcal{P}_N u. \tag{4.12}$$

Subtracting (4.12) from (4.9) gives

$$(\mathcal{I} - \mathcal{K}\mathcal{P}_N)(u - \widetilde{u}_N) = \mathcal{K}(\mathcal{I} - \mathcal{P}_N)u,$$

or equivalently,

$$(u - \widetilde{u}_N) = (\mathcal{I} - \mathcal{K}\mathcal{P}_N)^{-1}\mathcal{K}(\mathcal{I} - \mathcal{P}_N)u.$$

Hence,

$$\|u - \widetilde{u}_N\|_{L^2} \leq \|(\mathcal{I} - \mathcal{K}\mathcal{P}_N)^{-1}\| \|\mathcal{K}(\mathcal{I} - \mathcal{P}_N)u\|_{L^2}.$$

Since $(\mathcal{I}-\mathcal{P}_N)^2=(\mathcal{I}-\mathcal{P}_N)$, we have that

$$\|\mathcal{K}(\mathcal{I}-\mathcal{P}_N)u\|_{L^2}\leq\|\mathcal{K}(\mathcal{I}-\mathcal{P}_N)\|_{L^2}\|(\mathcal{I}-\mathcal{P}_n)u\|_{L^2}.$$

Since $\mathcal{K}$ is compact, we also have that $\mathcal{K}^*$ is compact (see Theorem 1.2 in Chapter 1). Then by compactness of $\mathcal{K}^*$ and Lemma 2 in Chapter 2, we have (see [7, p. 74])

$$\|\mathcal{K}(\mathcal{I}-\mathcal{P}_N)\|_{L^2}=\|\left[\mathcal{K}(\mathcal{I}-\mathcal{P}_N)\right]^*\|_{L^2}=\|(\mathcal{I}-\mathcal{P}_N)\mathcal{K}^*\|_{L^2}\to 0,\quad \text{as } N\to\infty.$$

Thus, we conclude that

$$\|u-\widetilde{u}_N\|_{L^2}\leq c\|(\mathcal{I}-\mathcal{P}_N)\mathcal{K}^*\|_{L^2}\|u-\mathcal{P}_Nu\|_{L^2}.$$

and see that $\|u-\widetilde{u}_N\|_{L^2}$ converges to zero more rapidly than does $\|u-\mathcal{P}_Nu\|_{L^2}$, or equivalently, $\|u-u_N\|_{L^2}$. The improvement in rate of convergence will depend on the rate at which $\|(\mathcal{I}-\mathcal{P}_N)\mathcal{K}^*\|_{L^2}\to 0$ as $N\to\infty$.

4.1.3 Numerical experiments

In the following we present some numerical examples to verify the convergence results discussed in the previous subsection.

Example 4.1. Consider

$$u(x)-\int_{-1}^{1}e^{\frac{1}{8}(x+1)^2(t+1)}u(t)dt=e^{x+1}-\frac{8(e^{\frac{1}{4}x(x+2)+9}-1)}{x^2+2x+9},\quad -1\leq x\leq 1,$$

where the exact solution of this equation is $u(x)=e^{x+1}$. Some numerical results are listed in Table 4.1. In this table, $|u(x)-u_N(x)|$ and $|u(x)-u_N^{it}(x)|$ are denote the absolute solution errors, where $u_N(x)$ and $u_N^{it}(x):=\widetilde{u}_N(x)$ are the corresponding the approximate and iterated solutions, respectively. In Figure 4.1, we plot the exact solution, the approximate and iterated solutions with $N=2,3$. It can be seen from both the table and figure that the iterated Legendre spectral-Galerkin solution is more accurate than the Legendre spectral Galerkin solution in approximating the exact solution. Figure 4.2 also illustrates the convergence order in the L^2 norm for both the Legendre spectral-Galerkin method and its iterated version.

Example 4.2. [1] Consider

$$u(x)-\frac{1}{2}\int_{-1}^{1}x^2tu(t)dt=f(x),\quad -1\leq x\leq 1,\tag{4.13}$$

where $f(x)$ is chosen so that for a non-negative constant k, the exact solution of this equation is $u(x)=\operatorname{erf}(x/\sqrt{k})$, which has a steep front at $x=0$ for small $k\ll 1$. We solve this example for $k=1/100$ and $1/1000$. The error in L^2 norm of the Legendre spectral Galerkin method and its iterated version are shown in Table 4.2. Moreover, Figure 4.2 also illustrates

TABLE 4.1: Some numerical results for Example 4.1.

x	$\lvert u(x)-u_2(x)\rvert$	$\lvert u(x)-u_2^{it}(x)\rvert$	$\lvert u(x)-u_3(x)\rvert$	$\lvert u(x)-u_3^{it}(x)\rvert$
0.999	2.43e−01	1.76e−03	3.26e−02	2.21e−05
0.753	1.38e−02	2.74e−04	1.07e−02	3.75e−06
0.352	8.61e−02	7.17e−04	6.50e−04	6.67e−06
0.001	1.29e−03	1.00e−03	9.98e−03	9.21e−06
−0.001	7.31e−03	1.01e−03	9.98e−03	9.22e−06
−0.352	7.06e−02	1.11e−03	5.69e−04	9.98e−06
−0.753	8.55e−03	1.15e−03	7.97e−03	1.02e−05
−0.999	1.48e−01	1.16e−03	2.19e−02	1.03e−05

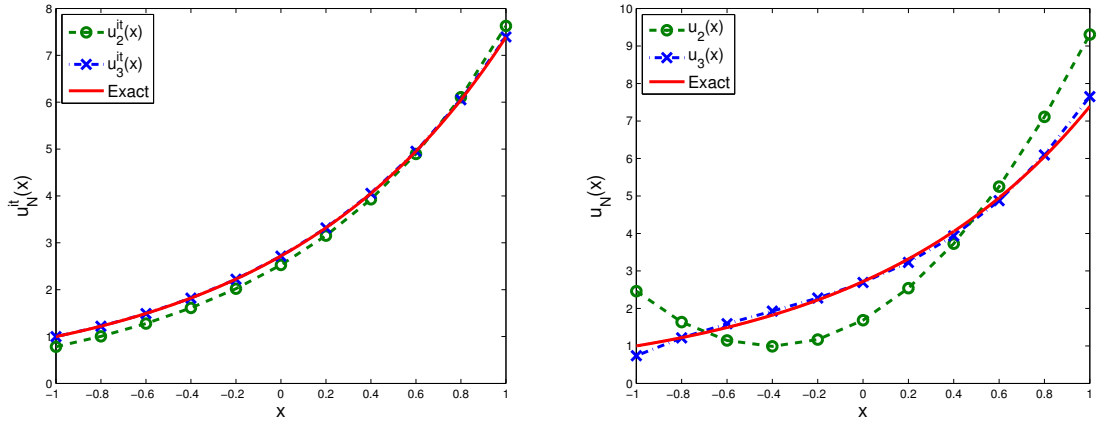

FIGURE 4.1: Plots of the exact solution, iterated (left) and approximate (right) solutions with $N = 2, 3$ for Example 4.1.

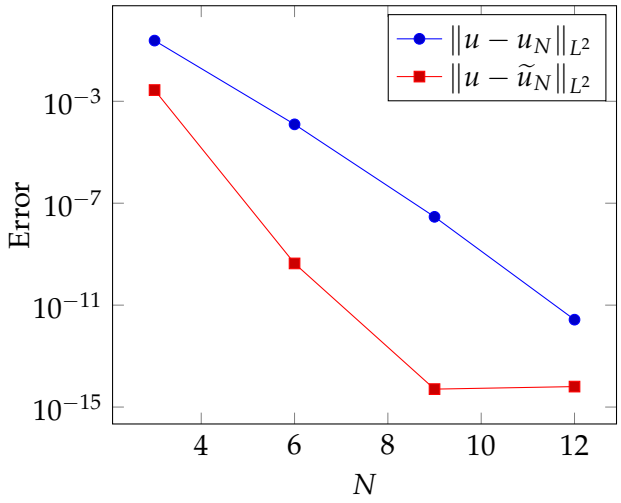

FIGURE 4.2: The convergence order under L^2 norm for Example 4.1.

the convergence order in the L^2 norm for both the Legendre spectral-Galerkin method and

its iterated version. As shown in both the table and figure, the iterated Legendre spectral-Galerkin solution is more accurate than the Legendre spectral Galerkin method.

TABLE 4.2: The error in L^2 norm for Example 4.2, with $k = 1/100$ and $1/1000$.

	$\|u - u_N\|_{L^2}$		$\|u - \widetilde{u}_N\|_{L^2}$	
N	$k = 1/100$	$k = 1/1000$	$k = 1/100$	$k = 1/1000$
8	2.64e−01	3.82e−01	5.76e−03	7.18e−03
16	8.87e−02	2.36e−01	5.04e−04	1.76e−03
32	5.58e−03	1.17e−01	2.32e−07	3.35e−04
64	1.22e−06	2.75e−02	5.22e−14	1.11e−05

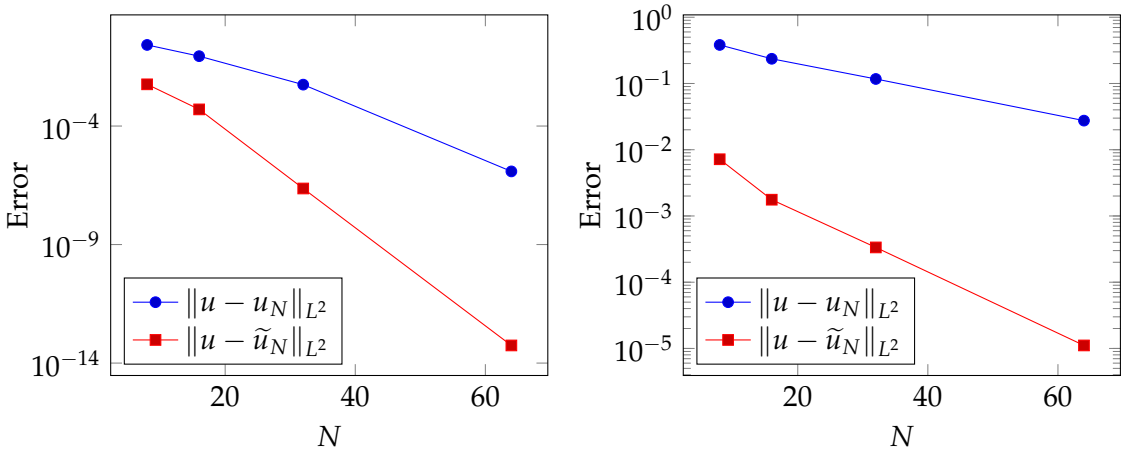

(A) $k = 1/100$ (B) $k = 1/1000$

FIGURE 4.3: The convergence order under L^2 norm for Example 4.2, with $k = 1/100$ and $1/1000$.

Example 4.3. [68] Consider

$$u(x) - \int_0^1 xtu(t)dt = \frac{r}{(x-1/2)^2 + r^2} - x \arctan\left(\frac{1}{2r}\right), \quad x \in [0,1],$$

whose solution is

$$u(x) = \frac{r}{(x-1/2)^2 + r^2}.$$

The transformed IE is

$$u(s) - \frac{1}{8}\int_{-1}^1 (s+1)(\xi+1)u(\xi)d\xi = \frac{4r}{s^2+4r^2} - \left(\frac{1+s}{2}\right)\arctan\left(\frac{1}{2r}\right), \quad s \in [-1,1],$$

with the transformed solution is $u(s) = \frac{4r}{s^2+4r^2}$. We solve this example for $r = 1/2$ and $1/10$. Figure 4.4a illustrates a comparison of the convergence rates between the Legendre

spectral-Galerkin method and its iterated version, and the SE/DE-Sinc collocation methods in [68]. Also, Figures 4.4b and 4.5 (left panel) show the error in L^2 norm of the Legendre spectral-Galerkin method and its iterated solution. It can be seen from the Figure 4.5 (left panel) that the error in L^2 norm obtained by the iterated solution is better than the Galerkin method, but the CPU time (right panel) by the Galerkin method is less compared to the iterated solution. From these figures, one can see that the errors decay exponentially, as the exact solution for this example is sufficiently smooth.

TABLE 4.3: Comparison results for Example 4.3, with $r = 1/2$ and $1/10$.

	$\|u - u_N\|_{L^2}$		$\|u - \widetilde{u}_N\|_{L^2}$	
N	$r = 1/2$	$r = 1/10$	$r = 1/2$	$r = 1/10$
8	1.84e−03	–	9.01e−07	9.78e−02
16	1.54e−06	2.18e−01	6.56e−13	3.90e−03
32	1.13e−12	8.99e−03	2.71e−16	6.73e−06
64	9.12e−15	1.55e−05	3.02e−16	2.01e−11

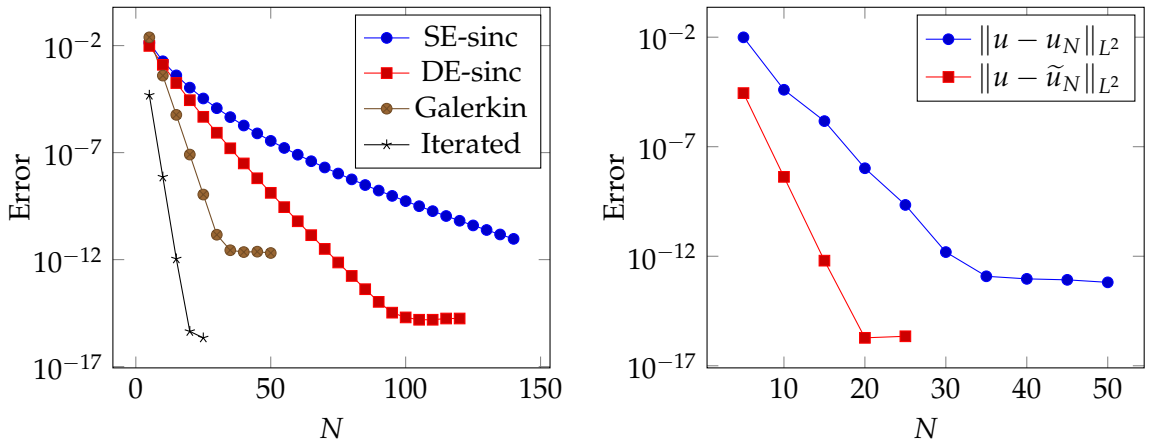

(A) The maximum absolute error

(B) The error in L^2 norm

FIGURE 4.4: Convergence with respect to N for Example 4.3, with $r = 1/2$.

4.2 Solving VIEs by using an adaptive spectral collocation method

Let $\Omega \equiv [0, x]$ in the equation (4.1), then this equation becomes

$$u(x) - \int_0^x k(x,t)u(t)dt = f(x), \quad 0 \leq x \leq 1. \tag{4.14}$$

where k and f are given functions, and u is the solution to be determined.

The authors [88] proposed a Legendre spectral collocation method for solving VIEs of the second kind together with a rigorous error analysis, whose kernel and solutions are

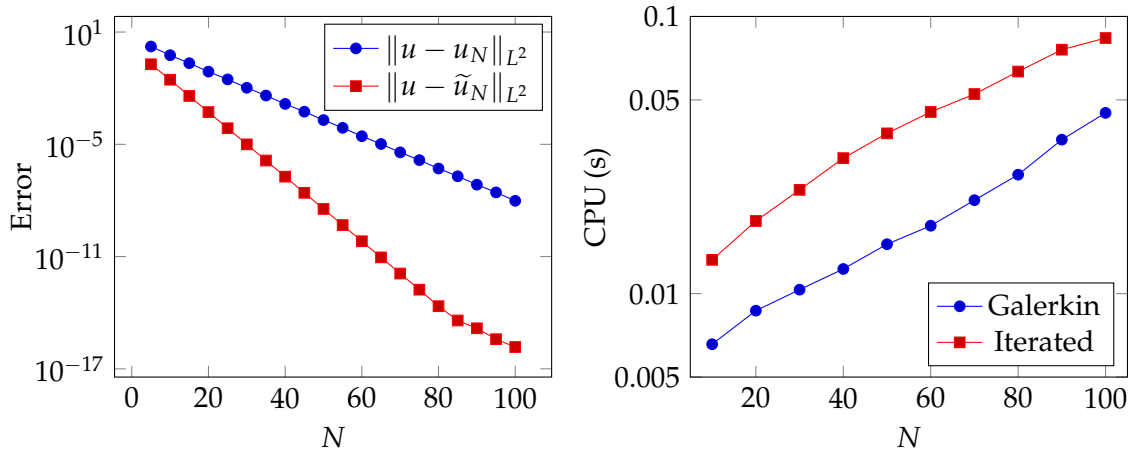

FIGURE 4.5: A comparison of errors in the L^2 norm (left) and the corresponding CPU time (right) with respect to N for the Galerkin solution and its iterated version for Example 4.3, with $r = 1/10$.

sufficiently smooth. In this work, we extend this method to a special case where the solution of the VIE (4.14) exhibits steep gradients or a steep front. To obtain a high-accuracy numerical solution for the equation (4.14), we need to use the change of variable transformations $x = \varphi_{0,1}(\nu; t)$ and $s = \varphi_{0,1}(\nu; \xi)$ in equation (4.14). Under these transformations, equation (4.14) becomes:

$$U_\nu(t) - \int_{-1}^{t} K_\nu(t, \xi) U_\nu(\xi) d\xi = F_\nu(t), \quad -1 \leq t \leq 1, \tag{4.15}$$

where $F_\nu(t) := f(\varphi_{0,1}(\nu; t))$,

$$K_\nu(t, \xi) := k(\varphi_{0,1}(\nu; t), \varphi_{0,1}(\nu; \xi)) \varphi'_{0,1}(\nu; \xi),$$

and the transformed solution $U_\nu(t) := u(\varphi_{0,1}(\nu; t))$ is smooth function.

In this section, we develop and analyze an adaptive spectral collocation method for VIEs of the second kind, which can achieve fast convergence and high accuracy despite the fact its solution exhibits steep gradients or a steep front. The strategy of the adaptive procedure is to transform the original equation into a new Volterra equation with smoother behavior, using an appropriate variable transformation to ensure the convergence of the Legendre spectral collocation method. Theoretical results on convergence rates and error estimates are provided in both the L^∞-norm and L^2-norm. Finally, several numerical examples are presented to demonstrate that the proposed method is preferable to its classical predecessor.

4.2.1 Adaptive spectral collocation method

In order to use the Legendre-Gauss quadrature formula to compute the integral term in (4.15), we transfer the integral interval $[-1, t]$ to the standard fixed interval $[-1, 1]$ using a

simple linear transformation

$$z(t,\theta) = \frac{1+t}{2}\theta + \frac{t-1}{2}, \quad -1 \leq \theta \leq 1.$$

Then, (4.15) becomes

$$U_\nu(t) - \int_{-1}^{1} \widetilde{K}_\nu(t, z(t,\theta)) U_\nu(z(t,\theta)) d\theta = F_\nu(t), \tag{4.16}$$

where

$$\widetilde{K}_\nu(t, z(t,\theta)) = \frac{1+t}{2} K_\nu(t, z(t,\theta)).$$

The spectral Legendre-collocation method for solving (4.16) is to find $U_\nu^N \in \mathbb{P}_N$, such that $U_\nu^N(t)$ satisfies equation (4.16) at the collocation points $\sigma_{N,i}$ $(0 \leq i \leq N)$, i.e.,

$$U_\nu^N(\sigma_{N,i}) - \int_{-1}^{1} \widetilde{K}_\nu(\sigma_{N,i}, z(\sigma_{N,i},\theta)) U_\nu^N(z(\sigma_{N,i},\theta)) d\theta = F_\nu(\sigma_{N,i}), \tag{4.17}$$

where $U_\nu^N(t)$ is expanded as

$$U_\nu^N(t) = \sum_{j=0}^{N} \widetilde{U}_{\nu,j} h_j(t), \tag{4.18}$$

with $\widetilde{U}_{\nu,j}$ $(0 \leq j \leq N)$ are the approximate values for $U_\nu(\sigma_{N,i})$. Substituting (4.18) into equation (4.17) and using a $(N+1)$-point Legendre-Gauss quadrature rule relative to the weights $\{\omega_{N,l}\}_{l=0}^N$ yields the following collocation equations:

$$\widetilde{U}_{\nu,i} - \sum_{j=0}^{N} \widetilde{U}_{\nu,j} \left(\sum_{l=0}^{N} \omega_{N,l} \widetilde{K}_\nu(\sigma_{N,i}, z(\sigma_{N,i}, \sigma_{N,l})) h_j(z(\sigma_{N,i}, \sigma_{N,l})) \right) = F_\nu(\sigma_{N,i}). \tag{4.19}$$

Using the following notations

$$\mathbf{U} = (\widetilde{U}_{\nu,0},,\ldots,\widetilde{U}_{\nu,N})^T, \ \ \mathbf{F} = (F_\nu(\sigma_{N,0}),\ldots,F_\nu(\sigma_{N,N}))^T,$$

$$\mathbf{A} = (a_{i,j}^{(\nu)})_{i,j=0}^N, \ \ a_{i,j}^{(\nu)} = \sum_{l=0}^{N} \omega_{N,l} \widetilde{K}_\nu(\sigma_{N,i}, z(\sigma_{N,i}, \sigma_{N,l})) h_j(z(\sigma_{N,i}, \sigma_{N,l})),$$

we obtain the matrix form

$$\mathbf{U} - \mathbf{A}\mathbf{U} = \mathbf{F}.$$

After solving the above linear system, we can find the approximate solution of the original (4.14) in the physical domain by means of relation (3.35).

4.2.2 Convergence analysis

The following theorems provide a convergence analysis of the adaptive numerical scheme described above in both the L^2-norm and the L^∞-norm

Theorem 4.1. *Let U_ν be the exact solution of the transformed Volterra equation (4.15) and U_ν^N be the numerical solution obtained using the spectral scheme (4.19). If $U_\nu \in H^m(I)$, then the*

following error estimate holds

$$\|U_\nu - U_\nu^N\|_{L^2(I)} \leq CN^{-m}\left(N^{\frac{1}{2}}\max_{t\in I}|K_\nu(t,z(t,\cdot))|_{\tilde{H}^{m;N}(I)}\|U_\nu\|_{L^2(I)} + |U_\nu|_{\tilde{H}^{m;N}(I)}\right).$$

Proof. The proof of this theorem is similar to that Theorem 4.1 in [88]. □

Theorem 4.2. *Let U_ν be the exact solution of the transformed Volterra equation (4.15) and U_ν^N be the numerical solution obtained using the spectral scheme (4.19) If $U_\nu \in H^m(I)$, then the following error estimate holds*

$$\|U_\nu - U_\nu^N\|_{L^\infty(I)} \leq CN^{\frac{1}{2}-m}\left(\max_{t\in I}|K_\nu(t,z(t,\cdot))|_{\tilde{H}^{m;N}(I)}\|U_\nu\|_{L^2(I)} + CN^{\frac{1}{4}}|U_\nu|_{\tilde{H}^{m;N}(I)}\right).$$

Proof. The proof of this theorem is similar to that Theorem 4.2 in [88]. □

4.2.3 Numerical experiments

In this subsection, we use the following examples to numerically verify the convergence results in Theorems 4.1 and 4.2.

Example 4.4. Consider

$$u(x) - \int_0^x xsu(s)ds = f(x), \quad 0 \leq x \leq 1, \tag{4.20}$$

where $f(x)$ is chosen so that the exact solution is

$$u(x) = \frac{10^{-1}}{10^{-2} + (x-0.5)^2}.$$

In Figure 4.6, the L^∞ and L^2 errors for the present method using the two-parameter mapping (3.23) ($\nu_1 = 5$, $\nu_2 = 0$) are compared with those of the classical method. From this figure, it is clear that the present method converges faster than the classical method, confirming the results of Theorems 4.1 and 4.2.

Example 4.5. Consider

$$u(x) - \int_0^x xsu(s)ds = f(x), \quad 0 \leq x \leq 1, \tag{4.21}$$

where $f(x)$ is chosen so that the exact solution is $u(x) = 1/(26 + 100x^2 - 100x)$. Figure 4.7 illustrates the L^∞ and L^2 errors of the present method using the two-parameter mapping (3.23) ($\nu_1 = 5, 10$ and $\nu_2 = 0$ fixed) and the classical method. This figure shows that our method converges faster than the classical method, with the improvement depending on the choice of the parameter mapping ν_1. Clearly, the error decays exponentially for the present method, while it decays geometrically for the classical method.

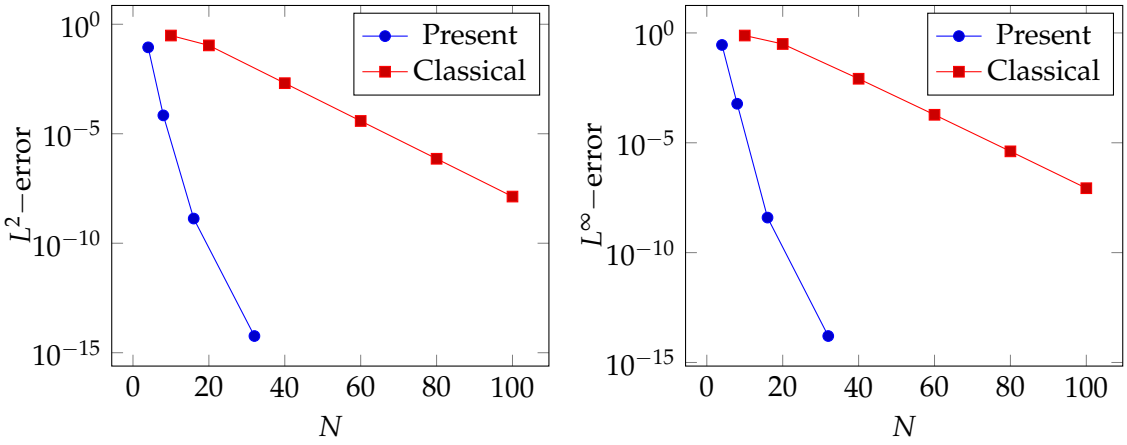

FIGURE 4.6: The L^∞ error (right) and the L^2 error (left) of the present method with $\nu_1 = 5$, $\nu_2 = 0$ and the classical method for Example 4.4.

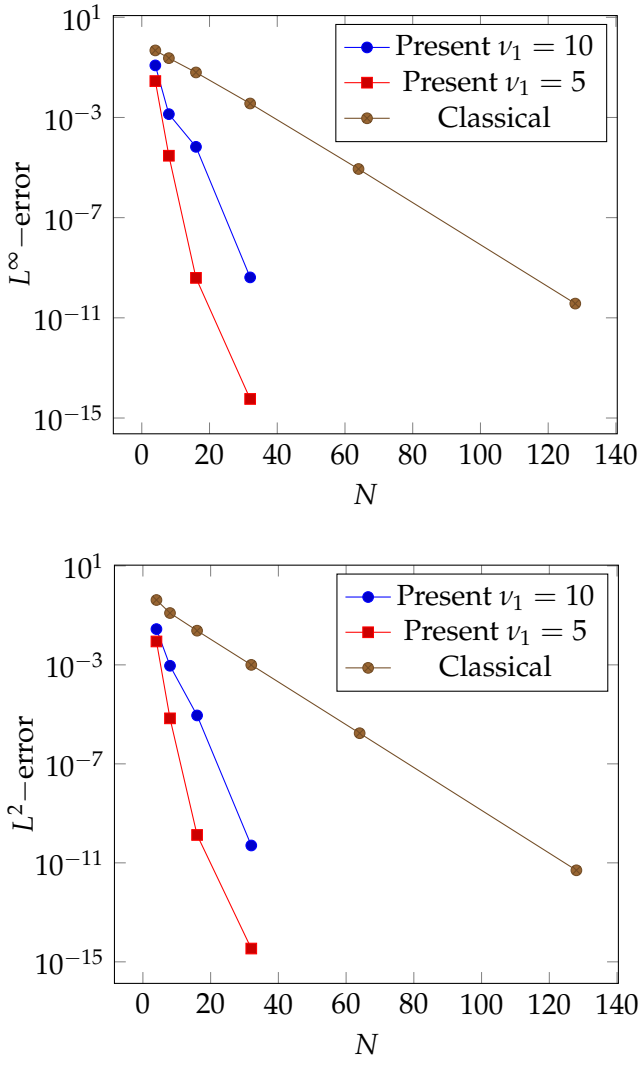

FIGURE 4.7: The convergence order under L^∞ norm (top) and L^2 norm (bottom) with respect to N for Example 4.5.

Example 4.6. Consider

$$u(x) - \int_0^x e^x s u(s) ds = f(x), \quad 0 \leq x \leq 1, \tag{4.22}$$

where $f(x)$ is chosen so that the exact solution is $u(x) = \arctan(100x)$. In Figure 4.8 (left), we plot the L^2-errors of the present method and the classical method, while in the right figure, we plot the corresponding CPU times, in seconds. From Figure 4.8, we see that the presented method is more accurate than the classical method, but the CPU time by the classical method is less than compared to the presented method. Also, Figure 4.9 shows relation between CPU time and errors in the L^2 norm for each method.

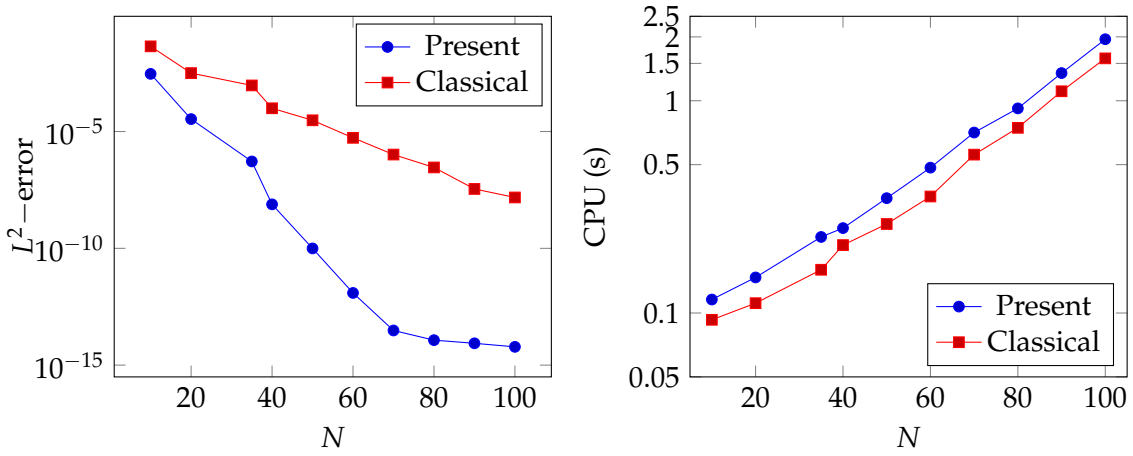

FIGURE 4.8: The convergence order under L^2 norm (left) and the corresponding CPU time (right) with respect to N for Example 4.6.

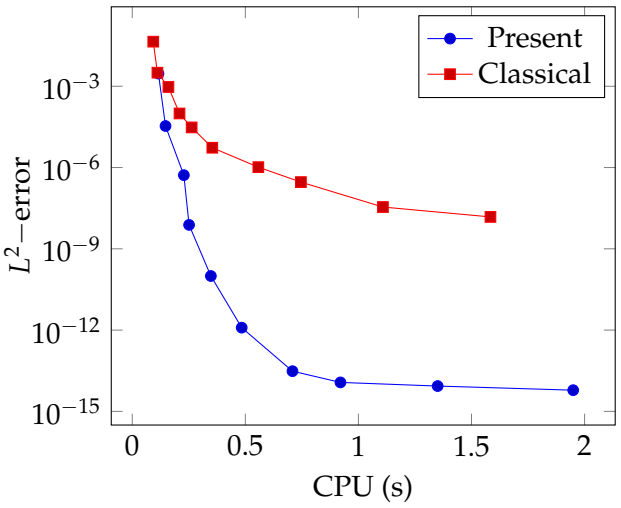

FIGURE 4.9: Relation between CPU time and errors in the L^2 norm for Example 4.6.

4.3 Solving FIEs by using an adaptive spectral collocation method

Let $\Omega \equiv [a, b]$ in the equation (4.1), then this equation becomes

$$u(x) - \int_a^b k(x,t)u(t)dt = f(x), \quad a \leq x \leq b. \tag{4.23}$$

where k and f are given functions, and u is the solution to be determined.

The content of this section is based on our research published in [1]. For the purposes of this thesis, the paper develops and analyzes an adaptive spectral collocation method for FIEs of the second kind, even if the equation exhibits localized rapid variations, steep gradients, or a steep front. The strategy of the adaptive procedure is to transform the original equation into an equivalent one with a sufficiently smooth behavior in order to ensure the convergence of the Legendre spectral collocation method without subdividing the domain of the IE, as usual, into the subintervals. Theoretical results on existence and uniqueness are discussed, and convergence rates and error estimates are provided in both the L^∞-norm and L^2-norm. Finally, several numerical examples are provided to show that the proposed method outperforms its classical counterparts as well as some other existing approaches.

4.3.1 Existence and uniqueness of solution

Note that the equation (4.23) can be rewritten as

$$(\mathcal{I} - \mathcal{K})u = f, \tag{4.24}$$

where

$$(\mathcal{K}u)(x) := \int_a^b k(x,t)u(t)dt, \quad a \leq x \leq b. \tag{4.25}$$

By employing (3.19), it becomes equivalent to the following equation

$$U_\nu(y) - \int_{-1}^1 K_\nu(y,\xi)U_\nu(\xi)d\xi = F_\nu(y), \quad -1 \leq y \leq 1. \tag{4.26}$$

where $F_\nu(y) := f(\varphi_{a,b}(\nu; y))$,

$$K_\nu(y,\xi) := k(\varphi_{a,b}(\nu; y), \varphi_{a,b}(\nu; \xi))\varphi'_{a,b}(\nu; \xi), \quad \nu \in \mathscr{D}_\nu, \tag{4.27}$$

and $U_\nu(y) := u(\varphi_{a,b}(\nu; y))$ is the smooth function that we need to estimate. Equation (4.26) can be also rewritten in operator form as follows:

$$(\mathcal{I} - \mathcal{K}_\nu)U_\nu = F_\nu, \tag{4.28}$$

where

$$(\mathcal{K}_\nu U_\nu)(y) := \int_{-1}^1 K_\nu(y,\xi)U_\nu(\xi)d\xi, \quad -1 \leq y \leq 1. \tag{4.29}$$

In the following theorems we discuss the existence and uniqueness of solution for the original operator (4.24) and the transformed operator (4.28).

Lemma 9. *For $\nu \in \mathscr{D}_\nu$, let's assume that*

$$\int_a^b \int_a^b |k(x,t)|^2 \frac{w_{J,\nu}(x)}{w_{J,\nu}(t)} dxdt = \beta_\nu^2 < \infty. \tag{4.30}$$

Then, the integral operators defined by (4.25) and (4.29) are bounded on $L^2_{w_{J,\nu}}(J)$ and $L^2(I)$, respectively.

Proof. By Cauchy-Schwarz inequality, we have

$$|\mathcal{K}u(x)|^2 \leq \left(\int_a^b |k(x,t)|^2 \frac{1}{w_{J,\nu}(t)} dt \right) \left(\int_a^b |u(t)|^2 w_{J,\nu}(t) dt \right).$$

This leads us to

$$\|\mathcal{K}u\|^2_{L^2_{w_{J,\nu}}(J)} = \left(\int_a^b \int_a^b |k(x,t)|^2 \frac{w_{J,\nu}(x)}{w_{J,\nu}(t)} dxdt \right) \|u\|^2_{L^2_{w_{J,\nu}}(J)} = \beta_\nu^2 \|u\|^2_{L^2_{w_{J,\nu}}(J)}.$$

Hence, we have $\|\mathcal{K}u\|_{L^2_{w_{J,\nu}}(J)} \leq \beta_\nu \|u\|_{L^2_{w_{J,\nu}}(J)}$. On the other hand, using (3.32) and (4.27), it is not hard to show that

$$\beta_\nu = \left(\int_{-1}^1 \int_{-1}^1 |K_\nu(y,\xi)|^2 dy d\xi \right)^{1/2}. \tag{4.31}$$

Thus, $K_\nu \in L^2(I \times I)$ and therefore $\mathcal{K}_\nu$ is bounded. □

Lemma 10. *Suppose that the assumption of Lemma 9 is fulfilled. Then the transformed integral operator $\mathcal{K}_\nu$ is compact from $L^2(I)$ into itself.*

Proof. The proof is similar to the Theorem 7 in [43, pp. 51–52]. □

Theorem 4.3. *Let the assumption in Lemma 9 be fulfilled. Furthermore, assume that the original homogeneous equation $(\mathcal{I} - \mathcal{K})u = 0$ has only the trivial solution $u \equiv 0$. Then (4.28) has a unique solution $U_\nu \in L^2(I)$ for any $f \in L^2_{w_{J,\nu}}(J)$. In this case, the unique solution of the original operator (4.24) in $L^2_{w_{J,\nu}}(J)$ is given by $u(x) = U_\nu(\psi_{a,b}(\nu; x))$.*

Proof. Under the assumption of Lemma 9, it follows immediately from Lemma 10 that the transformed integral operator $\mathcal{K}_\nu$ is compact on $L^2(I)$. On the other hand, if $(\mathcal{I} - \mathcal{K})$ is injective then $(\mathcal{I} - \mathcal{K}_\nu)$ is also injective. Therefore, by Theorem 3.4, p. 29 of [49], the operator $(\mathcal{I} - \mathcal{K}_\nu)^{-1}$ exists and is bounded. Then the transformed operator (4.28) has a unique solution $U_\nu \in L^2(I)$ for any $f \in L^2_{w_{J,\nu}}(J)$. Obviously, in such a case, the unique solution of Eq. (4.24) belongs to the weighted space $L^2_{w_{J,\nu}}(J)$ and is given by $u(x) = U_\nu(\psi_{a,b}(\nu; x))$. □

Corollary 4.1. *If the operator (4.24) has a unique solution in the weighted space $L^2_{w_{J,\nu}}(J)$, then the transformed operator (4.28) is uniquely solvable in $L^2(I)$, and vice versa.*

4.3.2 Adaptive spectral collocation method

Consider the transformed (4.26) in the linear functional equation form

$$U_\nu(y) - \mathcal{K}_\nu U_\nu(y) = F_\nu(y), \quad -1 \le y \le 1, \tag{4.32}$$

where $\mathcal{K}_\nu$ is the transformed integral operator defined by (4.29). Then, the spectral Legendre-collocation method approximates the solution of (4.32) by an element $U_\nu^N \in \mathbb{P}_N$, satisfying

$$U_\nu^N(\sigma_{N,i}) - \mathcal{K}_\nu U_\nu^N(\sigma_{N,i}) = F_\nu(\sigma_{N,i}), \quad 0 \le i \le N. \tag{4.33}$$

Using (3.17), the above equation can be rewritten in an operator form interpolation points, namely

$$U_\nu^N - \mathcal{I}_N \mathcal{K}_\nu U_\nu^N = \mathcal{I}_N F_\nu, \tag{4.34}$$

which can be considered as an equation in the whole space $\mathcal{C}(I)$ because any solution $U_\nu^N = \mathcal{I}_N \mathcal{K}_\nu U_\nu^N + \mathcal{I}_N F_\nu$ automatically belongs to $\mathbb{P}_N$. We expand the approximate solution U_ν^N as

$$U_\nu^N(y) = \sum_{j=0}^{N} \widetilde{U}_{\nu,j} h_j(y), \tag{4.35}$$

where $\widetilde{U}_{\nu,j}$ $(0 \le j \le N)$ are the approximate values for $U_\nu(\sigma_{N,j})$, such that $\{\widetilde{U}_{\nu,i}\}_{i=0}^N$ satisfies the following collocation equations:

$$\widetilde{U}_{\nu,i} - \sum_{j=0}^{N} a_{i,j}^{(\nu)} \widetilde{U}_{\nu,j} = F_\nu(\sigma_{N,i}), \quad 0 \le i \le N, \tag{4.36}$$

where

$$a_{i,j}^{(\nu)} = \sum_{l=0}^{N} K_\nu(\sigma_{N,i}, \sigma_{N,l}) h_j(\sigma_{N,l}) \omega_{N,l}. \tag{4.37}$$

Equation (4.36) yields a system of algebraic equations that can be represented in matrix form as follows:

$$(\mathbf{I} - \mathbf{A})\mathbf{U} = \mathbf{F}, \tag{4.38}$$

where $\mathbf{I}$ is the identity matrix, $\mathbf{A} = [a_{i,j}^{(\nu)}]_{i,j=0}^N$ is a matrix of size $(N+1) \times (N+1)$ with the elements as in (4.37), and

$$\mathbf{U} = [\widetilde{U}_{\nu,0}, \widetilde{U}_{\nu,1}, \ldots, \widetilde{U}_{\nu,N}]^T, \qquad \mathbf{F} = [F_\nu(\sigma_{N,0}), F_\nu(\sigma_{N,1}), \ldots, F_\nu(\sigma_{N,N})]^T.$$

Then the unknown vector $\mathbf{U}$ can be derived by solving the system (4.38) using Basic Linear Algebra Subroutines (BLAS). After determining the approximation $U_N(y)$ for the transformed (4.26) in the computational domain, we can determine the approximation for the solution of the original (4.23) in the physical domain by means of relation (3.35).

4.3.3 Convergence analysis

The purpose of the present section is to analyze the adaptive numerical scheme described above. Before presenting error estimates of the scheme, we first introduce the following standard Sobolev space and some useful lemmas which are usually required to obtain the convergence analysis.

For notational convenience, we denote by $\partial_y^r U$ the r-th order derivative of the function U, i.e., $\partial_y^r U := \partial^r U(y)/\partial y^r$. For $m \in \mathbb{N}$, define

$$H^m(I) = \{U : \partial_y^r U \in L^2(I),\ 0 \le r \le m\}, \tag{4.39}$$

equipped with the following norm

$$\|U\|_{H^m(I)} = \left(\sum_{r=0}^{m} \|\partial_y^r U\|_{L^2(I)}^2\right)^{\frac{1}{2}} = \left(\sum_{r=0}^{m} \int_{-1}^{1} |\partial_y^r U(y)|^2 dy\right)^{\frac{1}{2}}. \tag{4.40}$$

Thus, for $N \in \mathbb{N}$, it is convenient to introduce the semi-norm

$$|U|_{H^{m;N}(I)} = \left(\sum_{r=\min(m,N+1)}^{m} \|\partial_y^r U\|_{L^2(I)}^2\right)^{\frac{1}{2}}. \tag{4.41}$$

In the sequel, C will denote all generic constants independent of N, which are not necessarily the same. We quoted the following estimates from [26, Lemma 1] with the zeros of the Jacobi polynomials.

Lemma 11. *Assume that $U \in H^m(I)$, and denote by $\mathcal{I}_N U$ the interpolation operator associated with the Gauss points of the Legendre polynomials. Then the following estimates hold:*

$$\|U - \mathcal{I}_N U\|_{L^2(I)} \le C N^{-m} |U|_{H^{m;N}(I)}, \tag{4.42}$$

$$\|U - \mathcal{I}_N U\|_{\infty} \le C N^{\frac{1}{2}-m} |U|_{H^{m;N}(I)}. \tag{4.43}$$

Also, the following result quoted from [96].

Lemma 12. *For every bounded function U, there exists a constant C, independent of U such that*

$$\sup_N \|\mathcal{I}_N U\|_{L^2(I)} := \sup_N \|\sum_{j=0}^{N} U(\sigma_{N,j}) h_j(y)\|_{L^2(I)} \le C\|U\|_{\infty}, \tag{4.44}$$

where $h_j(y)$ is the Lagrange interpolation basis function associated with the Legendre collocation points $\{\sigma_{N,j}\}_{j=0}^N$.

The following result on the Lebesgue constant for Lagrange interpolation polynomials with the zeros of the Jacobi polynomials quoted form [61].

Lemma 13. *Assume that* $\{h_j(y)\}_{j=0}^{N}$ *are Lagrange interpolation polynomials associated with the Gauss points of the Legendre polynomials. Then*

$$\|\mathcal{I}_N\|_\infty := \max_{y\in I} \sum_{j=0}^{N} |h_j(y)| = \mathcal{O}(N^{\frac{1}{2}}). \tag{4.45}$$

The following theorems give the convergence analysis for the proposed adaptive numerical scheme in the L^2 and L^∞-norms, respectively.

Theorem 4.4. *Let* U_ν *be the exact solution of the transformed* (4.26) *and* U_ν^N *be the numerical solution produced by the spectral scheme* (4.36)*. If* $U_\nu \in H^m(I)$*, then for* $m > 1$*,*

$$\|U_\nu - U_\nu^N\|_{L^2(I)} \leq CN^{-m} \left(|F_\nu|_{H^{m;N}(I)} + \beta_\nu |U_\nu|_{H^{m;N}(I)} + K_\nu^* \|U_\nu\|_\infty \right), \tag{4.46}$$

where

$$K_\nu^* = \max_{\xi\in I} |K_\nu(.,\xi)|_{H^{m;N}(I)} + N \max_{0\leq l\leq N} |K_\nu(\sigma_{N,l},.)|_{H^{m;N}(I)}. \tag{4.47}$$

Proof. Let the transformed equation in (4.26)

$$U_\nu(y) = F_\nu(y) + \int_{-1}^{1} K_\nu(y,\xi) U_\nu(\xi) d\xi. \tag{4.48}$$

while using the approximate solution, we have

$$U_\nu^N(y) = \mathcal{I}_N F_\nu(y) + (\mathcal{I}_{N,N} K_\nu(y,.), \mathcal{I}_N U_\nu)_N. \tag{4.49}$$

Subtracting (4.48) from (4.49) gives

$$\begin{aligned} U_\nu(y) - U_\nu^N(y) &= F_\nu(y) - \mathcal{I}_N F_\nu(y) \\ &\quad + \int_{-1}^{1} K_\nu(y,\xi) U_\nu(\xi) d\xi - (\mathcal{I}_{N,N} K_\nu(y,.), \mathcal{I}_N U_\nu)_N \\ &= J_1^\nu(y) + J_2^\nu(y) + J_3^\nu(y), \end{aligned} \tag{4.50}$$

where

$$J_1^\nu(y) = F_\nu(y) - \mathcal{I}_N F_\nu(y), \tag{4.51}$$

$$J_2^\nu(y) = \int_{-1}^{1} K_\nu(y,\xi)(U_\nu(\xi) - \mathcal{I}_N U_\nu(\xi)) d\xi, \tag{4.52}$$

$$J_3^\nu(y) = \int_{-1}^{1} (K_\nu(y,\xi) - \mathcal{I}_{N,N} K_\nu(y,\xi)) \mathcal{I}_N U_\nu(\xi) d\xi. \tag{4.53}$$

By the triangle inequality, we have

$$\|U_\nu - U_\nu^N\|_{L^2(I)} \leq \|J_1^\nu\|_{L^2(I)} + \|J_2^\nu\|_{L^2(I)} + \|J_3^\nu\|_{L^2(I)}. \tag{4.54}$$

Now, we will try to find a suitable upper bound to the above norms on the right-hand side of inequality (4.54). Firstly, by Lemma 11, we obtain

$$\|J_1^\nu\|_{L^2(I)} = \|F_\nu - \mathcal{I}_N F_\nu\|_{L^2(I)} \leq CN^{-m}|F_\nu|_{H^{m;N}(I)}. \tag{4.55}$$

Next, by Cauchy-Schwarz inequality, Fubini's theorem and by the Lemma 11, we obtain

$$\begin{aligned}
\|J_2^\nu\|_{L^2(I)} &= \left(\int_{-1}^{1}\left|\int_{-1}^{1} K_\nu(y,\xi)(U_\nu(\xi) - \mathcal{I}_N U_\nu(\xi))d\xi\right|^2 dy\right)^{\frac{1}{2}} \\
&\leq \left\{\int_{-1}^{1}\left[\left(\int_{-1}^{1}|K_\nu(y,\xi)|^2 d\xi\right)\left(\int_{-1}^{1}|U_\nu(\xi) - \mathcal{I}_N U_\nu(\xi)|^2 d\xi\right)\right] dy\right\}^{\frac{1}{2}} \\
&= \beta_\nu \|U_\nu - \mathcal{I}_N U_\nu\|_{L^2(I)} \leq \beta_\nu CN^{-m}|U_\nu|_{H^{m;N}(I)},
\end{aligned} \tag{4.56}$$

On the other hand, by Cauchy-Schwarz inequality and from Lemma 12, we have

$$\begin{aligned}
\|J_3^\nu\|_{L^2(I)} &= \left(\int_{-1}^{1}\left|\int_{-1}^{1}(K_\nu(y,\xi) - \mathcal{I}_{N,N}K_\nu(y,\xi))\mathcal{I}_N U_\nu(\xi)d\xi\right|^2 dy\right)^{\frac{1}{2}} \\
&\leq \left\{\int_{-1}^{1}\left[\left(\int_{-1}^{1}|K_\nu(y,\xi) - \mathcal{I}_{N,N}K_\nu(y,\xi)|^2 d\xi\right)\left(\int_{-1}^{1}|\mathcal{I}_N U_\nu(\xi)|^2 d\xi\right)\right] dy\right\}^{\frac{1}{2}} \\
&\leq \left(2\int_{-1}^{1}\max_{\xi\in I}|K_\nu(y,\xi) - \mathcal{I}_{N,N}K_\nu(y,\xi)|^2 dy\right)^{\frac{1}{2}} \|\mathcal{I}_N U_\nu\|_{L^2(I)} \\
&\leq C\|U_\nu\|_\infty \max_{\xi\in I}\left(\int_{-1}^{1}|K_\nu(y,\xi) - \mathcal{I}_{N,N}K_\nu(y,\xi)|^2 dy\right)^{\frac{1}{2}}.
\end{aligned} \tag{4.57}$$

Applying the Minkowski inequality on the right-hand side (4.57), we get:

$$\begin{aligned}
\left(\int_{-1}^{1}|K_\nu(y,\xi) - \mathcal{I}_{N,N}K_\nu(y,\xi)|^2 dy\right)^{\frac{1}{2}} &\leq \left(\int_{-1}^{1}|K_\nu(y,\xi) - \mathcal{I}_N K_\nu(y,\xi)|^2 dy\right)^{\frac{1}{2}} \\
&\quad + \left(\int_{-1}^{1}|\mathcal{I}_N\left(K_\nu(y,\xi) - \mathcal{I}_N K_\nu(y,\xi)\right)|^2 dy\right)^{\frac{1}{2}} \\
&\leq \|K_\nu(.,\xi) - \mathcal{I}_N K_\nu(.,\xi)\|_{L^2(I)} \\
&\quad + \sqrt{2}\max_{y\in I}|\mathcal{I}_N(K_\nu(y,\xi) - \mathcal{I}_N K_\nu(y,\xi))|.
\end{aligned}$$

Therefore, by Lemmas 11 and 13, we obtain that

$$\begin{aligned}\|J_3^\nu\|_{L^2(I)} &\leq C\|U_\nu\|_\infty \Big(\max_{\xi\in I} \|K_\nu(.,\xi) - \mathcal{I}_N K_\nu(.,\xi)\|_{L^2(I)} \\ &\quad + \sqrt{2} \max_{0\leq l\leq N} \|K_\nu(\sigma_{N,l},.) - \mathcal{I}_N K_\nu(\sigma_{N,l},.)\|_\infty \|\mathcal{I}_N\|_\infty \Big) \\ &\leq CN^{-m} \max_{\xi\in I} |K_\nu(.,\xi)|_{H^{m;N}(I)} \|U_\nu\|_\infty \\ &\quad + CN^{\frac{1}{2}-m} N^{\frac{1}{2}} \max_{0\leq l\leq N} |K_\nu(\sigma_{N,l},.)|_{H^{m;N}(I)} \|U_\nu\|_\infty \\ &= CN^{-m} K_\nu^* \|U_\nu\|_\infty. \end{aligned} \tag{4.58}$$

Consequently, a combination of the above error bounds for equations (4.55), (4.56) and (4.58) leads to the desired estimate. □

Next, we will give the error estimate in L^∞-norm.

Theorem 4.5. *Let U_ν be the exact solution of the transformed (4.26) and U_ν^N be the numerical solution produced by the spectral scheme (4.36). If $U_\nu \in H^m(I)$, then for $m > 1$,*

$$\|U_\nu - U_\nu^N\|_\infty \leq CN^{\frac{1}{2}-m} \left(|F_\nu|_{H^{m;N}(I)} + \|\mathcal{K}_\nu\|_\infty |U_\nu|_{H^{m;N}(I)} + K_\nu^{**} \|U_\nu\|_\infty \right), \tag{4.59}$$

where

$$K_\nu^{**} = \max_{\xi\in I} |K_\nu(.,\xi)|_{H^{m;N}(I)} + N^{\frac{1}{2}} \max_{0\leq l\leq N} |K_\nu(\sigma_{N,l},.)|_{H^{m;N}(I)}. \tag{4.60}$$

Proof. By the triangle inequality we have

$$\|U_\nu - U_\nu^N\|_\infty \leq \|J_1^\nu\|_\infty + \|J_2^\nu\|_\infty + \|J_3^\nu\|_\infty. \tag{4.61}$$

Firstly, by Lemma 11, we obtain

$$\|J_1^\nu\|_\infty = \|F_\nu - \mathcal{I}_N F_\nu\|_\infty \leq CN^{\frac{1}{2}-m} |F_\nu|_{H^{m;N}(I)}. \tag{4.62}$$

Also by Lemma 11 we obtain that

$$\begin{aligned}\|J_2^\nu\|_\infty &= \max_{y\in I} \left| \int_{-1}^{1} K_\nu(y,\xi)(U_\nu(\xi) - \mathcal{I}_N U_\nu(\xi)) d\xi \right| \\ &\leq \|U_\nu - \mathcal{I}_N U_\nu\|_\infty \max_{y\in I} \int_{-1}^{1} |K_\nu(y,\xi)| d\xi \\ &\leq CN^{\frac{1}{2}-m} |U_\nu|_{H^{m;N}(I)} \|\mathcal{K}_\nu\|_\infty. \end{aligned} \tag{4.63}$$

On the other hand, by Cauchy-Schwarz inequality and the triangular inequality, it follows from Lemma 12 that

$$\begin{aligned}\|J_3^\nu\|_\infty &= \max_{y\in I}\left|\int_{-1}^{1}(K_\nu(y,\xi)-\mathcal{I}_{N,N}K_\nu(y,\xi))\mathcal{I}_N U_\nu(\xi)d\xi\right| \\ &\le \sqrt{2}\max_{y,\xi\in I}|K_\nu(y,\xi)-\mathcal{I}_{N,N}K_\nu(y,\xi)|\|\mathcal{I}_N U_\nu\|_{L^2(I)} \\ &\le \sqrt{2}\max_{y,\xi\in I}|K_\nu(y,\xi)-\mathcal{I}_{N,N}K_\nu(y,\xi)|\,(C\|U_\nu\|_\infty) \\ &\le C\|U_\nu\|_\infty\left(\max_{\xi\in I}\|K_\nu(.,\xi)-\mathcal{I}_N K_\nu(.,\xi)\|_\infty\right. \\ &\quad \left.+\max_{y\in I}\|\mathcal{I}_N\left(K_\nu(y,.)-\mathcal{I}_N K_\nu(y,.)\right)\|_\infty\right).\end{aligned}$$

Then, by Lemmas 11 and 13 we obtain that

$$\begin{aligned}\|J_3^\nu\|_\infty &\le CN^{\frac{1}{2}-m}\max_{\xi\in I}|K_\nu(.,\xi)|_{H^{m;N}(I)}\|U_\nu\|_\infty \\ &\quad + C\|U_\nu\|_\infty\left(\max_{0\le l\le N}\|K_\nu(\sigma_{N,l},.)-\mathcal{I}_N K_\nu(\sigma_{N,l},.)\|_\infty\|\mathcal{I}_N\|_\infty\right) \\ &\le CN^{\frac{1}{2}-m}\|U_\nu\|_\infty\left(\max_{\xi\in I}|K_\nu(.,\xi)|_{H^{m;N}(I)}+N^{\frac{1}{2}}\max_{0\le l\le N}|K_\nu(\sigma_{N,l},.)|_{H^{m;N}(I)}\right) \\ &= CN^{\frac{1}{2}-m}K_\nu^{**}\|U_\nu\|_\infty. \qquad (4.64)\end{aligned}$$

Consequently, a combination of the above error bounds for equations (4.62), (4.63) and (4.64) leads to the desired estimate. □

4.3.4 Numerical experiments

To verify the effectiveness and efficacy of the suggested adaptive method, several numerical examples are considered. Moreover, a comparison with classical and other recent existing methods is also given. The computations are executed with Matlab software on a Core i5-2520M CPU running at 2.5 GHZ and 4 GB RAM. In addition, we denote the condition number of the collocation system with respect to the 2-norm by κ. The CPU times are recorded in seconds.

Example 4.7. Consider

$$u(x)-\int_{-1}^{1}(\sin(2\pi x+\pi t)+\cos(3xt)+\frac{xt^2}{3})u(t)dt=f(x),\quad x\in[-1,1], \qquad (4.65)$$

where

$$f(x)=-\frac{x}{3\pi^2}+\cos(2\pi x)+\frac{6x\sin(3x)}{4\pi^2-9x^2}.$$

By using the one-parameter mapping (3.22), according to (3.21) and (3.32), the non-negative weight function on J is given by

$$w_{J,\nu}(x)=\psi'_{-1,1}(\nu;x)=\frac{\theta}{\nu}\cos(\theta x),\quad \nu\in\mathscr{D}_\nu:=(0,1). \qquad (4.66)$$

Thus, we have

$$\beta_\nu^2 = \int_{-1}^{1}\int_{-1}^{1} |k(x,t)|^2 \frac{\cos(\theta x)}{\cos(\theta t)} dxdt \leq (7/3)^2 \int_{-1}^{1}\int_{-1}^{1} \frac{\cos(\theta x)}{\cos(\theta t)} dxdt < \infty. \tag{4.67}$$

Indeed,

$$\int_{-1}^{1}\int_{-1}^{1} \frac{\cos(\theta x)}{\cos(\theta t)} dxdt = \frac{2\sin(\theta)}{\theta} \int_{-1}^{1} \frac{dt}{\cos(\theta t)} = \frac{2\sin(\theta)}{\theta^2} \ln\left[\frac{1+\sin(\theta)}{1-\sin(\theta)}\right]. \tag{4.68}$$

Recall that $\theta = \arcsin(\nu)$, hence we obtain

$$\int_{-1}^{1}\int_{-1}^{1} \frac{\cos(\theta x)}{\cos(\theta t)} dxdt = \frac{2\nu}{\arcsin^2(\nu)} \ln\left[\frac{1+\nu}{1-\nu}\right] < \infty, \tag{4.69}$$

because the argument of the logarithm is strictly positive. Therefore, the assumption of Lemma 9 is satisfied. On the other hand, by using the trigonometric identities for the sine function and the parity of cosine, it is not hard to show that the homogeneous integral equation of (4.65) has only the trivial solution $u \equiv 0$. Then, by Theorem 4.3, it follows that the transformed integral equation possesses a unique solution in $L^2(I)$ for any $f \in L^2_{w_{J,\nu}}(J)$.

In fact, the exact solution of (4.65) is $u(x) = \cos(2\pi x)$, which has periodic variations. A comparison of the absolute errors obtained by the present method and those obtained by the standard Legendre collocation approach in [30] are given in Table 4.4. The results clearly show the superiority of our method. Figure 4.10a shows the 2D contour plot of the $\log_{10} L^2$ errors, from which it can be seen that full spectral convergence is obtained over the entire range of ν-values extending from 0.4 to 0.6, and a much faster convergence rate is achieved with $\nu = 0.5$. Figure 4.10b shows the absolute error for $N = 15$ and $\nu = 0.5$. In further unreported results, the condition number in this example does not exceed 5.8 for all tested values of N and ν.

TABLE 4.4: Comparison of absolute errors with existing method for Example 4.7

	Method in [30]			Present method		
				$\nu = 0.87$	$\nu = 0.707$	$\nu = 0.5$
x	$N = 7$	$N = 9$	$N = 13$	$N = 7$	$N = 9$	$N = 13$
0.999	2.91e−01	4.77e−02	3.00e−04	6.16e−03	1.05e−05	2.33e−15
0.753	6.96e−02	1.58e−02	9.13e−04	7.08e−04	3.26e−06	7.98e−15
0.352	1.36e−01	1.39e−02	4.09e−05	8.28e−04	1.16e−06	5.21e−15
0.001	1.41e−01	1.75e−02	8.36e−05	1.24e−03	2.31e−06	5.55e−16
−0.001	1.41e−01	1.75e−02	8.36e−05	1.24e−03	2.31e−06	1.11e−16
−0.352	1.37e−01	1.39e−02	4.10e−05	1.06e−03	1.36e−06	2.66e−15
−0.753	7.15e−02	1.58e−02	9.13e−05	6.25e−04	3.11e−06	4.88e−15
−0.999	9.91e−01	4.77e−02	3.00e−04	5.95e−03	1.06e−05	3.66e−15

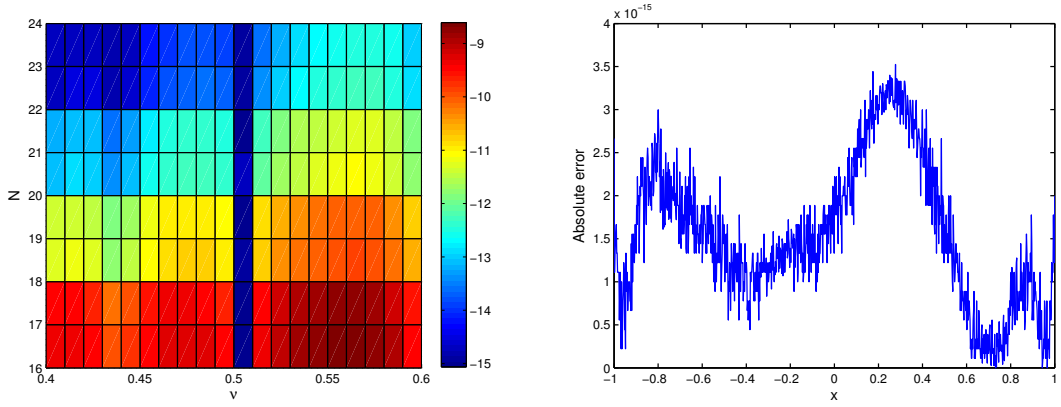

(A) $\log_{10}(L^2$ errors) versus N and ν

(B) Absolute error for $N = 15, \nu = 0.5$

FIGURE 4.10: Convergence rates and absolute error for Example 4.7.

Example 4.8. [24, Family 4 in Chap. 10] Consider

$$u(x) - \int_a^b (x - p_2)(t - p_3)u(t)dt = f(x), \quad x \in [a, b], \tag{4.70}$$

where

$$f(x) = \frac{r}{(x - p_1)^2 + r^2} - (x - p_2)r\left\{\frac{1}{2}\alpha(r) + \frac{(p_1 - p_3)}{r}\beta(r)\right\},$$

with

$$\alpha(r) = \ln\left[\frac{(b - p_1)^2 + r^2}{(a - p_1)^2 + r^2}\right], \quad \beta(r) = \arctan\left(\frac{b - p_1}{r}\right) - \arctan\left(\frac{a - p_1}{r}\right),$$

whose solution is

$$u(x) = \frac{r}{(x - p_1)^2 + r^2},$$

which has steep gradients near $x = p_1$. Depending on the equation parameters, we proceed in three cases. In all cases, we use the two-parameter mapping (3.23) with

$$\nu_1 = \frac{b - a}{2r}, \quad \nu_2 = \frac{2}{b - a}p_1 - \frac{b + a}{b - a}.$$

Case 1 $a = 0, b = 1, p_1 = 1/2$ and $p_2 = p_3 = 0$. Table 4.5 displays a comparison of the classical method and the present method for $r = 1/10$. The findings demonstrate that the present method successfully recovered the lost fast convergence observed in the classical method. Furthermore, this achievement was attained with exceptional accuracy and consistently low condition numbers. Figure 4.11 illustrates a comparison of convergence rates between the adaptive and the SE/DE-Sinc-collocation methods [67, 68] for $r = 1/2$. As it can be seen from this figure, all best accuracies were obtained with the sinc approximations for N listed $(N = 5, 10, 15, ..., 140)$ are obtained using the present method with N does not exceed 20.

Case 2 $a = -1$, $b = 1$, $p_i = 0$, $i = 1, 2, 3$. Table 4.6 presents the results for $r-$values as small as possible, indicating a satisfactory performance and a condition number close to 1 as r decreases. It is worth noting that, once again, the classical method has proven to be inadequate.

Case 3 $a = 0$, $b = 1$, $p_2 = 1/4$, $p_3 = 1/2$ and p_1 is chosen near the endpoints of the interval. Results for $r = 1/20$ are displayed in Table 4.7.

Additionally, Figure 4.12 illustrates the important effect of the two-parameter mapping (3.23) on the integrand of the equation.

TABLE 4.5: Comparison results for Example 4.8, Case 1 with $r = 1/10$

	Classical method			Present method		
N	L^∞ error	L^2 error	κ	L^∞ error	L^2 error	κ
8	2.43e+00	1.26e+00	1.56	2.96e−04	6.91e−05	1.56
12	1.25e+00	5.40e−01	1.57	5.52e−08	1.07e−08	1.56
16	6.34e−01	2.41e−01	1.57	3.14e−12	5.33e−13	1.56
20	3.15e−01	1.08e−01	1.58	1.06e−14	4.87e−15	1.56

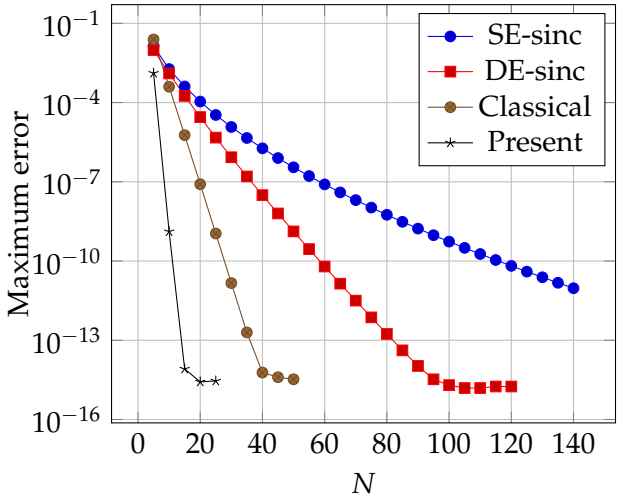

FIGURE 4.11: Convergence with respect to N for Example 4.8, Case 1 with $r = 1/2$.

TABLE 4.6: Results of the present method for Example 4.8, Case 2, $N = 20$

r	1/100	1/1000	1/10000	1/100000	1/1000000
L^∞ error	6.43e−14	8.59e−13	7.94e−12	8.89e−11	1.03e−09
L^2 error	4.79e−14	5.17e−13	4.58e−12	4.85e−11	4.50e−10
κ	1.53	1.00	1.00	1.00	1.00

TABLE 4.7: Comparison of the L^∞ errors for Example 4.8, Case 3

	Classical method				Present method			
N	$p_1 = 1/10$	κ	$p_1 = 9/10$	κ	$p_1 = 1/10$	κ	$p_1 = 9/10$	κ
8	1.06e+01	1.13	1.06e+01	1.13	6.15e−04	1.05	9.94e−04	1.16
16	3.63e+00	1.13	3.62e+00	1.13	9.13e−06	1.12	9.53e−06	1.37
32	3.81e−01	1.13	3.81e−01	1.13	9.16e−10	1.12	9.16e−10	1.35
64	3.36e−03	1.13	3.36e−03	1.13	5.33e−14	1.12	6.75e−14	1.35

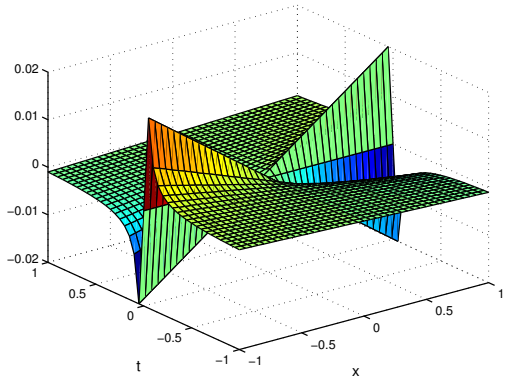

(A) Integrand, Case 2, $r = 1/1000$

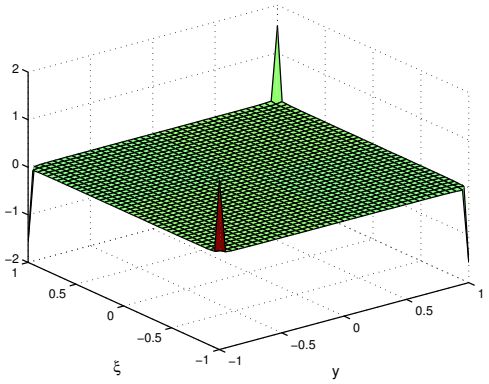

(B) Transformed integrand, Case 2, $r = 1/1000$

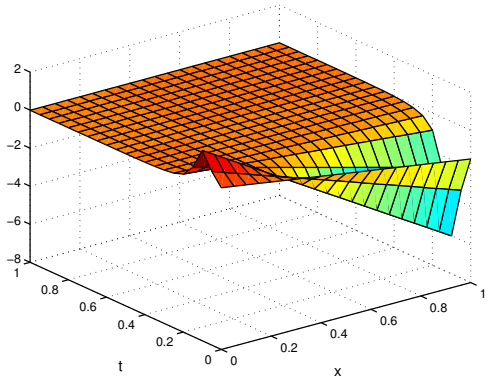

(C) Integrand, Case 3, $p_1 = 1/10$

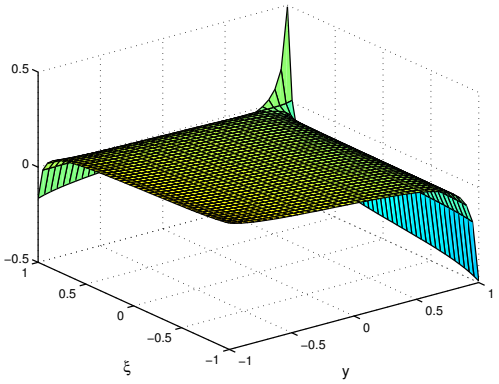

(D) Transformed integrand, Case 3, $p_1 = 1/10$

FIGURE 4.12: Effect of the mapping (3.23) on the integrand of Example 4.8

.

Example 4.9. Consider

$$u(x) - \frac{1}{2}\int_{-1}^{1}(x+t)u(t)dt = f(x), \quad x \in [-1,1], \tag{4.71}$$

where $f(x)$ is chosen so that for a non-negative constant k, the exact solution of this equation is $u(x) = 1/(1+kx^2)$, which has steep gradients near $x = 0$ for large $k \gg 1$, and is

often called Runge's function when $k = 25$. We solve this equation for $k = 25$ by using the two-parameter mapping (3.23) with $\nu = (5, 0)$. The comparison of the obtained results with those of the classical method is shown in Table 4.8. Figure 4.13 illustrates appropriate ranges for ν_1-parameter to obtain faster convergence rates when $k = 25$. Figure 4.14 shows the convergence between the present method by using the two-parameter mapping (3.23) with $\nu = (\sqrt{k}, 0)$ and the classical method. Based on this figure, it can be seen that our method is reliable and performs well in all cases, while the classical method degrades as k increases.

TABLE 4.8: Comparison results for Example 4.9, with $k = 25$

	Classical method			Present method		
N	L^∞ error	L^2 error	κ	L^∞ error	L^2 error	κ
8	2.61e−01	1.27e−01	4.03	2.96e−05	6.91e−06	3.91
12	1.29e−01	5.42e−02	4.07	5.52e−09	1.07e−09	3.95
16	6.41e−02	2.41e−02	4.09	3.14e−13	5.33e−14	3.95
20	3.17e−02	1.08e−02	4.11	1.11e−15	4.95e−16	3.96

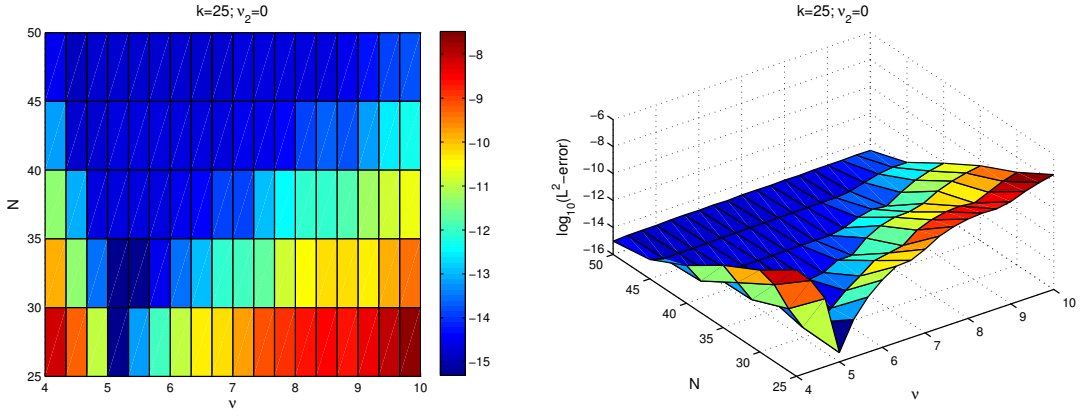

FIGURE 4.13: Convergence rates for Example 4.9

Example 4.10. Consider

$$u(x) - \frac{1}{2}\int_0^1 xe^{-t(1+x)}u(t)dt = f(x), \quad x \in [0, 1], \tag{4.72}$$

where $f(x)$ is chosen so that for an arbitrary constant k, the exact solution of this equation is

$$u(x) = \exp\left(-\frac{(x-\lambda)^2}{2k^2}\right),$$

which has steep gradients near $x = \lambda$. We solve this example for different values of k and fixed $\lambda = 1/2$, by using the two-parameter mapping (3.23) with $\nu = (1/10k, 0)$.

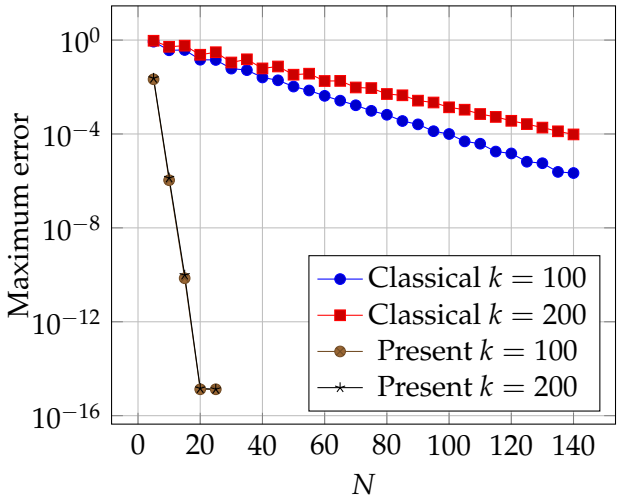

FIGURE 4.14: Convergence with respect to N for Example 4.9

In Table 4.9, we compare the L^∞ errors, condition numbers and CPU time between the present method and its classical one. Additional results are listed in Table 4.10. Figure 4.15 illustrates the region that we can choose the ν-parameter to provide a good estimate of the error for the given example. We observe that the accuracy is very sensitive over a small range of ν_2-parameter, but remains stable in a wide range of ν_1-parameter.

TABLE 4.9: Comparison results for Example 4.10, with $k = 0.05$

	Classical method			Present method		
N	L^∞ error	κ	CPU	L^∞ error	κ	CPU
16	1.78e−01	1.19	0.1199	5.58e−03	1.18	0.1253
32	4.54e−03	1.19	0.1235	2.04e−07	1.18	0.1322
64	4.79e−09	1.19	0.1514	2.00e−16	1.19	0.1550

TABLE 4.10: The L^∞ and L^2 errors of the present method for Example 4.10

	L^∞ error		L^2 error	
N	$k = 0.01$	$k = 0.005$	$k = 0.01$	$k = 0.005$
16	6.57e−02	7.80e−02	1.76e−02	2.17e−02
32	5.83e−06	4.29e−05	4.42e−06	6.10e−06
64	2.11e−10	1.74e−10	2.19e−11	5.11e−11

Example 4.11. Consider

$$u(x) - \frac{1}{2}\int_{-1}^{1} x^2 t u(t)dt = f(x), \quad x \in [-1, 1], \tag{4.73}$$

where $f(x)$ is chosen so that for a non-negative constant k, the exact solution of this equation is $u(x) = \text{erf}(x/\sqrt{k})$, which has a steep front at $x = 0$ for small $k \ll 1$. We solve this

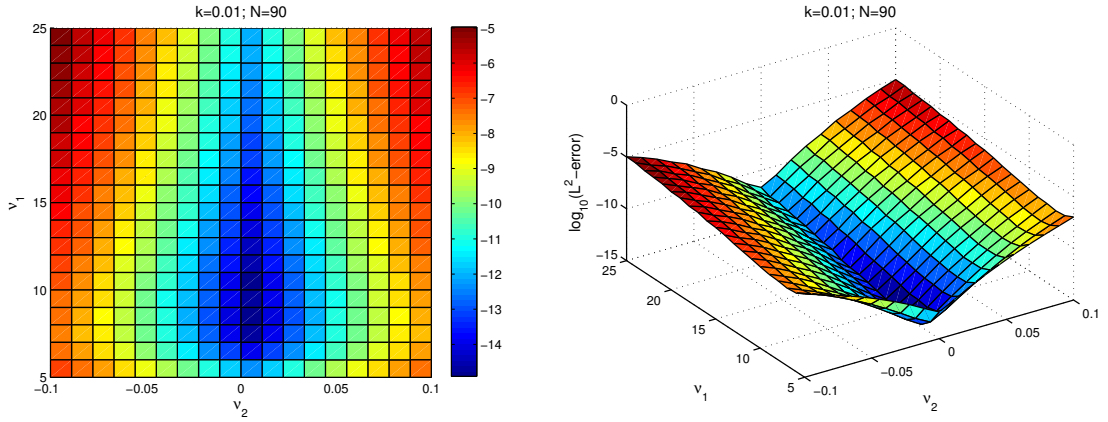

FIGURE 4.15: Optimal ν-parameters achieving the best accuracy Example 4.10.

equation for $k = 0.01$ by using the two-parameter mapping (3.23) with $\nu = (3, 0)$. The comparison of the obtained results with those of the classical method is shown in Table 4.11. The L^∞ and L^2 errors are given in Table 4.12.

TABLE 4.11: Comparison results for Example 4.11, with $k = 0.01$

	Classical method			Present method		
N	L^∞ error	κ	CPU	L^∞ error	κ	CPU
16	1.75e−01	1.38	0.1116	1.82e−03	1.31	0.1225
32	1.06e−02	1.39	0.1119	6.50e−08	1.33	0.1257
64	1.88e−06	1.40	0.1235	3.54e−14	1.34	0.1451

TABLE 4.12: The L^∞ and L^2 errors of the present method for Example 4.11

	L^∞ error		L^2 error	
N	$\nu_1 = 10$ $k = 10^{-3}$	$\nu_1 = 25$ $k = 10^{-4}$	$\nu_1 = 10$ $k = 10^{-3}$	$\nu_1 = 25$ $k = 10^{-4}$
16	4.85e−03	2.81e−02	1.77e−03	1.53e−02
32	3.58e−06	5.34e−05	4.46e−07	1.16e−05
64	1.69e−11	1.68e−10	1.86e−12	1.55e−11

Example 4.12. Consider

$$u(x) - \int_{-\infty}^{\infty} (x^2 + t^2) e^{-x^2 - t^2} u(t) dt = f(x), \quad x \in (-\infty, \infty), \tag{4.74}$$

where $f(x)$ is chosen so that for an arbitrary constant k, the exact solution of this equation is $u(x) = e^{-x^2} \cos(kx)$, which decays rapidly with oscillation. By truncating the interval

of integration $(-\infty, \infty)$ to $[-6, 6]$, and using the one-parameter mapping (3.22) with $\nu = 0.9$, it is found that the present method is more reliable than the classical method (see Table 4.13).

TABLE 4.13: Comparison results for Example 4.12, $N = 128$

	Classical method		Present method	
k	L^∞ error	L^2 error	L^∞ error	L^2 error
8	2.97e−15	2.11e−15	4.22e−15	1.58e−15
12	1.96e−08	1.72e−09	2.11e−15	8.20e−16
16	1.57e−03	1.63e−04	5.13e−12	3.68e−13

4.3.5 Analysis of results

The suggested approach can enhance the classical algorithm's efficiency by offering considerable computational benefits. Specifically, by employing the mapping strategy, as demonstrated in Example 4.8, the steep gradients that corrupt the numerical solution can be eliminated from the central part of the computational domain and confined to its boundaries. This not only reduces the computational cost but also substantially enhances the precision of the results. However, Example 4.7 demonstrates that the ν-parameter plays a crucial role in significantly improving convergence rates, particularly when the solution exhibits weak periodic variations. In essence, by slightly adjusting the grid points, the mapping strategy can achieve higher convergence rates.

Also, it is worth noticing that, when the usual mappings (3.22) and (3.23) approach the identity as $\nu \to 0$, the adaptive algorithm performs exactly as the classical algorithm.

Overall, the adaptive spectral method presented in this paper provides a powerful and flexible approach for solving FIEs, including those with localized rapid variations, steep gradients, or a steep front. Although we have not yet actually done so, it is also possible to extend this method to nonlinear IEs with similar challenging properties, and this is one of the goals of our future work.

Appendix A

Converting differential equations to integral equations

A.1 Converting initial value problem to Volterra integral equation

We show in this appendix how a initial value problem (IVP) can be transformed to an equivalent Volterra integral equation (VIE). The second-order IVP (1.2) is repeated here as

$$y''(x) + p(x)y'(x) + q(x)y(x) = g(x), \tag{A.1}$$

with the initial conditions

$$y(0) = \alpha,\ y'(0) = \beta,$$

where α and β are constants. The functions $p(x)$, $q(x)$ and $g(x)$ are continuous functions through the interval of discussion. Let us make transformation

$$y''(x) = u(x), \tag{A.2}$$

where $u(x)$ is a continuous function. By integrating both sides of (A.2) over the interval $[0, x]$ we obtain

$$y'(x) = \beta + \int_0^x u(t)dt. \tag{A.3}$$

Integrating both sides of equation (A.3) from 0 to x and applying the given initial condition at $x = 0$ yields

$$\begin{aligned} y(x) &= y(0) + x\beta + \int_0^x \int_0^t u(s)dsdt \\ &= \alpha + x\beta + \int_0^x \int_0^t u(s)dsdt, \end{aligned}$$

and using the formula that reduce double integral to a single integral we obtained that

$$y(x) = \alpha + \beta x + \int_0^x (x - t)u(t)dt. \tag{A.4}$$

Substituting (A.2) , (A.3) and (A.4) into the second-order IVP (A.1) yields

$$u(x) + p(x)\left[\beta + \int_0^x u(t)dt\right] + q(x)\left[\alpha + \beta x + \int_0^x (x-t)u(t)dt\right] = g(x).$$

Therefore the above equation can be written as the VIE of the second kind

$$u(x) = f(x) + \int_0^x k(x,t)u(t)dt,$$

where the kernel is given by

$$k(x,t) = -p(x) + q(x)(t-x)$$

and the free term is given by

$$f(x) = g(x) - [\beta p(x) + \alpha q(x) + \beta x q(x)].$$

A.2 Converting boundary value problem to Fredholm integral equation

We show in this appendix how a boundary value problem (BVP) can be transformed to an equivalent Fredholm integral equation (FIE). The two-point BVP (1.4) is repeated here as

$$y''(x) + p(x)y'(x) + q(x)y(x) = g(x), \tag{A.5}$$

with the boundary conditions

$$y(0) = \alpha,\ y(1) = \beta,$$

where α and β are given constants. Let us make transformation

$$y''(x) = u(x). \tag{A.6}$$

By integrating both sides of equation (A.6) from 0 to x we obtain

$$y'(x) = y'(0) + \int_0^x u(t)dt. \tag{A.7}$$

Integrating both sides of equation (A.7) from 0 to x and applying the given boundary condition at $x = 0$ yields

$$\begin{aligned} y(x) &= y(0) + xy'(0) + \int_0^x \int_0^t u(s)dsdt \\ &= \alpha + xy'(0) + \int_0^x \int_0^t u(s)dsdt, \end{aligned}$$

and using the formula that reduce double integral to a single integral we obtained that

$$y(x) = \alpha + xy'(0) + \int_0^x (x-t)u(t)dt. \tag{A.8}$$

Substitution of (A.6), (A.7) and (A.8) into the second-order BVP (A.5) yields

$$u(x) + p(x)\left[y'(0) + \int_0^x u(t)dt\right] + q(x)\left[\alpha + xy'(0) + \int_0^x (x-t)u(t)dt\right] = g(x)$$

which is rearranged to

$$\begin{aligned} u(x) + \alpha q(x) + [p(x) + xq(x)]\, y'(0) \\ + p(x)\int_0^x u(t)dt + q(x)\int_0^x (x-t)u(t)dt = g(x). \end{aligned} \tag{A.9}$$

The unknown constant $y'(0)$ can be determined by substituting $x = 1$ into (A.8), applying the boundary condition $y(1) = \beta$ and solving for $y'(0)$, yields

$$y'(0) = (\beta - \alpha) - \int_0^1 (1-t)u(t)dt, \tag{A.10}$$

which, when substituted into (A.9), yields

$$\begin{aligned} u(x) + \alpha q(x) + (\beta - \alpha)\,[p(x) + xq(x)] - (p(x) + xq(x))\int_0^1 (1-t)u(t)dt \\ + p(x)\int_0^x u(t)dt + q(x)\int_0^x (x-t)u(t)dt = g(x) \end{aligned}$$

or equivalently

$$\begin{aligned} u(x) =& g(x) - \alpha q(x) - (\beta - \alpha)(p(x) + xq(x)) \\ &+ \int_0^x [(1-t)\,[p(x) + xq(x)] - p(x) - (x-t)q(x)]\, u(t)dt \\ &+ \int_x^1 (1-t)(p(x) + xq(x))u(t)dt. \end{aligned}$$

Therefore the above equation can be written as the FIE of the second kind

$$u(x) = f(x) + \int_0^1 k(x,t)u(t)dt,$$

where the free term is given by

$$f(x) = g(x) - \alpha q(x) - (\beta - \alpha)[p(x) + xq(x)]$$

and the kernel is given by

$$k(x,t) = \begin{cases} -(p(x) + (x-1)q(x))t, & 0 \le t \le x, \\ \\ (p(x) + xq(x))(1-t), & x \le t \le 1. \end{cases}$$

For more details on converting boundary value problems (BVPs) to Fredholm integral equations (FIEs) and initial value problems (IVPs) to Volterra integral equations (VIEs), see, e.g. [44, 71].

Conclusion and perspectives

In this thesis, we have presented accurate spectral solution methods for Volterra and Fredholm IEs, which naturally arise from the mathematical modeling of initial and boundary value problems associated with ordinary and partial DEs.
At first, we have applied the Legendre spectral Galerkin method and its iterated version to solve FIEs of the second kind and analyzed their convergence in the L^2 norm. The numerical results obtained in Subsection 4.1.3 show that the iterated Legendre spectral Galerkin solution provides a better approximation than the Legendre spectral Galerkin method. Hence, the iterated Legendre spectral-Galerkin solution improves over the Legendre spectral-Galerkin solution. The advantage of this method is that its convergence behavior depends solely on the smoothness properties of the solution and kernel.
Secondly, we have developed and analyzed an adaptive spectral collocation method for Volterra and Fredholm IEs of the second kind, where the underlying solution exhibits localized rapid variations, steep gradients, or a steep front. The suggested approach can enhance the efficiency of the classical algorithm by providing significant computational advantages. This is particularly achieved through the use of a mapping strategy, as shown in the numerical results presented in Subsections 4.3.4. These results clearly show that our method is better than the classical method for such problems.
The main advantages of the suggested approach include:

(i) Dynamically adjust resolution based on solution characteristics;

(ii) Implement moving grid points for capturing the localized rapid variations in the solution of the given problem;

(ii) Clustering of grid points around steep gradients or a steep front to effectively track critical features of the solution.

The perspectives are:

- Extending the results obtained in this thesis to nonlinear IEs with similar challenging properties.
- Extending the results obtained in this thesis to higher-dimensions IEs with similar challenging properties.

These issues will be addressed in future work.

Bibliography

[1] I. Abdennebi and A. Rahmoune. "Adaptive spectral solution method for Fredholm integral equations of the second kind". In: *Numer. Algor.* 96 (2023), pp. 975–998. DOI: 10.1007/s11075-023-01671-1.

[2] N.H. Abel. "Auflösung einer mechanischen Aufgabe". In: *J. Die Reine Angew. Math.* 1 (1826), pp. 153–157.

[3] N.H. Abel. "Solution de quelques problemesa l'aide d'intégrales définites, oeuvres completes, 1, 16–18". In: *Grondahl, Christiania, Norway* (1881).

[4] M. Abramowitz and I.A. Stegun. *Handbook of Mathematical Functions with Formulas, Graphs, and Mathematical Tables*. Dover Publications, New York, 1992.

[5] K. Adamiak. "Application of integral equations to solving inverse problems of stationary electromagnetic fields". In: *Int. J. Numer. Methods Eng.* 21.12 (1985), pp. 1447–1458. DOI: 10.1002/nme.1620210807.

[6] K. E. Atkinson. "A survey of numerical methods for solving nonlinear integral equations". In: *The Journal of Integral Equations and Applications* (1992), pp. 15–64.

[7] K.E. Atkinson. *The Numerical Solution of Integral Equations of the Second Kind*. 1st. Cambridge: Cambridge Univ. Press, 1997.

[8] K.E. Atkinson and W. Han. *Theoretical Numerical Analysis*. Springer Verlag, Berlin, 2nd edition, 2005.

[9] K.E. Atkinson and F. Potra. "The discrete Galerkin method for nonlinear integral equations". In: *J. Integral Equations Appl.* (1988), pp. 17–54.

[10] K.E. Atkinson and F.A. Potra. "On the discrete Galerkin method for Fredholm integral equations of the second kind". In: *IMA Journal of Numerical Analysis* 9.3 (1989), pp. 385–403.

[11] K.E. Atkinson and F.A. Potra. "Projection and iterated projection methods for nonlinear integral equations". In: *SIAM Journal on Numerical Analysis* 24.6 (1987), pp. 1352–1373. DOI: doi.org/10.1137/0724087..

[12] S. Benyoussef and A. Rahmoune. "Efficient spectral-collocation methods for a class of linear fredholm integro-differential equations on the half-line". In: *J. Cmoput. Appl. Math.* 377 (2020), p. 112894. DOI: 10.1016/j.cam.2020.112894.

[13] M. Bôcher. *An introduction to the study of integral equations*. 10. University Press, 1926.

[14] J. P. Boyd. *Chebyshev and Fourier spectral methods*. Dover Publications, 2000.

[15] C. Brezinski and M. Redivo-Zaglia. "Extrapolation methods for the numerical solution of nonlinear Fredholm integral equations". In: *Journal of Integral Equations and Applications* 31.1 (2019), pp. 29 –57. DOI: 10.1216/JIE-2019-31-1-29.

[16] H. Brunner. *Volterra integral equations: an introduction to theory and applications*. Vol. 30. Cambridge University Press, 2017.

[17] H. Brunner and P. J. van der Houwen. "The numerical solution of Volterra equations". In: *CWI Monographes* vol 3. (1986), p.588.

[18] C. Canuto et al. *Spectral Methods: Evolution to Complex Geometries and Applications to Fluid Dynamics*. New York: Springe-Verlag, 2007.

[19] C. Canuto et al. *Spectral methods: Fundamentals in Single Domains*. 1st. Berlin: Springe-Verlag, 2006.

[20] C. Canuto et al. *Spectral Methods in Fluid Dynamics*. New York: Springe-Verlag, 1988.

[21] W. G. Charles. "Integral equations of the first kind, inverse problems and regularization". In: (2007), p. 37.

[22] Z. Chen, C.A. Micchelli, and Y. Xu. *Multiscale Methods for Fredholm Integral Equations*. Cambridge University Press, 2015.

[23] P. J. Davis and P. Rabinowitz. *Methods of Numerical Integration*. Academic Press, New York, 1984.

[24] L. M. Delves and J. L. Mohamed. *Computational methods for integral equations*. Cambridge: Cambridge University Press, 1988.

[25] Z. Denkowski, S. Migórski, and N. S. Papageorgiou. *An introduction to nonlinear analysis: theory*. Springer Science & Business Media, 2013.

[26] E.H. Doha et al. "Shifted Jacobi spectral collocation method with convergence analysis for solving integro-differential equations and system of integro-differential equations". In: *Nonlinear Analysis: Modelling and Control* 24.3 (2019), pp. 332–352. DOI: 10.15388/NA.2019.3.2.

[27] B. Doman. *The classical orthogonal polynomials*. World Scientific: Singapor, 2015.

[28] S. E. El-Gendi. "Chebyshev solution of differential, integral and integro-differential equations". In: *Comput. J.* 12 (1969), pp. 282–287. DOI: 10.1093/comjnl/12.3.282.

[29] N. Engibaryan. "On a problem in nonlinear radiative transfer". In: *Astrophysics* 2.1 (1966), pp. 12–14.

[30] Z.K. Eshkuvatov et al. "Effective approximation method for solving linear fredholm-volterra integral equations". In: *Numer. Algebra Control Optim.* 7.1 (2017), pp. 77–88.

[31] R. Farengo, Y.C. Lee, and P.N. Guzdar. "An electromagnetic integral equation: application to microtearing modes". In: *Phys. Fluids.* 26.12 (1983), pp. 3515–3523. DOI: 10.1063/1.864112.

[32] D. Funaro. *Polynomial approximation of differential equations*. Springer-Verlag, Berlin, 1992.

[33] N. Georg et al. "Enhanced adaptive surrogate models with applications in uncertainty quantification for nanoplasmonics". In: *International Journal for Uncertainty Quantification* 10.2 (2020).

[34] M.A. Golberg. *Numerical solution of integral equations*. Plenum Press, New York, 1990.

[35] M.A. Golberg. *Numerical Solution of Integral Equations*. Plenum Press, New York, 1990.

[36] I.G. Graham, S. Joe, and L. Sloan. "Iterated Galerkin versus iterated collocation for integral equations of the second kind". In: *IMA J. Numer. Anal.* 5 (1985), pp. 355–369. DOI: 10.1093/imanum/5.3.355.

[37] Charles W Groetsch. "Integral equations of the first kind, inverse problems and regularization: a crash course". In: *Journal of Physics: Conference Series*. Vol. 73. 1. IOP Publishing. 2007, p. 012001.

[38] B.-Y. Guo. "Jacobi spectral approximations to differential equations on the half line". In: *Journal of Computational Mathematics* (2000), pp. 95–112.

[39] B.-Y. Guo and L.-L. Wang. "Jacobi approximations in non-uniformly Jacobi-weighted Sobolev spaces". In: *J. Approx. Theory* 128.1 (2004), pp. 1–41.

[40] W. Hackbusch. *The Concept of Stability in Numerical Mathematics*. Berlin: Springer, 2014.

[41] S. Heinrich and P. Mathé. "The Monte Carlo Complexity of Fredholm Integral Equations". In: *Mathematics of Computation* 60.201 (1993), pp. 257–278. ISSN: 00255718, 10886842. DOI: https://doi.org/10.2307/2153165. (Visited on 09/16/2023).

[42] H.M. Wang H.J. Ding and W.Q. Chen. "Analytical solution for the electroelastic dynamics of a nonhomogeneous spherically isotropic piezoelectric hollow sphere". In: *Arch. Appl. Mech.* 73 (2003), pp. 49–62.

[43] H. Hochstadt. *Integral Equations*. Wliey: Wiley Classics Library, 2011.

[44] A. Jerri. *Introduction to Integral Equations with Applications*. New York: Marcel Dekker, 1985.

[45] S. Jiang and V. Rokhlin. "Second kind integral equations for the classical potential theory on open surfaces II". In: *J. Comput. Phys.* 195.1 (2004), pp. 1–16. DOI: 10.1016/j.jcp.2003.10.001.

[46] Y.-J. Jiang. "On spectral methods for Volterra-type integro-differential equations". In: *Journal of computational and applied mathematics* 230.2 (2009), pp. 333–340.

[47] D. R. Kincaid and E. W. Cheney. *Numerical analysis: mathematics of scientific computing*. Vol. 2. American Mathematical Soc., 2009.

[48] D. A. Kopriva. *Implementing spectral methods for partial differential equations: Algorithms for scientists and engineers*. Springer Science & Business Media, 2009.

[49] R. Kress. *Linear integral equation*. New York: Springer-Verlag, 1998.

[50] R. Kress. *Linear Integral Equations*. Applied Mathematical Sciences: Springer New York, 2014.

[51] E. Kreyszig. *Introductory functional analysis with applications*. John Wiley & Sons, 1.

[52] V.V. Kulish and V.B. Novozhilov. "Integral equation for the heat transfer with the moving boundary". In: *J. Thermophys. Heat Trans.* 17.04 (2003), pp. 538–540. DOI: 10.2514/2.7653.

[53] A. Kumar. "An analytical solution to applied mathematics-related love?s equation using the boubaker polynomials expansion scheme". In: *J. Frankl. Inst.* 347.9 (2010), pp. 1755–1761. DOI: 10.1016/j.jfranklin.2010.08.008.

[54] P. M. Lima et al. "Finite element solution of a linear mixed-type functional differential equation". In: *Numerical Algorithms* 55 (2 2010), pp. 301–320. ISSN: 1572-9265. DOI: https://doi.org/10.1007/s11075-010-9412-y.

[55] Y. Liu. "Application of the chebyshev polynomial in solving fredholm integral equations". In: *Math. Comput. Model.* 50.3 (2009), pp. 465–469. DOI: 10.1016/j.mcm.2008.10.007.

[56] E. R. Love. "The electrostatic field fo two equal circular co-axial conducting disks". In: *Quart. J. Mech. Appl. Math.* 2.4 (1949), pp. 428–451. DOI: 10.1093/qjmam/2.4.428.

[57] M. Heydari M. Tafakkori-Bafghi GB. Loghmani and X. Bai. "Jacobi-Picard iteration method for the numerical solution of nonlinear initial value problems". In: *Wiley* (2019).

[58] K. Maleknejad, H. Derili, and S. Sohrabi. "Numerical solution of Urysohn integral equations using the iterated collocation method". In: *International Journal of Computer Mathematics* 85.1 (2008), pp. 143–154.

[59] K. Maleknejad, K. Nouri, and M. Yousefi. "Discussion on convergence of legendre polynomial for numerical solution of integral equations". In: *Appl. Math. Comput.* 193.2 (2007), pp. 335–339. DOI: 10.1016/j.amc.2007.03.062.

[60] B. Mandal and S. Bhattacharya. "Numerical solution of some classes of integral equations using bernstein polynomials". In: *Appl. Math. Comput.* 190.2 (2007), pp. 1707–1716. DOI: 10.1016/j.amc.2007.02.058.

[61] G. Mastroianni and D. Occorsio. "Optimal systems of nodes for Lagrange interpolation on bounded intervals". In: *Journal of Computational and Applied Mathematics* 134 (2001), pp. 325–341. DOI: 10.1016/S0377-0427(00)00557-4.

[62] S.G. Mikhlin. *Integral Equations and Their Applications to Certain Problems in Mechanics, Mathematical Physics and Technology*. New York: Macmillan, 1964.

[63] G. V. Milovanovic and D. Joksimovic. "Properties of boubaker polynomials and an application to love's integral equation". In: *Appl. Math. Comput.* 224 (2013), pp. 74–87. DOI: 10.1016/j.amc.2013.08.055.

[64] B. L. Moiseiwitsch. *Integral equations*. CourierCorporation, 2011.

[65] E. D. Muhammet. "A numerical approach for singularly perturbed reaction diffusion type Volterra-Fredholm integro-differential equations". In: *Journal of Applied Mathematics and Computing* (2023). ISSN: 1865-2085. DOI: https://doi.org/10.1007/s12190-023-01895-3.

[66] E. D. Muhammet et al. "A second-order numerical approximation of a singularly perturbed nonlinear Fredholm integro-differential equation". In: *Applied Numerical Mathematics* 191 (2023), pp. 17–28. ISSN: 0168-9274. DOI: https://doi.org/10.1016/j.apnum.2023.05.008.

[67] T. Okayama. "Sinc-collocation methods with consistent collocation points for Fredholm integral equations of the second kind". In: (2023). DOI: 10.48550/arXiv.2301.12692.

[68] T. Okayama, T. Matsuo, and M. Sugihara. "Improvement of a Sinc-collocation method for Fredholm integral equations of the second kind". In: *BIT Numer. Math.* 51.2 (2011), pp. 339–366. DOI: 10.1007/s10543-010-0289-x.

[69] A. Quarteroni. *Numerical Models for Differential Problems*. Third Edition. Springer, 2017.

[70] M. Rabbani et al. "Computational projection methods for solving Fredholm integral equation". In: *Applied Mathematics and Computation* 191.1 (2007), pp. 140–143.

[71] M. Rahman. *Integral Equations and their Applications*. WIT Press, 2007.

[72] A. Rahmoune. "On the numerical solution of integral equations of the second kind over infinite intervals". In: *J. Appl. Math. Cmoput.* 66 (2021), pp. 129–148. DOI: 10.1007/s12190-020-01428-2.

[73] A. Rahmoune. "Spectral collocation method for solving fredholm integral equations on the half-line". In: *Appl. Math. Comput.* 219.17 (2013), pp. 9254–9260. DOI: 10.1016/j.amc.2013.03.043.

[74] A. Rahmoune and A. Guechi. "A rational spectral collocation method for solving fredholm integral equations on the whole line". In: *Int. J. Copmput. Sci. Math.* 13 (2021), pp. 32–41. DOI: 10.1504/IJCSM.2021.114184.

[75] A. Rahmoune and A. Guechi. "Sinc-Nystrom methods for Fredholm integral equations of the second kind over infinite intervals". In: *Appl. Numer. Math.* 157 (2020), pp. 579–589. DOI: 10.1016/j.apnum.2020.07.013.

[76] A. Ralston and P. Rabinowitz. *A First Course in Numerical Analysis*. New York: Dover Publications, Mineola, 2001.

[77] T. J. Rivlin. *Chebyshev Polynomials: From Approximation theory to Algebra & Number Theory*. Second Edition, Dover Publications, Inc. Mineola, New York, 2020.

[78] J. Shen, T. Tang, and L-L. Wang. *Spectral methods. Algorithms, Analysis and Applications*. Springer Series in Computational Mathematics. Berlin: Springer, 2011.

[79] J. Shen, T. Tang, and Li-L. Wang. *Spectral methods. Algorithms, Analysis and Applications*. Heidelberg: Springer Berlin, 2011. ISBN: 978-3-642-27097-0.

[80] J. Shen and L. L. Wang. "Error analysis for mapped legendre spectral and pseudospectral methods". In: *SIAM J. Numer. Anal.* 42.1 (2004), pp. 326–349. DOI: 10.1016/j.crme.2004.09.013.

[81] D. Slepian. "Some comments on Fourier analysis, uncertainty and modeling". In: *SIAM Rev.* 25.3 (1983), pp. 379–393. DOI: 10.1137/1025078.

[82] I. H. Sloan. "Improvement by iteration for compact operator equations. Mathematics of Computation". In: *Mathematics of Computation* 30.136 (1976), pp. 758–764.

[83] F. Smithies. *Integral equations*. no.49,CUPArchive, 1958.

[84] V.V. Sobolev. *Course in Theoretical Astrophysics*. Izdatel'stvo Nauka Nauka, Moscow, 1985.

[85] I. Stakgold and M.J. Holst. *Green's functions and boundary value problems*. John Wiley & Sons, 2011.

[86] G. Szegö. *Orthogonal Polynomials*. New York: Amer. Math. Soc., 1967.

[87] T. Tang. *Spectral and high-order methods with applications*. Science Press Beijing, 2006.

[88] Xu X. Tang T. and J. Cheng. "On spectral methods for Volterra integral equations and the convergence analysis". In: *J Comput. Math* 26.1 (2008), pp. 825–837.

[89] L. N. Trefethen. *Spectral Methods in Matlab*. SIAM, Philadelphia, 2000.

[90] L.N. Trefethen. *Approximation theory and approximation practice*. Society for Industrial and Applied Mathematics (SIAM), 2013.

[91] L.N. Trefethen. *Spectral methods in MATLAB*. SIAM, 2000.

[92] H. Wang. "How much faster does the best polynomial approximation converge than Legendre projection?" In: *Numerische Mathematik* 147.2 (2021), pp. 481–503.

[93] H.-Y. Wang and S.-H. Xiang. "On the convergence rates of Legendre approximations". In: *SIAM journal on numerical analysis* 81.278 (2012), pp. 861–877.

[94] A.M. Wazwaz. *Linear and Nonlinear Integral Equations: Methods and Applications*. 1st. Berlin: Springer, 2011.

[95] Z. XIE, X. LI, and T. Tang. "Convergence analysis of spectral Galerkin Methods for Volterra type integral equations". In: *J. Sci. Comput.* 53 (2012), pp. 414–434.

[96] Y. Yang et al. "Convergence Analysis of Legendre-Collocation Methods for Nonlinear Volterra Type Integro Equations". In: *Advances in Applied Mathematics and Mechanics* 7.1 (2015), pp. 74–88. DOI: 10.4208/aamm.2013.m163.

ملخص

يركز العمل البحثي المقدم في هذه الأطروحة على تحسين سرعة تقارب الطرق العددية لحل المعادلات التكاملية. غالبا ما تقدم هذه المعادلات سلوكا معقدا للغاية، مما يشكل تحديات كبيرة للتقنيات العددية التقليدية، لاسيما من حيث التقارب والدقة. لمعالجة هذه التحديات، قمنا بتطوير وتحليل طريقة التجميع الطيفي التكيفي لمعادلات فريدهولم وفولتيرا التكاملية من النوع الثاني، والتي يمكن أن تحقق تقاربا سريعا ودقة عالية على الرغم من أن حلها يظهر تباينات سريعة موضعية، أو تدرجات حادة، أو جبهة حادة. تم تنفيذ التكيف باستخدام عائلة مناسبة من التعيينات الفردية لتوليد معادلة جديدة بسلوك أكثر سلاسة يمكن تقريبها بدقة أكبر. يمكن للطريقة المقترحة تحقيق دقة أسية عن طريق ضبط تعيين يعتمد على المعلمة في التقريب النمطي وفقا للمعطيات المقدمة. أخيراً، تم تقديم العديد من الأمثلة الرقمية لإظهار أن الطريقة المقترحة أفضل من طريقتها الكلاسيكية وبعض الطرق الأخرى الموجودة مع عدد أقل نسبيا من درجات الحرية.

كلمات المفتاحية : معادلات تكاملية خطية، تعيينات لتحسين الدقة، طريقة التجميع الطيفي التكيفي، الدقة الطيفة، تحليل التقارب.

Abstract

The research work presented in this thesis focuses on improving the convergence speed of numerical methods for solving integral equations. These equations often introduce a very complex behavior, posing significant challenges to traditional numerical techniques, particularly in terms of convergence and accuracy. To address these challenges, we have developed and analyzed an adaptive spectral collocation method for Fredholm and Volterra integral equations of the second kind, which can achieve fast convergence and high accuracy despite the fact that its solution exhibits localized rapid variations, steep gradients, or a steep front. Adaptivity is implemented using a suitable family of one-to-one mappings to generate a new equation with smoother behavior that can be approximated more accurately. The proposed method can achieve exponential accuracy by adjusting a parameter-dependent mapping in the modal approximation according to the given data. Finally, several numerical examples are given to show that the proposed method is preferable to its classical method and some other existing approaches with a relatively smaller number of degrees of freedom.

Keywords : Linear integral equations, mappings for improved accuracy, adaptive spectral collocation method, spectral accuracy, convergence analysis.

Résumé

Le travail de recherche présenté dans cette thèse se concentre sur l'amélioration de la vitesse de convergence des méthodes numériques pour résoudre des équations intégrales. Ces équations introduisent souvent un comportement très complexe, posant des défis importants aux techniques numériques traditionnelles, notamment en termes de convergence et de précision. Pour relever ces défis, nous avons développé et analysé une méthode spectrale adaptative de collocation pour les équations intégrales de Fredholm et de Volterra du second type, qui peut atteindre une convergence rapide et une grande précision, malgré le fait que sa solution présente des variations rapides localisées, des gradients abrupts ou un front abrupt. L'adaptativité est implémentée en utilisant une famille de transformations appropriées pour générer une nouvelle équation avec un comportement plus lisse qui peut être approximée plus précisément. La méthode proposée peut atteindre une précision exponentielle en ajustant une transformation appropriée dépendant d'un paramètre dans l'approximation modèle selon les données fournies. Enfin, plusieurs exemples numériques sont donnés pour montrer que la méthode proposée est préférable à son méthode classique et à d'autres approches existantes avec un nombre relativement plus petit de degrés de liberté.

Mots clés : Équations intégrales linéaires, transformations appropriées pour une précision améliorée, méthode spectrale adaptative de collocation, convergence spectrale, analyse de la convergence.